SSI report

SSI Rapport
2005:20

Rapport från Statens strålskyddsinstitut
tillgänglig i sin helhet via www.ssi.se

Expert Panel Elicitation of Seismicity Following Glaciation in Sweden

Stephen Hora and Mikael Jensen

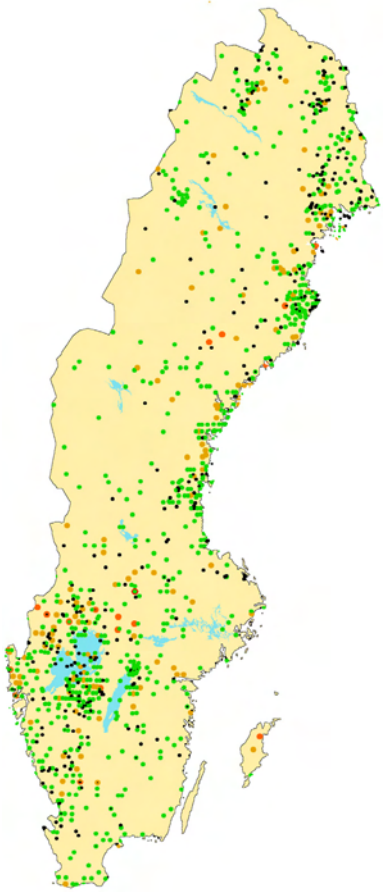

Statens strålskyddsinstitut
Swedish Radiation Protection Authority

SSI's Activity Symbols

Ultraviolet, solar and optical radiation
Ultraviolet radiation from the sun and solariums can result in both long-term and short-term effects. Other types of optical radiation, primarily from lasers, can also be hazardous. SSI provides guidance and information.

Solariums
The risk of tanning in a solarium are probably the same as tanning in natural sunlight. Therefore SSI's regulations also provide advice for people tanning in solariums.

Radon
The largest contribution to the total radiation dose to the Swedish population comes from indoor air. SSI works with risk assessments, measurement techniques and advises other authorities.

Health care
The second largest contribution to the total radiation dose to the Swedish population comes from health care. SSI is working to reduce the radiation dose to employees and patients through its regulations and its inspection activities.

Radiation in industry and research
According to the Radiation Protection Act, a licence is required to conduct activities involving ionising radiation. SSI promulgates regulations and checks compliance with these regulations, conducts inspections and investigations and can stop hazardous activities.

Nuclear power
SSI requires that nuclear power plants should have adequate radiation protection for the general public, employees and the environment. SSI also checks compliance with these requirements on a continuous basis.

Waste
SSI works to ensure that all radioactive waste is managed in a manner that is safe from the standpoint of radiation protection.

Mobile telephony
Mobile telephones and base stations emit electromagnetic fields. SSI is monitoring developments and research in mobile telephony and associated health risks.

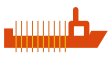

Transport
SSI is involved in work in Sweden and abroad to ensure the safe transportation of radioactive substances used in the health care sector, industrial radiation sources and spent nuclear fuel.

Environment
"A safe radiation environment" is one of the 15 environmental quality objectives that the Swedish parliament has decided must be met in order to achieve an ecologically sustainable development in society. SSI is responsible for ensuring that this objective is reached.

Biofuel
Biofuel from trees, which contains cesium, for example from the Chernobyl accident, is an issue where SSI is currently conducting research and formulating regulations.

Cosmic radiation
Airline flight crews can be exposed to high levels of cosmic radiation. SSI participates in joint international projects to identify the occupational exposure within this job category.

Electromagnetic fields
SSI is working on the risks associated with electromagnetic fields and adopts countermeasures when risks are identified.

Emergency preparedness
SSI maintains a round-the-clock emergency response organisation to protect people and the environment from the consequences of nuclear accidents and other radiation-related accidents.

SSI Education
is charged with providing a wide range of education in the field of radiation protection. Its courses are financed by students' fees.

EDITORS / REDAKTÖRER : Stephen Hora* and Mikael Jensen

* University of Hawaii at Hilo

SSI rapport: 2005:20
december 2005
ISSN 0282-4434

TITLE / TITEL: Expert Panel Elicitation of Seismicity Following Glaciation in Sweden / Formella Expertbedömningar av Jordskalv efter Nedisning i Sverige.

SUMMARY: The Swedish Radiation Protection Authority, the Swedish Nuclear Power Inspectorate and the Swedish Nuclear Fuel and Waste Management Company have jointly carried out a project on expert panel elicitation on the issue of glacial induced Swedish earthquakes.

Following a broad nomination procedure, 5 experts were chosen by a selection committee of 4 professors within Earth sciences disciplines. The 5 experts presented judgments about the frequency of earthquakes greater the magnitude 6 within 10 km for two Swedish sites, Oskarshamn and Forsmark, in connection with a glaciation cycle. The experts' median value vas 0,1 earthquakes for one glaciation cycle.

SAMMANFATTNING: Statens strålskyddsinstitut, Statens kärnkraftinspektion och Svensk Kärnbränslehantering AB har tillsammans genomfört ett projekt med formella expertutfrågningar i ämnet jordskalv i Sverige i samband med nedisning.

Efter ett brett nomineringsförvarande har 5 experter valts ut av en urvalskommitté av 4 professorer inom området. De 5 experterna har givit bedömningar om frekvensen av jordskalv större än magnitud 6 inom tio kilometer, för två platser i Oskarshamn och Forsmark, i samband med en nedisning. Medianvärdet av experternas bedömningar var 0,1 jordskalv för en glaciationscykel.

Statens strålskyddsinstitut
Swedish Radiation Protection Authority

Content

Figures

Appendices

1 Background

1.1 The technique of expert panel elicitation, EPE

In the safety assessment of the final disposal of radioactive waste, expert judgement in many different forms will undoubtedly play a significant role. The method of formal expert elicitation reported here was developed by the US NRC during the safety studies of nuclear reactors and provides the basis for expert judgement methods used in the license application for the WIPP [Ref.1]. The method is also used in the UK but in Continental Europe the experience of formal expert panel elicitation studies is very modest, with the exception of work done in the University of Delft [Ref. 2]. The technique has been studied within many disciplines. Examples of fields that have contributed to probability elicitation are decision analysis, psychology, risk analysis, Bayesian statistics, mathematics and philosophy.

In a Swedish Radiation Protection Authority's (SSI) report an example is given of work in Sweden, exploring the technique. A more general background is given in [Ref. 3]. Quantification of subjective probabilities is employed in a number of circumstances. These include:

issues that concern political decisions

- when there is likely to be public scrutiny of the uncertainties,
- in situations requiring impartial judgments,
- in cases where there are potential legal action,

combined with issues that concern scientific questions

- when data exist only from analogue situations (one might know the solubility of one mineral and might use this information to infer the solubility of another mineral),
- when scaling up from experiments to target physical processes is not direct (scaling of mean values is often much simpler than rescaling uncertainties), and
- when the uncertainties are significant relative to the demonstration of compliance.

Several, and perhaps all, of these criteria are relevant to the final disposal of radioactive waste.

Professor Stephen Hora, used as a consultant in this study, of the University of Hawaii, has been directly involved in the development of these methods over the past twenty years [Ref. 4,5,6,7].

1.2 Formation of a research project

Based on the assumption that both operator and regulators may have an interest in the method of expert panel elicitation, a common research project was suggested by SSI at a meeting in November 2004. SSI had invited the operator, the Swedish Nuclear Fuel and Waste Management Company, SKB, the Swedish Nuclear Power Inspectorate, SKI, and representatives from the two municipalities involved in SKB's ongoing site investigation (2005), Östhammar and Oskarshamn. At the meeting Prof. Stephen Hora from the University of Hawaii at Hilo was invited as an expert on the method.

1.3 The role of the project and roles of the project participants

The project is thus not set up as a part of the ongoing operator-regulator license activities but as a pure research project of interest to all parties. The participants present at the meeting November 2004 agreed to act as a steering committee. The practical work was to be made by SSI and SKI, mainly through Mikael Jensen and Eva Simic. SKB, through its representative Raymond Munier, took part in an observing capacity, and also offered to place its databases at the project's disposal, to meet the need for such data, as asked for by the experts. The project was financed jointly by the authorities SSI and SKI and the operator SKB.

For purposes of transparency, the finances were administrated within SSI, using SSI's economic reporting system.

2 Project formulation

2.1 Scientific matters

The quantity or quantities for elicitation were discussed at the first meeting.. The municipalities' representatives were in favour of seismicity issues but several possibilities were discussed, e.g. the future fate of the Baltic Sea shoreline. Finally, two questions on seismicity following glaciation were defined:

1. What will be the frequency of magnitude 6.0 or greater earthquakes within 10 km of Forsmark and Oskarsham during the immediate post glaciation period assuming that the average thickness of ice above the repository reached a maximum of 1000 meters, 2000 meters, 3000 meters? Give an uncertainty distribution for this quantity at each repository under these three assumptions about thickness of the ice overlay.

2. Given a magnitude 6.0, 7.0, and 8.0 earthquake occurring within 10 km of a repository in Forsmark and Oskarham, give an uncertainty distribution for the maximum displacement (slip or shear) in an existing or new fracture in the repository. Your uncertainty distribution should include the possibility that no displacement occurs with the repository.

2.2 The procedure for nomination and selection

A letter inviting to nominate was sent out to 23 organisations (Appendix 1 – in Swedish), a group of organisations or stakeholders that has shown an interest in the Swedish Waste Program; this group is usually invited to review SKB's research plan. While this was an open and transparent method, it became obvious after a while that it did not yield a great number of experts. Therefore, a number of additional experts were nominated within the project's reference group. A number of experts declined to participate, in some cases because of the relatively short time between the additional nomination and the first meeting, around 6 weeks and even shorter for some. In the end of the process, 16 experts remained. Four experts were chosen to form a selection group, who selected 5 experts among the 16 nominees. The selection group was made up by Prof. Jimmy Stigh, University of Gothenburg, Prof. Roland Roberts, Uppsala University, Prof. Ove Stephansson, the Swedish Royal Technical University and Prof. Giorgio Ranalli, Carleton University, Canada.

The selection implied that relevant disciplines corresponding to the two questions needed to be addressed. Instructions were given in Appendix 2. It was noted that some experts who felt

they were qualified in only one of the 2 questions, did not take the opportunity to disqualify themselves on one question and participate on the other. Rather they preferred to depart from the process altogether. Most of these experts looked on question 1 as problematic. It was then decided to give additional instructions to the selection committee, to the effect that the committee should focus on experts in question 2, in case it could not find 5 experts qualified to answer both questions (Appendix 3).

2.3 Timetable

The group set up a timetable on the first November meeting, based on suggestions from Prof. Hora that implied that the project would have to be carried out during the first half of 2005. Information activities were to follow in the fall of 2005 directed at the two municipalities.

3 Selection of experts and preparatory work

3.1 The selection.

The selection committee had a meeting on April 12. Their report is attached as Appendix 4.

The selection committee considered that "the proposed group has the competence to address both of the questions, albeit that the field of excellence of the different experts varies significantly from person to person" (Appendix 4).

The selection committee selected 5 experts:

- John Adams, Geological Survey of Canada, Natural Resources Canada,
- Hilmar Bungum, NORSAR, also affiliated to the University of Oslo,
- James Dieterich, University of California, Riverside,
- Kurt Lambeck, The Australian National University, Canberra, and
- Björn Lund, University of Uppsala.

The committee also selected two reserves, to functions in case any expert experienced unforeseen problems with participation.

By April 29, the selected experts had all agreed to the arrangements made by SSI for the project, so the reserves did not have to be called in. At this point the remaining experts were notified that they were not selected.

3.2 The first meeting of the expert group

The first meeting took place at SSI the 17-18 of May 2006. The experts were given a presentation by Stephen Hora on the technique of elicitation of subjective probability. The rest of the meeting's two days were used to discuss the questions.

Although two experts, Adams and Dieterich, thought they might give the second problem some consideration, it soon became clear from the discussion that it would be difficult to cover both questions, given the restriction of 5 days of consultancy between the two meetings.

The second issue is not addressed further in the elicitation process. Information on the issue is included in Adam's and Bungum's reports.

The first question was changed in two steps. Before the meeting, based on discussion between SSI, SKI and SKB, it was suggested that the glaciation should be assumed to be similar to the Weichsel glaciation, in order to define the circumstances and sequences of events during the glaciation, thereby avoiding the need of a large number of additional assumptions, which would be the case if a glaciation in general was assumed.

The issue nevertheless required some assumptions to be made, as was unfolded by the discussion. Among other things the experts wanted information about cumulative earthquakes from two 20-year periods 65-84, 85-2004 in an area 1985-2000 in three different areas of Sweden, one of which includes the two sites, shown in Fig 1. Earthquake locations on the map are from the Swedish National Seismic Network (SNSN) 2000-2005.

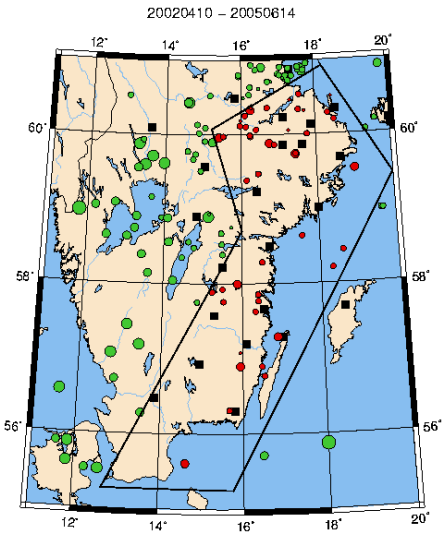

Figure 1.

The polygon defining the southeast area of Sweden (From Lund's presentation, June 20, 2005).

In the end of the discussion the group agreed on the following formulation of the first elicitation issue:

> What will be the frequency of moment magnitude 6.0 or greater earthquakes per unit area (e.g. per 100 sq. km) in the middle and south of Sweden (Forsmark and Oskarshamn) during a glacial cycle (app. 100 000 a) assuming conditions similar to the Weichsel glaciation? Give an uncertainty distribution for this quantity for each area.

Assume

- the maximum moment magnitude of 7,6 (nominal value for Dehls Pärve fault), and
- a seismogenic thickness of 30 km.

In addition, a minimum common set of references was given according to the list below:

- Additional material to be submitted on stress load from Kurt Lambeck for the two sites.
- Material from SKB regarding earthquakes in the polygon for two time periods.
- SKB Publication TR-99-03.

- Clark H. Fenton, C.H., Adams, J., and Stephen Halchuk, S., 2005. Seismic Hazards Assessment for Radioactive Waste Disposal Sites in Regions of Low Seismic Activity. Geotechnical and Geological Engineering (preprint, paper to appear Fall 2005).
- POSIVA 2003-10 Glacial Rebound and Crustal Stress in Finland.
- Stewart, I.S., J. Sauber & J. Rose (eds.): Glacio-seismotectonics: Ice sheets, crustal deformation and seismicity, Quat. Sci. Rev., 19, pp. 1367-1389.

During the cause of the project, the panel agreed that the form of much of the data input, earthquakes within a 100 km radius, made it logical to give the results using that unit area, i.e. earthquakes during a glaciation cycle per 31416 km^2, i.e. from an area within 100 km from the given sites. Numerical results in this report could be converted to refer to a 10-km distance, closer to the original area unit, by dividing by 100.

4 The elicitation

4.1 The second expert group meeting – presentation and elicitation

A one and one-half day elicitation meeting was held in Stockholm on June 20th and 21st, 2005. The first part of the meeting consisted of presentations by each of the experts concerning how they had analyzed the two elicitation questions. It became apparent that the experts were exceptionally well prepared to answer questions about the frequency of seismic events of various magnitudes during periods of ice intrusion and withdrawal as well as during periods of relative stability.

The experts produced a written account of their work available in appendices 5-9. These were in some cases finalised after the meeting. They were all available shortly after the second expert meeting.

Each expert was allotted approximately one hour for presentation. Handouts and/or slides were used to facilitate the presentations. Each presentation period was followed by a discussion period that was generally quite lively. After the presentations had been completed, the experts worked with the elicitation team on an individual basis to provide their judgments as probability distributions. These sessions and findings are summarized in the order in which they occurred.

4.2 Hilmar Bungum

This expert addressed the issue of uncertainty in the frequency of seismic events by encoding the uncertainty in a lognormal distribution. He did not distinguish between the two sites. The parameter of σ, of his distribution carries the uncertainty and was empirically linked to the uncertainty in the Guttenberg-Richter curve through uncertainty in the 'a' and 'b' parameters. The encoded value for σ is 0.47 while the median value for the distribution is established by using an 'a' parameter of 4.21 which is the observed value for the Lappland data. The resulting probability distribution is shown in the following table. Here the extreme values of the frequency are obtained by truncating the distribution at three standard deviations above and below the mean. The answers were given for a 100,000-year period and have been scaled from an area of 100 km^2 to an area with a radius of 100 km.

Figure 1 Uncertainty Distribution for Magnitude 6 or Greater – Forsmark and Oskarshamn (Bungum)

Cumulative Probability	0.000	0.023	0.159	0.50	0.84	0.98	1.00
Frequency of Magnitude 6 or Greater	0.008	0.60	1.74	5.1	14.9	43.7	374

4.3 James Dieterich

Professor Dieterich used the stress calculations of Kurt Lambeck as a basis for his judgments. He employed a mechanical model using Lambeck's glaciation stress calculations to which tectonic and gravitational stresses were added to obtain total stress figures. A Columb failure criterion was used in the model to determine when the total stress was sufficient to induce a seismic event. The model was run over time varying three factors. These factors accounted for stressing state and failure uncertainty, parameter uncertainty, and model uncertainty, respectively. The elicited distributions incorporate all these sources of uncertainty. The distributions are for the number of magnitude 6 or greater events over 100,000 years in an area with 100 km radius.

Figure 2 Uncertainty Distribution for Magnitude 6 or Greater – Forsmark and Oskarshamn (Dieterich)

Uncertainty Distribution for Magnitude 6 or Greater – Forsmark and Oskarshamn (Dieterich)

Cumulative Probability	0.00	0.05	0.25	0.50	0.75	0.95	1.00
Oskarshamn	1.4	4.1	21	42	83	206	247
Forsmark	0.8	2.4	12	24	47	118	142

4.4 Björn Lund

The judgments of Dr. Björn Lund are based upon the assumed maximum magnitude event, 7.6, and the current, ice-free, seismicity rate rate and the ice model stresses of Lambeck. Lund used a model of background and glacial stress using nodes to represent potential event locations. Five steps were used to evaluate the magnitudes and frequencies of events at each time period. These are:

1. Generate area with nodes of random stress, some above the failure stress.

2. Add the evolving, ice sheet generated, stress field which has all nodes at

   or below failure.

3. Count connected nodes as one event, number of nodes gives magnitude.

4. Count up the events to a frequency-magnitude relation.

5. Generate new background area for the next time step to avoid repeating events.Lund's judgments were provided for a 100,000-year period with an area of radius of 100 km. The judgments differentiated between the frequency of events at Forsmark and Oskarshamn with Forsmark having the higher frequency.

Figure 3 Uncertainty Distribution for Magnitude 6 or Greater – Forsmark and Oskarshamn (Bjorn Lund)

Cumulative Probability	0.00	0.25	0.50	0.90	1.00
Oskarshamn	0.0	2.25	4.5	80	200
Forsmark	0.8	4	7	123	200

4.5 John Adams

Adams compared 4 sources of earthquake rate information: worldwide SCC earthquakes, Swedish earthquakes, Lappland faults, and Mörner's catalogue of Swedish paleoearthquakes. Adams adjusted the magnitude estimates of Mörner downward to create a Guttenberg-Richter curve. The adjustment brought Mörner's estimate of the Parve event in line with the assumed value of magnitude 7.6 used in this study. The uncertainty in the frequency of magnitude six events was deduced from the lower physical bound of 0.0 and comparison to the Australian and Canadian frequencies. The judgments were given for a radius of 100 km and 100,000 years. No differences between Oskarshamn and Forsmark were given. The resulting uncertainty distribution is:

Figure 4 Uncertainty Distribution for Magnitude 6 or Greater – Forsmark and Oskarshamn (Adams)

Cumulative Probability	0.00	0.25	0.50	0.75	1.00
Frequency of Magnitude 6 or Greater	0	3	12	45	200

4.6 Kurt Lambeck

Professor Lambeck provided an extensive analysis of glacial loading for both the Forsmark and Oskarshamn sites. His analysis indicated that the greatest seismic hazard occurs at the rim of the ice cap as the ice cap advances and retreats. Because the ice cap is larger when the rim is at Oskarshamn than when the rim is at Forsmark, the seismicity at Oskarshamn will be greater as the rim of the cap passes over the site than when the rim of the cap passes over Oskarshamn. The analysis of loading and unloading was used in the analyses of Drs. Dieterich and Lund. Dr. Lambeck did not provide an uncertainty distribution for magnitude 6 or greater events but he did provide information from which such a distribution could be imputed. Specifically, Dr. Lambeck provided an uncertainty distribution for the frequency of a magnitude 7.6 or greater event. Employing these values and a range of slope values of the Gutenberg-Richter relationship, representative of the various data sets used in the analysis, we

are able to construct an uncertainty distribution. We caution that this is an imputed distribution that was not directly assessed by the expert.

Professor Lambeck provided a best estimate of the frequency of a 7.6 magnitude or greater event with 100 km^2 of Oskarshamn as 1/350 with uncertainty bounds of 1/1000 (lower) and 1/100 upper. The estimates for Forsmark are smaller with a best estimate of the frequency of 1/20,000 with lower and upper uncertainty limits of 1/200,000 and 1/8,000 respectively. Figure 5 shows these uncertainty values with the frequencies translated to a radius of 100 km.

Figure 5 Frequency of 7.6 or Larger Events in a 100 km Radius (Kurt Lambeck)

	Lower Limit	Best Estimate	Upper Limit
Oskarshamn	0.31	0.90	3.14
Forsmark	0.0016	0.016	0.039

The second translation applied to Lambeck's values is to convert from magnitude 7.6 or greater events to magnitude 6.0 or greater events. This translation requires a value for the slope, b, of the Gutenberg-Richter relationship. As a demonstration, four values representative of the data sets presented by the experts in this study are used. These values are 0.8, 0.9, 1.0, and 1.1; the larger the slope, the greater the ratio between the frequencies of 6.0 and 7.6 or larger events. Note that the quantity b below normally is given as the slope of the relationship on a natural log plot; values below are b-values for base 10 log plots.

Specifically, $f_{6.0}/f_{7.6} = 10^{b(7.6 - 6.0)}$ where f_p is the frequency of magnitude p or greater events. Figure 6 shows the translated uncertainty distributions for each of the sites.

Figure 6 Translated Uncertainty Distributions, 100 km Radius and Magnitude 6.0 or Greater

	Slope b	Lower Limit	Best Estimate	Upper Limit
Oskarshamn	0.8	6.0	17.1	60
	0.9	8.7	24.7	87
	1	12.5	35.7	125
	1.1	18.1	51.7	181
Forsmark	0.8	0.030	0.30	0.75
	0.9	0.043	0.43	1.08
	1	0.063	0.63	1.56
	1.1	0.090	0.90	2.26

5 The resulting combined distributions

The individual distributions of four experts, excluding Lambeck's uncertainty distributions that are not commensurable, were combined to give a single distribution by averaging probabilities. Denote a cumulative probability function or distribution function of the ith expert by $F_i(x)$. The combined distribution is given by

$$G(x) = \frac{1}{m}\sum_{i=1}^{m} F_i(x)$$

where m is the number of experts and $G(x)$ is the resulting combined distribution.

Figures 7 and 8 are graphical representations of the elicited and combined distributions for Oskarshamn and Forsmark respectively.

Figure 7 Cumulative frequency of earthquakes with magnitude > 6 within 100 km from the Oskarshamn site during a glaciation cycle.

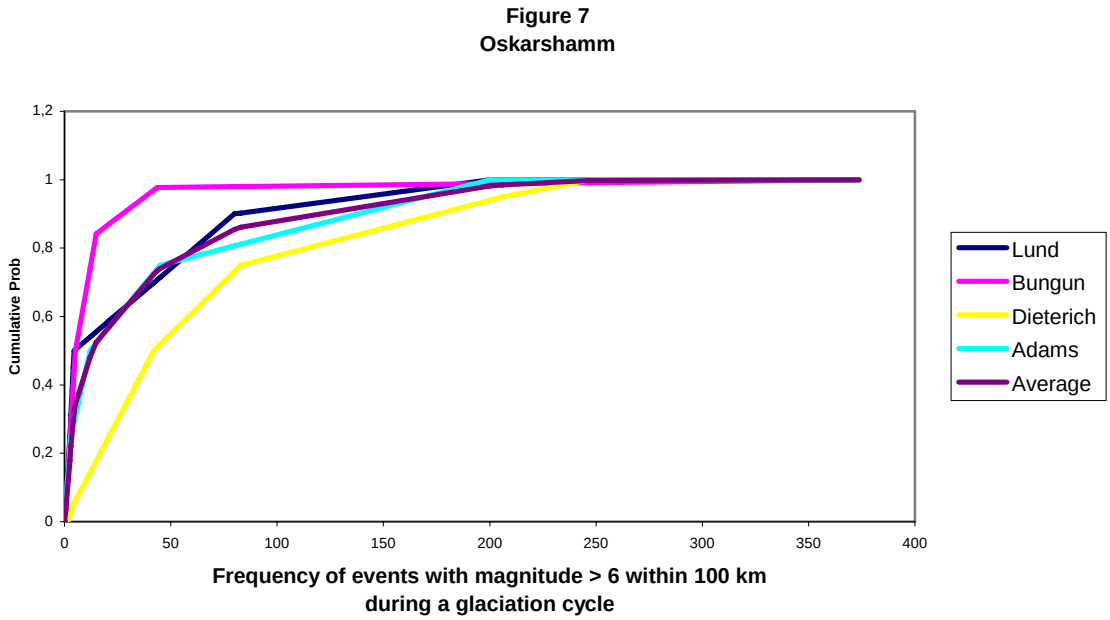

Figure 8 Cumulative frequency of earthquak*es* with magnitude > 6 within 100 km from the Forsmark site during a glaciation cycle.

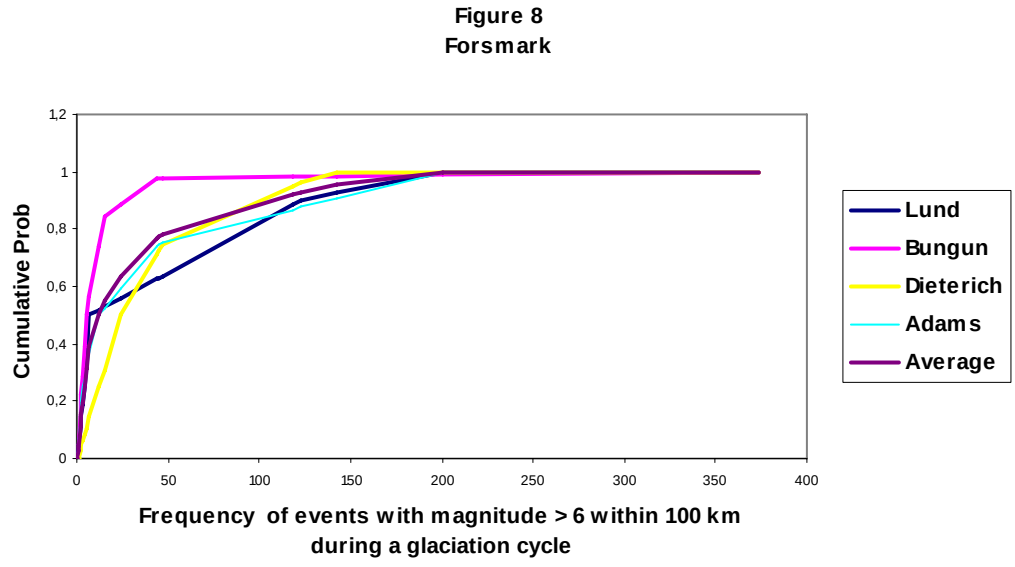

The numerical values of the frequencies and the averaged cumulative probabilities are given in the following tables.

Figure 9 Combined Cumulative Distribution for Oskarshamn

Frequency	0.00	0.01	0.60	1.40	1.74	2.50	3.00	4.10	4.50	5.09	12.0
Cumulative Probability	0.00	0.00	0.03	0.09	0.12	0.18	0.22	0.29	0.32	0.34	0.48

Freq. Cont	14.9	21.0	42.0	43.7	45.0	80	83	200	206	247	374
Cum. Prob., continued	0.52	0.57	0.72	0.73	0.74	0.85	0.86	0.98	0.98	1.00	1.00

Figure 10 Combined Cumulative Distribution for Forsmark

Frequency	0	0.01	0.6	0.8	1.74	2.4	3	4	5.09	7	12
Cumulative Probability	0.00	0.00	0.03	0.04	0.11	0.16	0.20	0.25	0.31	0.39	0.50

Freq. Cont	14.9	24	43.7	45	47	118	123	142	200	374
Cum. Prob., continued	0.55	0.63	0.76	0.77	0.78	0.92	0.93	0.95	1.00	1.00

The combined probability density distribution for Oskarshamn and Forsmark is given in figures 11 and 12 below.

Figure 11. Combined probability density distribution for Oskarshamn. Frequency of event with magnitude > 6 within 100 km during a glaciation cycle

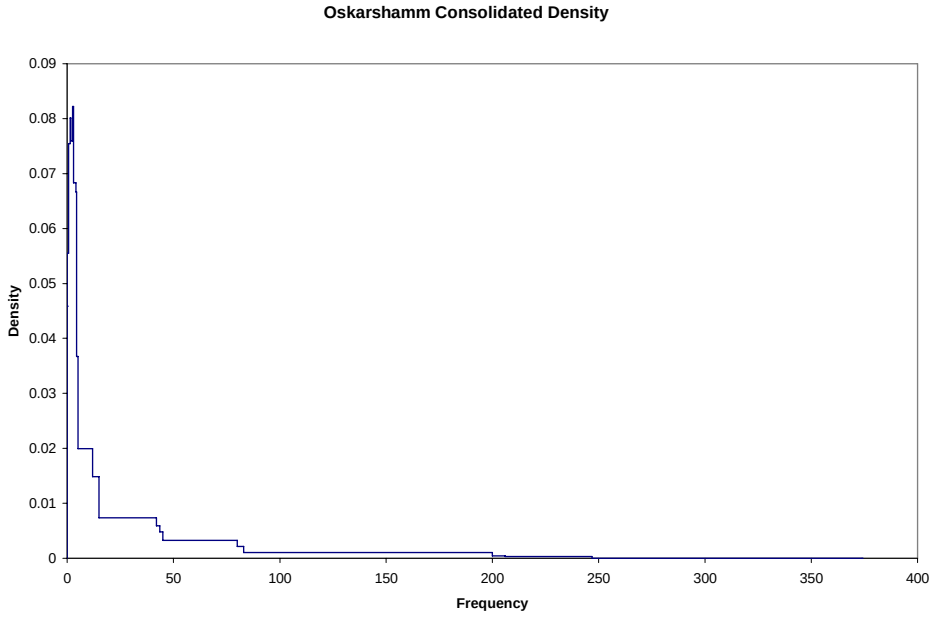

Figure 12. Combined probability density distribution for Forsmark. Frequency of event with magnitude > 6 within 100 km during a glaciation cycle

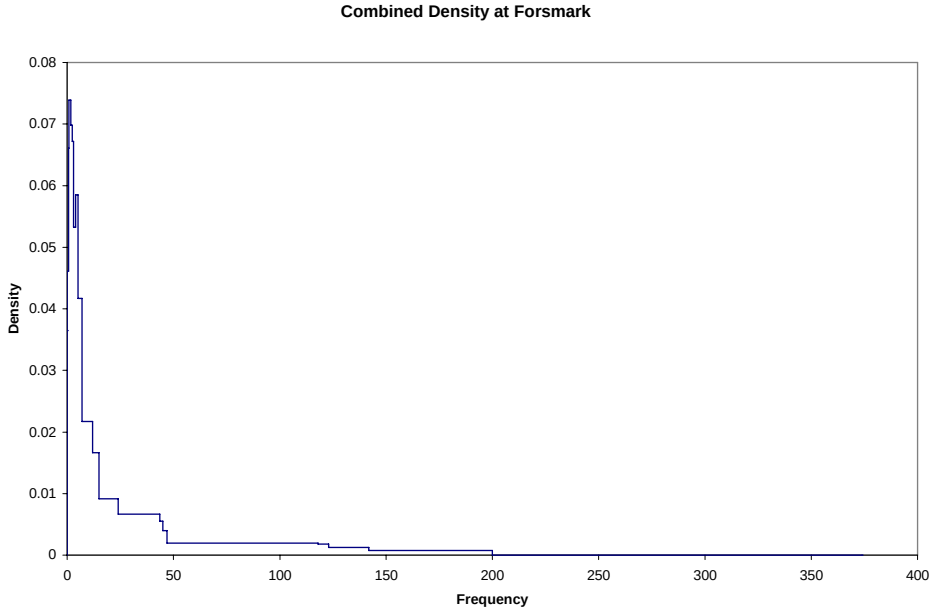

6 Discussion

As mentioned earlier the project is designed to produce elicitation results, but not to comment on implications for repository safety. Such inferences may be made later by any of the participants in the project, or any reader. The discussion is therefore limited mainly to the elicitation technique.

6.1 The unit of the result

As mentioned above the experts discussed the elicitation issue using number of earthquakes within a 100 km radius. Using a 10 km radius the answer in terms of the 50% fractal is 0.1 earthquakes within 10 km per 100 000 years or one glaciation, similar to the Weichsel glaciation.

6.2 The nomination process

In the election process a large number of Swedish organisations were invited to nominate candidates. However, the actual number of candidates nominated from these Swedish sources was small. Several candidates had to decline participation because of the relatively short time for practical planning. The combination of academic disciplines required by the two different issues, may have had an effect on the selection committee's choices. It cannot be ruled out that the expert group had been different if one of the issues had been abandoned earlier in the process.

6.3 Application of expert knowledge to the first elicitation issue

There is a widely heard hypothesis that glaciation and in particular the de-glaciation process causes seismic activity. All experts presented a guarded view in this respect. On the contrary, the issue was considered very difficult and required more calculation than is normal in such elicitations. This is also noticeable in the individual expert reports in the appendices 5-9.

6.4 The experts estimations and their independence

The spread between the experts' estimates is unusually narrow for elicitations. The expert's distributions all have the bulk of probability between 0 – 50 earthquakes per 100 000 a.

Lambeck's estimates is presented separately since it is not directly commensurable with the other distributions, in that it requires a choice of b for which he could not offer an estimate, but his values are well in accordance the other experts for all choices of b. His best estimate (50% cumulative probability) actually lies within the span off all 4 other experts for all choices of b except for b =1.1 (Lambeck's number for that choice ofb yields 52 earthquakes per 100 000 a, higher than Dieterich's 42).

The experts also emphasised the possibility that the frequency might be quite small. The cumulative probability of the 5% level is less than 1 earthquake in 100 000 a, and 25% lies between 3 and 4 (3 for Oskarshamn and 4 for Forsmark)!

The narrow range of distributions makes it natural to discuss to the question of independence, since Lambeck's calculation of stress load during a glaciation cycle is part of the reference documentation and referred to by all experts. Although Lund's and Dieterich's approach differs significantly, e.g. with different results for Oskarshamn and Forsmark, they both used

Lambeck's calculated stress loads to calculate their distribution. Adams' work, including empirical data, must be considered to have a high degree of independence. Bungum also falls in the more independent category, presenting a more independent view.

6.5 Differences between the two sites

The possibility of differences between the two sites has been mentioned, e.g. by the Geological Survey of Sweden, summarised by SSI and SKI, in the following passage on SKB's safety report SR 97:

> *The Swedish Geological Survey (SGU) emphasizes that there seems to be a causal relationship between deglaciation and displacement movements which should warrant further research. SGU lacks a compilation and analysis of available geological and hydrogeological data that could provide important information on the rock type or tectonic environment that can generally be considered to be the most favourable for a repository.* (Ref. 8)

As can be seen from the figures 7 and 8 there is virtually no difference to be seen between the two sites in the experts' estimations of the elicitated quantities. This is not to say that there couldn't be differences in other formulations of earthquake frequency, or in earthquake consequences at the respective sites.

7 Conclusion

The experience of this project has revealed a number of circumstances to take into account in formal elicitation.

7.1 Nominating procedure

The nomination procedure was similar to procedures from some cases in the US. However, the number of interested stakeholders in the US is higher than in Sweden and it is doubtful whether a longer list of Swedish organisations would have improved the result to render more candidates. Another more important issue is the very fact that the project was research oriented rather than part of the licence dialogue. A suggestion was made to include commercial methods and advertise in key magazines for candidates. A strict protocol will always give advantages in transparency, but there must always be provisions of external or corrective manoeuvres if the outcome threatens the whole process, as the case was when the process provided quite too few nominations. In any case, it is difficult to imagine a timescale shorter than 6 month as for the present project.

7.2 Preparation

The issue to be presented to the experts has to be prepared thoroughly. In the beginning of the project there were proposals both for one and two elicitation issues. As the project unfolded it is obvious that it would have been better to limit the issues to one. The project would thus have benefited from more preparation on this issue possibly including a so-called dry run, such as a small-scale elicitation exercise with in-house experts. The issue used in this report was a choice between several alternatives. However, in a situation where the choice of issues are in a more intense focus, whether for the authorities in a license dialogue or for SKB in

establishing bases for decision on a safety case, there would probably be much more focus on an issue before a formal elicitation would be made.

7.3 The number of experts

Particularly the issue of interdependence underlined the value of having more than just a few experts in the procedure. Prof. Hora recommended to use at least 3 and pointed to 5-6 as the maximum. Although the number of experts has bearing on the economy, the choice of no less than 5 can be recommended on practical grounds. It ensures a minimum number of experts available for the final combined distribution in case of incapacities for various reasons. In the present study, three different lines of thinking remain even if Lund and Dieterich are considered to use the same approach as Lambeck.

7.4 The value of formal expert judgement and when to use the technique

The different participating organisations may take somewhat different views on the value of the method and when to use it, considering the present experiences, but some general observations can be made.

The technique has shown to

- provide a clear answer, given the stated conditions,
- constitute a powerful tool for illuminating a limited, well defined, scientific area, and
- give, through the discussions throughout the project, new insights on the formulation of the problem in the field of glacial induced earthquakes.

It remains to be seen if the result will be supported or commented within the scientific community. There are a number of cases where formal expert judgement would not be warranted and in some cases where external input is required, an external review team may be the answer. Such a team is more flexible in their work and may still be transparent. The method described here may be used when the issue is well defined and there is good understanding of the need for the combination of disciplines that might be needed in the process.

The familiarity in Sweden with formal expert panel elicitation is strongly limited. It is the hope of the authors that this report will help to spread information about the result of this study and the technique of expert panel elicitation.

8 References

1. Kotra, J.P., M.P. Lee, N.A. Eisenberg, A.R. DeWispelare, Branch Technical Position on the Use of Expert Elicitation in the High-Level Radioactive Waste Program, U.S. Nuclear Regulatory Commission, NUREG-1563, 1996.

2. Harper, F.T., M.L.Young, S.C. Hora, L.A. Miller, C.H. Lui, M.D. McKay, J.C. Helton, L.H.J. Goossens, R.M. Cooke, J. Pasler-Sauer, B. Kraan, and J.A. Jones, *Probability Accident Consequence Uncertainty Analysis*, Vols. 1-3, USNRC and CEC DG XII, (NUREG/ CR-6244, EUR 15855 EN) , Brussels, 1994.

3. S. Hora, M. Jensen, *Expert Judgement Elicitation*, SSI report 2002:19.

4. Harper, F.T., M.L.Young, S.C. Hora, L.A. Miller, C.H. Lui, M.D. McKay, J.C. Helton, Rechard, R.P., K, Trauth, J.S. Rath, R.V. Guzowski, S.C. Hora and M.S. Tierny, The Use of Formal and Informal Expert Judgments when Interpreting Data for Performance Assessments SAND92-1148, Sandia National Laboratories, 1993.

5. Trauth K. S.C. Hora, and R.P. Rechard, Expert Judgment as Input to Waste Isolation Pilot Plant Performance-Assessment Calculations, SAND91-0625, Sandia National Laboratories, 1993.

6. Trauth, K., S.C. Hora and R.V. Guzowski, A Formal Expert Judgment Procedure for Performance Assessments of the Waste Isolation Pilot Plant, SAND93-2450, Sandia National Laboratories, 1994.

7. Hora, S.C., Nuclear Waste and Future Societies: A Look into the Deep Future, Technological Forecasting and Social Change, 56, 155-70, 1997.

8. SSI's and SKI's joint review of SR 97, SKI Report 01:3 also available as SSI-report 2001:02

9 Post scriptum

At a late stage in the project, several comments have reached the authors, worthwhile to mention.

During his work to finalise his work, on of the experts, Lund, reached the conclusion that he could not separate the two sites in terms of earthquake frequency. Another expert, Bungum, in his comment of the elicitation report, pointed out that the earthquake frequency used for the 0 and 100 % actually refer to his frequencies estimated at ±3 σ. At a later time, after a closer examination of the elicitation report, essentially section 4 of this report, he also questioned whether his values for 1 and 2 σ should not have been attributed lower probabilities, 0,68 instead of 0,84 for 1 σ and 0.95 instead of 0,98 for 2 σ.

Using the simple averaging formula for of probabilities, $G(x) = \frac{1}{m}\sum_{i=1}^{m} F_i(x)$, described in section 5, it can immediately be seen that neither comment would change the result in any significant way. For this reason, and in the interest of a timely presentation, no other action is made than to present the comments here.

One additional conclusion can be drawn, inspired in part by the discussion with Bungum, namely that it might be advisable to put more emphases on the quality assurance aspect of the elicitation. The elicitation was made on a strict timetable with several experts leaving for departing flights hours after their contribution and they would not have been available to follow up questions that might have come up at the end of the elicitation series, covering two days.

Appendix 1

AoM

2005-02-02 Dnr. 2004/2376-26

Inbjudan till nominering av experter till formell expertutfrågning (Expert Panel Elicitation)

Med detta brev vill SSI och SKI bjuda in olika aktörer i det svenska kärnavfallsprogrammet att bidra med nomineringar inom ett projekt kring formell expertutfrågning, så kallad Expert Panel Elicitation.

Frågorna som ställs till experterna rör jordskalv efter en nedisning, och formuleringen ges i bilaga 1. I bilaga 2 ges en beskrivning av tekniken med formella expertutfrågningar såsom den läggs upp i vår studie. Bland annat ska en urvalskommitté bestående av 3 medlemmar utses, vilken sedan ska välja ut 5 experter inom området seismologi. Vi hoppas därför på ett allsidigt underlag för urvalskommittén. Frågorna kan komma att modifieras något i en senare diskussion med experterna.

Vi tar tacksamt emot expertnomineringar från er organisation. Vi föreslår av praktiska skäl att varje deltagande organisation begränsar sig till högst tre nomineringar.

Syftet är att pröva en internationellt etablerad metod för att beskriva hur olika experters bedömningar kan ge en viss typ av samlad överblick i en fråga där, av olika skäl, inget uppenbart svar kan ges. Vi har valt en fråga som relaterar till säkerhetsanalysen för ett slutförvar för använt kärnbränsle. Myndigheterna SSI och SKI administrerar projektet och samråder med en referensgrupp som består av representanter från myndigheterna, SKB och platsundersökningskommunerna. SKB agerar som observatör inom projektet och kommer att ställa sina databaser och referenser till experternas förfogande om de så önskar. Projektet finansieras lika av SSI, SKI och SKB. De formella utfrågningarna leds av prof. Stephen Hora, University of Hawaii at Hilo.

Nomineringarna kan skickas till Statens strålskyddsinstitut, Mikael Jensen, 171 16 Stockholm och måste vara SSI tillhanda senast den 21 februari.

Med vänlig hälsning

Mikael Jensen Eva Simic

Statens strålskyddsinstitut Statens kärnkraftinspektion

Sändlista

KASAM

Lunds tekniska högskola/universitet - Geologiska Institutionen

Uppsala universitet, Institutionen för geovetenskaper

Chalmers Tekniska Högskola - Geologiska Institutionen

Göteborgs universitet - Geologiska Institutionen

Umeå universitet - Institutionen för ekologi, miljö och geovetenskap

Kungliga Tekniska Högskolan - Institutionen för Mark- och Vattenteknik

Stockholms Universitet - Geovetenskapliga Ämnesrådet

Luleå Tekniska Universitet

SGU

Hultsfreds kommun

Svenska Naturskyddsföreningen

Greenpeace – Sverige

Fältbiologerna Rikskansliet

Folkkampanjen mot kärnkraft och kärnvapen

Avfallskedjans Förening – Ingrid Sörlander

Avfallskedjans Nätverk – Olov Holmstrand

Avfallskedjan – Bertil Alm

OSS

Miljöförbundet Jordens vänner

Miljövänner för kärnkraft

Föreningen kärnteknik

Appendix 2

Dnr. 2004/2376-26 07 March 2005

INSTRUCTIONS TO THE SELECTION COMMITTEE

BACKGROUND

A project has been launched with the aim to use the technique of formal expert panel elicitation on an issue of interest within the Swedish radioactive waste program. The purpose is twofold: (1) to explore the merits of the method of formal elicitation (2) to evaluate how and why expert opinions differ on the scientific issue at hand. The project is a research activity, and is not part of any regulatory action on behalf of the Swedish authorities.

The project is monitored by a steering committee with members from the Swedish radiation Protection Authority, SSI, the Swedish Nuclear Poser Inspectorate, SKI, the Swedish Nuclear Fuel and Waste Management Company, SKB, and the municipalities of Östhammar and Oskarshamn, presently hosting site investigations. The project is lead by SSI and SKI.

The two questions posed to the experts are given in appendix A.

A number of experts have been nominated based on suggestions from a wide selection of Swedish organisations. Only 5 experts will be used in the panel, and a selection committee will select these among all nominees. The instruction to the committee is given below.

THE NUMBER OF EXPERTS

5 experts must be chosen, with 2 additional experts as reserves.

SCREENING FOR MOTIVATIONAL BIAS AMONG NOMINATED EXPERTS

Several types of motivational bias are possible in connection with expert judgement. In regulatory work, it is required that consulting experts, assisting the regulator in external reviews, do not have close ties with the regulated organisation.

The project's steering committee has decided that there is no ground for restrictions in this regard, since the elicitation occurs within a common research project. However, as a compromise to avoid possible misunderstanding within the public, the committee has decided that the experts, in order to be selected must

- not presently be working as SKB staff member
- not presently be employed by SKB as a consultant

The project's steering committee will screen nominees in this respect by asking experts to submit relevant information with respect to SKB.

SCIENTIFIC CRITERIA

The selection committee should aim to select experts best suited to answer the questions given. The experts will be asked to provide scientific merits, such as academic positions and recognition, and to list relevant papers.

Scientific width

It is advantageous to approach questions by several disciplines, methods or models. This should also be reflected in the selection committee's aim and choices, if reasonably achievable. If any balance is struck between scientific standing and diversity of approaches, this should be documented.

The selection committee's criteria

The committee should create a written set of critieria based on their own interpretation of the questions, for the purpose of the selection work and to use in the selection of experts.

MODUS OPERANDI

A chairman, who will report the work to the committee through Mikael Jensen and Eva Simic, heads the selection committee members.

Two day's work is allocated for the selection, one of which in the form of a meeting, possibly at SSI or SKI who will arrange for a meeting room. Only the members of the selection committee are present at the meeting.

An intricate voting system is not required but the choices made of experts from the list of nominees should be motivated and documented, as well aspossible disagreements. Committee members may also submit shared or individual comments.

Mikael Jensen Swedish Radiation Protection AuthoritySE-171 16 Stockholm, SwedenEmail address: mikael.jensen@ssi.se Phone +46 8 729 7100 Eva SimicSwedish Nuclear Power InspectorateSE-106 58 Stockholm, SwedenEmail Address: eva.simic@ski.sePhone +46 8 6988400

APPENDIX /to Appendix 2/ Questions to the experts in English.

1. What will be the frequency of magnitude 6.0 or greater earthquakes within 10 km of Foresmark and Oskarsham during the immediate post glaciation period assuming that the average thickness of ice above the repository reached a maximum of 1000 meters, 2000 meters, 3000 meters? Give an uncertainty distribution for this quantity at each repository under these three assumptions about thickness of the ice overlay.

2. Given a magnitude 6.0, 7.0, and 8.0 earthquake occurring within 10 km of a repository in Forsmark and Oskarham, give an uncertainty distribution for the maximum displacement (slip or shear) in an existing or new fracture in the repository. Your uncertainty distribution should include the possibility that no displacement occurs with the repository.

Appendix 3

Additional instructions to the selection committee

6 april 2005 Dnr. 2004/2376-26

TO THE MEMBERS OF THE SELECTION COMMITTEE

This is to inform you that the additional instructions have been formulated, to avoid a possible conflict between experts on issues related to question 1 vs. question 2.

The contacts made with nominated experts have revealed a certain number of abstentions and experts hesitating to participate related to problems with question 1.

Notwithstanding the committee's particular judgements, the project needs to ensure that the process does not come to a halt because of lack of candidates on one of the two questions.

The additional instruction is as follows. The committee should, as previously instructed, search for a panel of 5 persons, knowledgeable in both areas covered by question 1 and 2. If the committee finds it difficult to find a full panel of 5 candidates with high level of expertise in both fields, a panel of 5 experts in the area covered by question 2 should be chosen (even if 5 candidates attributable to question 1 also may be found).

In addition to this, assuming a panel covering both questions cannot be found, 2 experts should be chosen on the area covered by question 1. In that case it is valuable to the project to have this additional information as potential assistance in the definition of boundary conditions and other assumptions that must be made regarding question 2.

Appendix 4

The selection committee's report

2005-04-22

Notes regarding a meeting in Uppsala 12 april 2005 for panel selection for an expert panel elicitation regarding earthquake risks within the Swedish radioactive waste program.

Participants in the selection committee: Giorgi Ranalli, Carl*e*ton University, Ottawa,Roland Roberts, Uppsala University, Uppsala, Ove Stephansson, GeoForschungsZentrum, Potsdam, Jimmy Stigh, Gothenburg University.

Roland Roberts acted as secretary for the meeting.

Mikael Jensen (SSI) participated in the introductory part of the meeting, but then left and did not participate in the selection committee's discussions regarding the proposed experts.

The meeting commenced with a short introduction from Mikael Jensen (SSI) regarding the aims and boundary conditions of the procedure, together with some comments on the responses from the various proposed experts. Some of these had expressed doubts about the depth of their competence in one of the two questions (Note from SSI 6 April 2005, Dnr 2004/2376-26). While the issue and the additional instructions to the selection committee were discussed, no specific information about which proposed experts had expressed reservations was provided.

The scientists considered for selection to the expert panel were the following *(in alphabetical order)*

John Adams

Franck Audemard Mennessier

Hilmar Bungum

Kevin Coppersmith

James Dieterich

Kurt Lambeck

Björn Lund

Ian Main

Arthur McGarr

Peter Mora

Robert Muir-Wood

Nils-Axel Mörner

Hossein Shomali

Walter Silva

Ragnar Slunga

Per-Einar Tröften

All of these had supplied CVs.

Information on some of the proposed experts came very late prior to the meeting, which limited the possibilities of the selection committee to follow up this information.

Criteria for selection

The selection committee first discussed relevant criteria for the choice of the expert panel. Expertise in the following areas was considered relevant:

Crustal and mantle rheology

Crustal stress regime in general and in Fennoscandia

Deformation modeling: General and specific competence

Documented broad scientific perspective

General geological background

General geophysical background

General knowledge of glaciation/deglaciation processes (ice sheet models etc)

Knowledge of direct deformation measurements (GPS) etc in general and/or Fennoscandia.

Knowledge of fracture systems in crystalline rocks – general and specific

Laboratory measurements of rock physics

Knowledge of shield environments

Paleoseismology

Post-glacial rebound studies

Rock mechanical competence

Rock stresses

Seismic/aseismic movements

Seismic risk studies

Seismicity in Sweden

Statistical seismology

Strong ground motion studies

Theoretical understanding of current knowledge of slip processes

Prior to discussing the candidates, some generalities were discussed. These included how possible conflicts of interest should be handled. This was not regarded as a problem due to the clear guidelines given.

The form of the CV from most of the experts was sub-optimal in that these were not formulated specifically regarding competence in the area of the exact questions to be answered.

Prior to and after making the selections, the group discussed in detail the differences in competence necessary to optimally answer both questions 1 and 2. It is considered that the proposed group has the competence to address both of the questions, albeit that the field of excellence of the different experts varies significantly from person to person.

All proposed experts were considered to be highly competent in areas relevant for the questions to be addressed.

A conscious ambition was to avoid selecting experts with very similar backgrounds and experiences.

Only scientific competence was considered in making the selections.

The selection committee's recommendations

The committee was requested to recommend a group of 5 experts, with an additional 2 reserves. The group recommends (in alphabetical order): Adams, Bungum, Dieterich, Lambeck, and Lund, with McGarr and Slunga as reserves.

Comments on the experts proposed to form the panel (alphabetical order)

Adams (Canada)

Has worked with post-glacial faulting in Precambrian shields, and is well recognized in the field. Expertise in hazard analysis. Has limited local knowledge e.g. of seismicity in Fennoscandia. Not primarily engaged in numerical modeling of crustal stresses but has worked with in-situ stress.

Bungum (Norway)

Expertise in neotectonics, the seismicity and state of stress in Fennoscandia. Has worked extensively with probabilistic seismological hazard analysis and its application to large constructions

Dieterich (USA)

Extensive experience in seismic risk and hazard assessment (head of the relevant unit at USGS) and the relevant rock mechanical issues (mechanisms of slip etc). Not an expert on the local conditions in Fennoscandia, and has not worked extensively with issues related to glaciation.

Lambeck (Australia)

Is regarded as a world leader in postglacial rebound and lithospheric rheology. Has scientific pondus. Knows Fennoscandian geology well.

Lund (Sweden)

Works with the effects of glacial loading/unloading on the stresses in the crust; specifically in relation to earthquake motions. Works with relevant numerical modeling. Has local expertise, including regarding Swedish seismicity.

Reserves

McGarr (USA)

Has a similar profile to Dieterich but has had less exposure to the issues relevant for the specific questions to be addressed.

Slunga (Sweden)

Very knowledgable regarding seismology in general and specifically Fennoscandian seismicity.

Concluding remarks

In the view of the selection committee, the recommended panel shows a very satisfactory mixture of established competence in the questions to be addressed, experience in similar geological environments, and familiarity with local conditions.

While all the proposed experts considered had supplied information about their background and experience, the form, quantity and level of detail in this information varied. The panel suggests that explicit instructions on the form of information to be supplied could have enhanced the procedure.

Appendix 5

On the Probable Rate of Magnitude ≥6 Earthquakes Close to a Swedish Site During a Glacial Cycle

John Adams

Geological Survey of Canada

7 Observatory Crescent

Ottawa K1A 0Y3

Canada

jadams@nrcan.gc.ca

Revised version 13 July 2005

Background

This work was carried out as Adams' contribution to an international panel of experts convened by the Swedish Radiation Protection Authority (SSI). The purpose of the panel was to evaluate a methodology for estimating uncertain values through elicitation of expert judgment (Hora and Jensen, 2002). The values were not intended to be used in any hazard assessment for a repository. However, the questions were chosen to be interesting and challenging and have results potentially useful to future workers. Two questions were intended to be addressed, but 97% of the effort was spent on question #1. While the approach is considered sound, and the assumptions are stated for the most part, numbers in this report should be regarded as preliminary, given the short period of time allocated to the work. The Geological Survey of Canada was reimbursed for Adams' time and SSI paid all travel expenses to attend the two panel sessions.

Elicitation issue 1

"What will be the frequency of moment magnitude 6.0 or greater earthquakes per unit area (e.g. per 100 sq. km) in the middle and south of Sweden (Forsmark and Oskarshamn) during a glacial cycle (appr 100 000 a) assuming conditions similar to the Weichel glaciation? Give an uncertainty distribution for this quantity for each area."

A common set of references was distributed, and two common assumptions provided:

- the maximum moment magnitude of 7.6 (nominal value for Dehls' Pärve fault).
- a seismogenic thickness of 30 km"

Approach to Question 1

The hypothesis I used to establish the required distribution of rates is that the long-term seismicity rate in Sweden is the same as that of other Stable Craton Cores ("SCC") analyzed by Fenton at al. (2005), i.e. Sweden, like virtually all of the continental cores, is being squeezed by plate–boundary interactions and is deforming very slowly, chiefly through reverse faulting. The internal deformation rates are so slow they are below the threshold for direct determination using current GPS methods. I test the hypothesis by trying to reconcile both the low contemporary seismicity rate in Sweden, and the high seismicity rate that occurred immediately following deglaciation with the SCC rate. The reconciliation needs an assessment of the completeness of the information and then additional assumptions to process the results.

My model for explaining the burst of deglacial stress release is essentially that of Johnston (1989), that these earthquakes represent the rapid release of tectonic strain accumulated over tens of thousands of years while the weight of the icesheet inhibited reverse faulting. Johnston (1989, p. 596) foreshadowed the quantitative approach used here. The first-order model for cumulative rates is given in Figure 1a for a continent without glaciation and Figure 1b for a glaciated continent. Figure 1c shows a postulated history of earthquake rates, where the deficit relative to the SCC rate during glaciation and the surplus after are intended to match in deformation rate (but not necessarily in area, which on this plot represents seismicity rate). No earthquake strain release is allocated to the bending strains due to the ice load. However a certain modulation of the rates might be considered at the onset of the ice load, in a manner analogous to reservoir-induced seismicity where the bending effects of the load and

increased hydrostatic pressures trigger faults that were previously a considerable margin away from being unstable (Fig. 1d).

The lack of any earthquake strain release allocated to the bending strains due to the ice load is a highly unusual postulate. I defend this a worthwhile because

1. It could be abandoned if it proves implausible to reconcile the rates of deglacial earthquakes with other rates.
2. Symmetry requires that if the reverse fault slips during the deglacial earthquakes are due to the return of the crust to its "unbent" state, equivalent normal fault slips should have occurred during the onset of the icesheet load. One might plausibly argue that the evidence for these has been eroded away, but this appears not to be the case in northern Sweden where the cold-based icesheet preserved geomorphic features from the prior glaciation. Maps of the extent of wet-based icesheet in time and space would be very useful to judge the likely preservation of evidence in different parts of Sweden. ***Note:*** *The identification of even one large normal-slip fault in northern Sweden dating in the range 25-100 kyr and striking parallel to the ice margin would invalidate much of the following argument.*
3. Large regions of Canada with high contemporary unbending strains seem to have no earthquakes.
4. Mazzotti et al. (in prep.) compared current GPS and seismic deformation rates in eastern Canada with the predicted deformation modeled from postglacial rebound and concluded that the strength of the eastern North American lithosphere is large enough that the postglacial rebound deformation is accommodated almost entirely as elastic deformation of the upper crust and does not require brittle faulting.

Models that have been considered

Five models have been considered to make the estimates. It is not intended that every model be given the same weight, rather I am looking to see if consistency occurs among the estimates.

1. Rates from Worldwide Stable Craton Cores

1.1 Nature of the evidence

The evidence is the instrumental record of M>4.75 earthquakes in worldwide Stable Craton Cores.

1.2 Assumptions

- Sites of concern in Sweden have equivalent tectonic stability to those chosen by Fenton et al. (2005) to represent SCC stability
- There is no reason to exclude Australia, which accounts for nearly half of the worldwide earthquakes considered (rates would roughly be halved if Australia were to be excluded)
- The annual worldwide rate is 0.18 M≥6 per 50,700,000 km^2
- The upper bound for the SCC dataset was taken to be 7.0 (not 7.8 as for the other analyses) and it is assumed that the rate of M≥6 is not affected by this choice (however, the deformation rates will be – see discussion later on future work)

1.3 Analysis

The data fit the SCC magnitude-recurrence curve quite well for M>4¾, the assumed completeness level (Fig. 2). The annual rate of M≥6 per 31415 km^2 (100-km radius circle) is established fairly directly in Table 1 without consideration of the effects of icesheet load. Using the SCC data the standardized rate for the glacial cycle (100 000 years) would be 11. A separate entry in Table 1 shows the results for Australia. Using the Australian data the standardized rate for the glacial cycle would be 100. For comparison the standardized rate for a moderately-active continental zone, "Gatineau" (Adams and Halchuk, 2003), in eastern Canada is about 400.

1.4 Uncertainty in estimates

Judged by the data on Figure 2, the uncertainty in the rate of M≥6 events is quite small, a factor of 2 or less. However this only captures the aleatory (randomness) uncertainty, and there is almost certainly additional epistemic (model) uncertainty in the assumptions that should be considered.

2. Rates extrapolated from Swedish seismicity rates provided to the Panel

2.1 Nature of the evidence

The evidence is the instrumental record of Swedish earthquakes.

2.2 Assumptions

- The three source regions chosen by the panel represent the contemporary variability in earthquake rates in Sweden
- The catalog is complete for M≥3.0 since 1965 (at this level, the rates for 1965-1984 and 1985-2004 are about the same)
- The magnitude, M (where M is not **M**, which is another abbreviation for Mw), for the catalog values is directly equivalent to Mw (may not be true, see note below)
- For extrapolation from M=3 to M=6, a b-value equivalent to the worldwide SCC rate should be used instead of a calculated b-value.

2.3 Analysis

Rates were graphically extrapolated to larger magnitudes using the rate for M≥3, the worldwide SCC b-value, and a Mx of 7.0 (Fig. 3). This b-value was considered appropriate as the worldwide SCC data set is fairly populous and homogeneous in magnitude. b=0.8 is not the most extreme value, as the Australian dataset has b=0.67; however the value is a little smaller than b = 0.9 ± 0.03 I determined from Kagan's (1999) "universal β value" for the moment-magnitude frequency, using the assumption that the earthquake magnitude scales used are identical with the moment magnitude scale.

The standardized rates for an area of 31,415 km^2 for 100 kyr (equivalent to the glacial cycle considered) given in Table 1 are 62 for NE Sweden coast, 8 for SE Sweden, and 71 for SW Sweden. Note that in the contemporary eastern Canadian catalog the local magnitude overestimates Mw by about 0.4 units; if a similar bias exists in the Sweden local magnitude scale, each rate would be a factor of 3 lower (as is annotated on Fig 3).

Different rates for similar regions were given by LaPointe et al. (1999), as summarized in Table 1. The two rates for southern Sweden are a little lower than, but comparable to, other rates in Table 1, but the northern two rates are much lower. The rea-

son for their lower rates is their high b-values, 1.35 and 1.26, as given in table 4-1 of LaPointe et al. (1999). In my view, high b-values often represent inadequate data, or inconsistent magnitude scales, or both.

2.4 Uncertainty in estimates

The rates of M≥3.0 are somewhat uncertain, but this is a small part of the uncertainty due to the assumption that b=0.8. The use of alternative, yet still plausible, b-values could give rates for M≥6 that differ by an order of magnitude (see Fig. 8). The smaller values of b give the higher estimates (see section on future work).

3. Rates from Deglacial events in Northern Sweden

3.1 Nature of the evidence

The evidence is the record of postglacial faults discovered over the past 40 years in Lappland. The faults were overlooked during a century of geological mapping, but most were recognized as young scarps in 1960's and 1970's by their geomorphic characteristics: length continuity, consistent upthrown side, cross-cutting of young features, etc. While the list of smaller features is still being added to, it is plausible that most (if not all) of the larger faults in Lappland have been found. Confirming a postglacial fault involves identifying a potential geomorphic scarp, and then confirming its postglacial earthquake origin. Low, short or discontinuous scarps, resulting from small (M~6) earthquakes, can easily be overlooked, particularly if they follow old Precambrian structures.

3.2 Assumptions

- "deglacial" is used instead of "postglacial". Deglacial earthquakes occurred in the earliest part of postglacial times. "End-glacial" would be a synonym.
- The region of "big" deglacial faults in northern Norway/Sweden/Finland is termed "Lappland" (but a more extensive area than the Swedish province of the same name), and has an area of about 275,000 km^2 (450 km NW-SE x 625 km NE-SW)
- All the big deglacial faults in Lappland have been found and are as listed in Dehls et al. (2000)
- All the fault offsets represent single events which occurred circa 9000 yBP
- The time period represented by the faulting is 1000 years
- Moment magnitudes are as listed in Dehls et al. (2000)

- The largest listed event, Pärve (magnitude 7.6 according to Dehls, but note that others have estimated it to be as high as M8.2), represents the largest event that occurred (i.e. no larger fault has been missed).
- For maximum likelihood curve fitting, asymptotic to an assumed upper-bound magnitude, the appropriate upper-bound magnitude is 0.2 units above the value for the Pärve Fault (i.e., Mx=7.8)
- The size distribution of deglacial faults can be determined from the listed moment magnitudes and additional assumptions about the b-value
- Seismogenic crust thickness is taken to be 30 km
- The period of tectonic strain inhibition prior to the deglacial faulting episode is taken from Figure 10 of Lambeck (2005). I have used 42 kyr for Forsmark (but potentially it could be as long as 90 kyr); it is possible that the period was longer than 42 kyr in Lappland.

3.3 Analysis

Fig 4 shows the magnitude-frequency distribution of earthquakes in Lappland deduced from the reported deglacial faults. To plot the rates it has been assumed that all events occurred in a 1000-year time period, that is, the rate for the largest earthquake is taken to be 0.001 per annum, and the rates for the others follow.

Two fitted curves are shown, the first (green) is approximately a direct fit to the data, and the second (red) a fit to the data when the b-value is constrained to the worldwide SCC rate of 0.8, which is a fairly typical b-value. The first, unconstrained fit has a very low b-value, and if viewed in the context of worldwide earthquake populations might appear to represent "characteristic" earthquake behavior (i.e. situations where a plate-boundary fault ruptures in a few big earthquakes of similar size, but the rates of small earthquakes are much fewer than in the standard case). Such behavior is *possible* in Lappland, if the deglacial behavior is atypical of contemporary SCC seismicity. However, for this dataset it is believed instead that the data are incomplete at small magnitudes.

If the second fitted relationship is correct, there are many unidentified earthquakes less than magnitude ~7, shown by the gap between the rate of postglacial earthquakes (black dots) and the red curve. At M=6 this gap is about 36 (predicted) – 10 (actual) = 26 events for the cumulative plot. As the two curves agree at M7.0 we are missing 26 M6 (6<M<7) events and know of only 4, i.e. from neotectonic mapping we have so far found only $1/7^{th}$ of the expected number of events. It is not too surprising that magnitude ~6 events might be under-reported in the fault mapping because: 1) the scarps of M6 events can be subtle even in open ground, and hidden in vegetated land, and 2) not all magnitude 6 events (especially M6.0-6.2 earthquakes) need break surface. Fenton et al. (2005) estimate one in three M6 events would not break surface,

based on the size dimensions of M6 ruptures and a presumed-uniform distribution of earthquakes with depth in the 30-km-thick seismogenic crust.

In my opinion the second fit is the more likely; the first fit could be taken to be a lower bound. The only reason for an even lower rate would be if some faults in the Dehls et al. (2000) list are misidentified as deglacial faults and/or if the magnitudes of the events are overestimated. The latter seems unlikely, given that competing magnitudes for some of the events (e.g. Bungum et al., 2005) are larger, not smaller

Rates of M≥6 per 31415 km^2 (100-km radius circle) are established for the deglacial period in Table 1. If the deglacial events represent tectonic strain accumulated over the 42 kyr period when the icesheet inhibited earthquakes, then the standardized rate for the glacial cycle would be 10.

3.4 Uncertainty in estimates

A priori we do not know that b=0.8 is correct. However, the use of alternative, yet plausible b-values could give rates for M≥6 that differ by a factor of only 1.6 (see Fig. 8). In contrast to dataset 2, it is the larger values of b that give higher estimates (see section on future work).

4. Rates from Deglacial events in all of Sweden

4.1 Nature of the evidence

The evidence is the record of surface faulting used in section 3, greatly augmented by evidence of ground shaking due to large earthquakes. The additional types of evidence (some types more controversial than others) include landslides, rock deformation, sediment deformation, sediment liquefaction, turbidites, tsunamis, and varve deformation and varve turbidites (Morner, 2003, p. 304; Morner, 2004). The key evidence is the sedimentary record of shaking within the varved clay deposits. The varved sediments comprise tens to thousands of fairly regular annual layers, but also uncommon abnormal layers. Some of the abnormal layers appear to represent the result of earthquake shaking, chiefly deformed layers, liquefied sediments and unusually thick layers interpreted as earthquake-triggered turbidity currents (or the result of tsunamis). Individual exposures of varved sediments may contain the sedimentary record of several episodes of earthquake shaking occurring a few years to a few hundred years apart. By correlation of thickness and other sedimentary characteristics DeGeer built up a master chronology of varve sedimentation for Sweden. By relating the sequences of varves in individual exposures to each other and to the master chronology it is possible to show that an abnormal sedimentation event in one exposure happened at the same time (to within 1 year) of an abnormal event in another exposure. By extending the method to many outcrops Morner and workers have shown that a given abnormal layer occurred at the same time in many different places; this evidence is then most simply explained as due to a single event, an earthquake. The extent of the area disturbed is related to the size of the earthquake, and the location of the area affected gives an indication of where the earthquake occurred. The importance of the earthquakes recorded in the varved sediments is that several events close in time can be distinguished from each other (difficult if not impossible to do from the deglacial fault scarps), the date of the event can be determined, and the size of the earthquake can be estimated, all without needing to identify the causative fault. Morner supports the evidence from the varved sequences with additional types of evidence, arguing that the coincident timing and areal extent of these features is additional support for their earthquake origin.

4.2 Assumptions

- The region considered is termed "Sweden", and has an area of 500,000 (rounded from 450,000 km^2 for convenience, and to accommodate some underwater faults). The region encompases the shaded area on Morner's map (2003, p. 302).
- The earthquakes are as listed in Table 2 of Morner (2003) page 306-307.
- All the entries dating to older than 7999 yrBP represent single events which occurred "soon" after deglaciation (note: the catalogue may contain duplicates, if some dates were mis-determined, ie. the correct varve correlations between sites were not made)

- The time period represented by the faulting is 1000 years, but that window is diachronous (i.e. 12,000-11,000 in southern Sweden, 9500-8500 in northern Sweden)
- Morner's magnitude classes have the following numerical equivalents in order to plot them: ">>8" = 8.2, >8 = 8.0, >7 = 7.3, ~7 = 7.0, 6-7 = 6.6, >6 = 6.3, ~6 = 6.0, the rest plotted at 5.0. The largest events are not inconsistent with the upper estimate on the magnitude of the Pärve (M8.2). For consistency with Lappland analysis, a second plot with the assigned magnitudes reduced by 0.6 units (i.e., 8.2 minus 7.6) was made.
- For curve fitting, the appropriate upper-bound magnitude is 0.2 units above the value for the largest magnitude class
- The size distribution of earthquakes can be determined from the listed magnitudes and additional assumptions about the b-value
- The period of tectonic strain inhibition represented by the deglacial faulting episode is taken from Figure 10 of Lambeck (unpub., 2005). The average of 42 kyr for Forsmark (but potentially it could be as long as 90 kyr) and 30 kyr for Oskarshamn was used, 36 kyr.

4.3 Analysis

Fig 5 shows the magnitude-frequency distribution of earthquakes in Sweden deduced from Morner's reported paleoseismic events older than 7999 yrBP. To plot the dots it has been assumed that all events occurred in a 1000-year time period, that is, the rate for the largest earthquake is taken to be 0.001 per annum, and the rates for the others follow.

Two fitted curves are shown, the first (green) is approximately a direct fit to the data, and the second (red) a fit to the data with a b-value constrained to the worldwide SCC rate of 0.8, which is a fairly typical b-value. The unconstrained fit has a very low b-value, like a "characteristic" earthquake behavior. However, for this dataset it is believed that the data are incomplete at small magnitudes.

If the second fitted relationship is correct, there are many unidentified earthquakes less than magnitude ~7½ (gap between the rate of postglacial earthquakes (black dots) and the red curve). At M=6 this gap is about 200 (predicted) – 34 (actual) = 166 events. Hence we are missing about 166 events, and have so far found only $1/6^{th}$ of the expected number of events, more-or-less the same fraction as for the Lappland analysis. It is not too surprising that magnitude ~6 events might be somewhat underreported in the Morner paleoseismic record because despite the areal extent of his sites across Sweden some areas large enough to contain the strong shaking from M6 events might not have been sampled.

Figure 6 shows the effect of reducing Morner's magnitude estimates by 0.6 units. This is a convenient speculative reduction, based on 1) the size of the largest identified deglacial earthquake (Pärve Fault) being taken as M7.6 for consistency with the Lappland analysis, and 2) the sense that magnitudes of continental earthquakes are often over-estimated (relative to plate boundary events) because the efficient propagation of energy in the shield rocks leads to very large areas of strong shaking effects (New Madrid, U.S.A. is a classic example). The unidentified-earthquake analysis is then as follows. At M=6 the gap is about 80 (predicted) – 28 (actual) = 52 events. Hence we are missing about 50 events, and have so far found only 1/3 of the expected number of events. This estimate of under-reporting of events in the Morner paleoseismic record is less extreme than the preceding analysis and is probably more consistent with the lower level of effort needed to spot earthquakes from shaking evidence, instead of needing to find a fault scarp.

Rates of M≥6 per 31415 km^2 (100-km radius circle) are established for the 1000-year deglacial period in Table 1. If the deglacial events represent tectonic strain accumulated over the (average for Sweden) 36 kyr period when the icesheet inhibited earthquakes the standardized rate for the glacial cycle would be 35 (taking Morner's magnitudes) to 14 (using reduced magnitudes).

4.4 Uncertainty in estimates

Without reviewing the evidence for each earthquake in Morner's catalog in detail, it is difficult to assess the uncertainty in the above estimates.

5. Rates from post-deglacial events in all of Sweden

5.1 Nature of the evidence

The evidence is similar to that in section 4, except that only the post-7999 yBP events are used.

5.2 Assumptions

- The region considered is termed "Sweden", and has an area of 500,000 (rounded from 450,000 km^2 for convenience, and to accommodate some underwater faults). The region encompases the shaded area on Morner's map (2003, p. 302).
- The earthquakes are as listed in Table 2 of Morner (2003) page 306-307.
- All the entries dating to younger than 7999 yrBP represent single events unrelated to deglaciation (note: the catalogue may contain duplicates, if some dates were mis-determined, ie. the correct varve correlations between sites were not made)

- The time period represented by the faulting is 9000 years (approximate conversion from radiocarbon years to calibrated years).
- Morner's magnitude classes have the following numerical equivalents in order to plot them: ">>8" = 8.2, >8 = 8.0, >7 = 7.3, ~7 = 7.0, 6-7 = 6.6, >6 = 6.3, ~6 = 6.0, the rest plotted at 5.0. The largest events are not inconsistent with the upper estimate on the magnitude of the Pärve (M8.2). For consistency with Lappland analysis, a second calculation with the assigned magnitudes reduced by 0.6 units (i.e., 8.2 minus 7.6) was made.
- For curve fitting, the appropriate upper-bound magnitude is 0.2 units above the value for the largest magnitude class
- The size distribution of earthquakes can be determined from the listed magnitudes and additional assumptions about the b-value

5.3 Analysis

Figure 7 shows the magnitude-frequency distribution of earthquakes in Sweden deduced from Morner's reported paleoseismic events younger than 7999 yrBP. To plot the dots it has been assumed that all events occurred in a 9000-year time period, that is, the rate for the largest earthquake is taken to be 0.00011 per annum, and the rates for the others follow.

Instead of repeating the analyses in section 4, I note that the rate of the post-deglacial earthquakes (red dots) is approximately $1/15^{th}$ the rate of the deglacial earthquakes (black dots). Therefore I use the rates from section 4 reduced by a factor of 15. Comments on the completeness of the data, etc would be proportionately similar.

Rates of $M \geq 6$ per 31415 km^2 (100-km radius circle) are established for the 9000-year post-deglacial period in Table 1. The standardized rate for the glacial cycle would be 84 (taking Morner's magnitudes) to 34 (using reduced magnitudes). These rates may be a little on the high side if the period around 7000-7999 yBP included some residual deglacial events.

5.4 Uncertainty in estimates

Without reviewing the evidence for each earthquake in Morner's catalog in detail, it is difficult to assess the uncertainty in the above estimates.

Conclusions

In my view, the agreement between the Lappland and Sweden deglacial rates is good and argues that Morner's work should be given more credence in future assessments. Determining paleoearthquakes from shaking evidence such as sediment disturbance is a valid technique, and although it is less direct than mapping a fault scarp it can probably identify more earthquakes and with lower effort. However the evidence needs to be closely scrutinized, as for example was done for potential postglacial faults in Norway during the NEONOR project.

The processed standardized deglacial rates, 10 from Lappland and 14 from Sweden, are very similar to the average SCC rate of 11. Thus the hypothesis that the deglacial events represent the rapid release of accumulated tectonic deformation of the Fennoscandian shield (rather than being dominated by unbending earthquakes) is not rejected. Indeed if we accept the hypothesis, the deglacial rates could provide a good (since the time period is longer, ~40,000 years) estimate of the long-term tectonic deformation of the Fennoscandian shield.

There is room in the uncertainty for unbending earthquakes, but they are not required for the reconciliation. Unbending earthquakes summing to ten times the SCC rate are probably excluded, but unbending earthquakes summing to 1-2 times the SCC rate are probably not.

Contemporary seismicity rates *may* be similar to both the deglacial-derived and SCC rates, but in the analysis presented here are higher and in SKB's analysis lower. Additional work on the magnitude scale and appropriate b-values is warranted. Uncertainties are likely to remain large unless the b-value can be constrained.

On the basis of the hypothesis proposed, there would be no difference between the Forsmark and Oskarshamn sites over a glacial cycle (though the shorter duration of glacial load inhibition for Oskarshamn would argue that the deglacial burst of activity would have been less intense there).

The study requested five parameters to describe my assessment of the distribution, they are as follows:

Parameter	Standardized rate *	Comments
Upper limit	200	Sweden is more similar to Australian SCC and/or significant bending earthquakes occur; Sweden is only half as active as Canadian source zone "Gatineau"
Upper quartile	45	halfway in log-space between 10 and 200
Best estimate	12	From SCC, Lappland and Sweden deglacial rates
Lower quartile	3	halfway in log-space between 1 and 10
Lower limit	0	Site is more stable than average, or statistical chance that if the correct value is 12, no events could happen

* Standardized rate is the rate of M≥6 earthquakes within 100 km distance over a period of 100,000 years

Four suggestions for future work

The analysis here is based on earthquake rates, primarily earthquake rates greater than 6. This may be the correct approach in the context of the long-term safety of a waste repository, but it relies heavily on the b-value and choosing the correct size-distribution model for the largest earthquakes. In regard to the b-value adopted, note the opposite consequences of different b-values used for the extrapolation of common small earthquakes to predict the rate of M~6 earthquakes and for the extrapolation of extremely-rare large deglacial faults to predict the rate of M~6 earthquakes (Fig. 8). In regard to the size-distribution model adopted, an especial concern might be whether the conditions at the time of deglaciation promoted cascading fault-to-fault ruptures so that single magnitude 7 events happened, instead of three to thirty individual magnitude 6 events spread out in both space and time. Those two scenarios might have different implications for vault stability.

A parallel analysis should be undertaken in terms of the deformation rate, obtained by integrating the magnitude-recurrence relationship. As noted in the discussion of Figure 1, the matching between the accumulation during the glaciation and the release immediately afterwards should be done in terms of the deformation, not the number of earthquakes. This integration is very sensitive to the upper-bound magnitude chosen, however. A spreadsheet calculation for Lappland using the SCC rates and following the method of Mazzotti and Adams (in press) which can incorporate a wide range of uncertainties into the analysis and allows easy testing of the sensitivity to various pa-

rameter choices is illustrated on Figure. 9. The median deformation rate across Sweden is 0.04 mm/yr using Mx=7.8 for consistency with the deglacial analysis, interpreted as shortening normal to the Norwegian margin. If Mx=7.0 is taken, as for the SCC analysis of Fenton et al. (2005), the rate is 0.012 mm/yr. If Mx=8.2 is taken, as for the upper estimates of the Pärve Fault, the rate is 0.08 mm/yr. Thus the SCC (and the similar Swedish) rates suggest geological shortening at 10-80 m per million years.

Morner's 2003 table of Swedish paleoearthquakes should be analyzed more rigorously, both in terms of re-assessing the evidence for each event and its likely magnitude, and then reanalyzing the events in terms of those that are deglacial separate from those that represent post-deglacial or "normal SCC" activity, together with analyzing northern and southern Sweden separately.

The existence of recognized postglacial fault scarps in Lappland but their absence in southern Sweden is a continuing puzzle that needs to be addressed. Some have considered that the tectonic environments in northern and southern Sweden were different, such that large deglacial earthquakes did not happen in the south. Others, including Morner, see evidence for large deglacial earthquakes in southern Sweden, but are unable to finger the fault scarps in a way that would convince the sceptics. Morner has proposed that both regions had deglacial earthquakes. Based on the areas of strongest shaking being centred near the ice front and the presence of large amounts of angular rock debris he suggests that the fault scarps produced in the south were just inside the ice margin and were destroyed by outward movement of the ice even as the ice front was melting back. Fault scarps produced in the north were just outside the ice margin and were preserved. Morner's model should be testable by determining the timing of stress changes relative to ice front position implied, as is possible with recent detailed models of icesheet history (e.g. by Lambeck) for northern and southern Sweden. Conditions that would promote the deglacial earthquakes to occur inside the ice sheet would be rapid thinning (to reduce the load) of the icesheet without rapid melt-back of the ice front.

Elicitation issue 2

> "Given a magnitude 6.0, and 8.0 earthquake occurring at a point 10 km from a repository in a granitic type of rock, give an uncertainty distribution for the maximum displacement (slip or shear) in an ex-

isting fracture in the repository (/a disc of 1 sq. km x 50 m ?/). Your uncertainty distribution should include the possibility that no displacement occurs within the repository."

Possible Approach to Question 2

The phrasing of this question suggests an empirical approach, rather than a rock mechanics approach. If the disc is taken to be 1 km in diameter and it is variously tried with different amounts of slip (the amounts of slip have to be a plausible fraction of the diameter), then the slip event can be characterized as an earthquake of magnitude m. The empirical question can then be phrased in terms of aftershock studies as "what is the probability that an aftershock of magnitude m will occur x km from the rupture plane of an earthquake of magnitude M". In answering the question, there would need to be a careful selection of datasets, in terms of the appropriateness of the rock type and the quality of the aftershock locations. The benefit of phrasing the question in this way is that once the empirical relation is found it can be used as in a hazard calculation viz to give the total probability of a slip event of magnitude m (i.e. displacement d) given all M at all distances x.

Acknowledgements

Stephen Halchuk assisted with fitting the magnitude-recurrence relations and reviewing the text for clarity, and Stephane Mazzotti provided the deformation spreadsheet. Feedback from the panel experts and conveners is appreciated.

References

Bungum, H., Lindholm, C., and Faleide, J.J., 2005. Postglacial seismicity offshore mid-Norway with emphasis on spatio-temporal-magnitudal variations. Marine Geology, 22:137-148.

Dehls, J.F., Olesen, O., Bungum, H., Hicks, E.C., Lindholm, C.D.& Riis, F., 2000. Neotectonic map: Norway and adjacent areas. Geological Survey of Norway, Trondheim.

Clark H. Fenton, C.H., Adams, J., and Stephen Halchuk, S., 2005. Seismic Hazards Assessment for Radioactive Waste Disposal Sites in Regions of Low Seismic Activity. Geotechnical and Geological Engineering (to appear)

Hora, S., and Jensen, M., 2002. Expert judgement elicitation. Swedish Radiation Protection Authority (SSI) Report 2002:19, 12 pp.

Johnston, A.C., 1989. The effect of large ice sheets on earthquake genesis. in Gregersen, S., and Basham, P.W., (eds) Earthquakes at North Atlantic Passive Margins: Neotectonics and Postglacial Rebound, p. 581-599. Kluwer Academic Publishers, Dordrecht 1989.

Kagan, Y.Y., 1999. Universality of the seismic moment-frequency relation. Pure and Applied Geophysics, 155:537-573.

Lambeck, K., 2005. Glacial load stresses. Note for SSI, Stockholm, May 2005, 20 pp.

LaPointe, P.R., Cladouhos, T., and Follin, S., 1999. Calculation of displacement on fractures intersecting canisters induced by earthquakes: Aberg, Beberg and Ceberg examples. SKB Report TR-99-03 103 pp.

Mazzotti, S. and Adams, J. (2005). Rates and uncertainties on seismic moment and deformation in eastern Canada. In press, Journal of Geophysical Research.

Mazzotti, S., James, T.S., Henton, J., and Adams, J., (in preparation). GPS Crustal Strain, Postglacial rebound, and seismic hazard in eastern North America: the St Lawrence valley example. Revised after review, Journal of Geophysical Research.

Morner, N-A., 2003. Paleosemicity of Sweden – a novel approach. Nils-Axel Morner, see http://www.pog.su.se/04public/public.htm, Stockholm, 320 pages.

Morner, N-A., 2004. Active faults and paleoseismicity in Fennoscandia, especially Sweden. Primary structures and secondary effects. Tectonophysics 380:139-157.

Table 1 Comparative estimates of standardized rate

Model	Source	Region	Area (square km)	Figure number	a	b	Upper-bound magnitude,Mx	Time span (years)	Rate M≥6 off the graph (per annum)	Rate of M≥6 per million square km per kyr	Rate per 31415 square km per kyr	Length of glacial load inhibition, kyr	Rate M≥6 per 31415 square km per 100 kyr	Useable for distribution estimate?
1	Stable Craton Core seismicity (Fenton et al., 2005)	Worldwide	50700000	Figure 2	4.1	0.80	7.0	40-100	0.18	3.6	0.1	0	11	yes
	Stable Craton Core seismicity (Fenton et al., 2005)	Australia	3500000		-	0.67	7.0	40-100	0.11	31.4	1.0	0	99	high
	Adams and Halchuk (2003), moderate activity zone, Canada	Gatineau	32300		3.1	0.90		40-100	0.004	123.8	3.9	0	389	high
2	Panel Area NE, 40 yrs for M>3	Swedish coast	152625	Figure 3		0.80		40	0.003	19.7	0.6	0	62	yes
	Panel Area SE, 40 yrs for M>3	SE Sweden	117800	Figure 3		0.80		40	0.0003	2.5	0.1	0	8	yes
	Panel Area SW, 40 yrs for M>3	SW Sweden	88000	Figure 3		0.80		40	0.002	22.7	0.7	0	71	perhaps
	Seismicity (SKB TR-99-03)	Southern Sweden	145000			1.04						0	7	yes
	Seismicity (SKB TR-99-03)	Lake Vanern	77000			0.98						0	16	yes
	Seismicity (SKB TR-99-03)	Gulf of Bothnia	186000			1.26						0	1	minimum
	Seismicity (SKB TR-99-03)	Northern Sweden	375000			1.35						0	1	minimum
3	Deglacial faults (Dehls et al. 2000), free-fit	Northern Sweden	275000	Figure 4	-0.2	0.06	7.8	1000	0.01	36.4	1.1	42	3	minimum
	Deglacial faults (Dehls et al. 2000), constrained slope	Northern Sweden	275000	Figure 4	3.4	0.80	7.8	1000	0.036	130.9	4.1	42	10	yes
4	Deglacial earthquakes (Morner, 2003) pre-7999 events, free-fit	Sweden	500000	Figure 5	0.7	0.35	8.4	1000	0.035	70.0	2.2	36	6	minimum
	Deglacial earthquakes (Morner, 2003) pre-7999 events, constrained slope	Sweden	500000	Figure 5	4.1	0.80	8.4	1000	0.2	400.0	12.6	36	35	perhaps
	Deglacial earthquakes (Morner, 2003) pre-7999 events, constrained slope, magnitudes adjusted down 0.6 units	Sweden	500000	Figure 6	3.7	0.80	7.8	1000	0.08	160.0	5.0	36	14	yes
5	Post-Deglacial earthquakes (Morner, 2003), free-fit	Sweden	500000	Figure 7	-	-	8.4	9000	0.002	4.7	0.1	0	15	minimum?
	Post-Deglacial Earthquakes (Morner, 2003), constrained slope	Sweden	500000		-	0.80	8.4	9000	0.013	26.7	0.8	0	84	high?
	Post-Deglacial Earthquakes (Morner, 2003), constrained slope, magnitudes minus 0.6	Sweden	500000		-	0.80	7.8	9000	0.005	10.7	0.3	0	34	yes

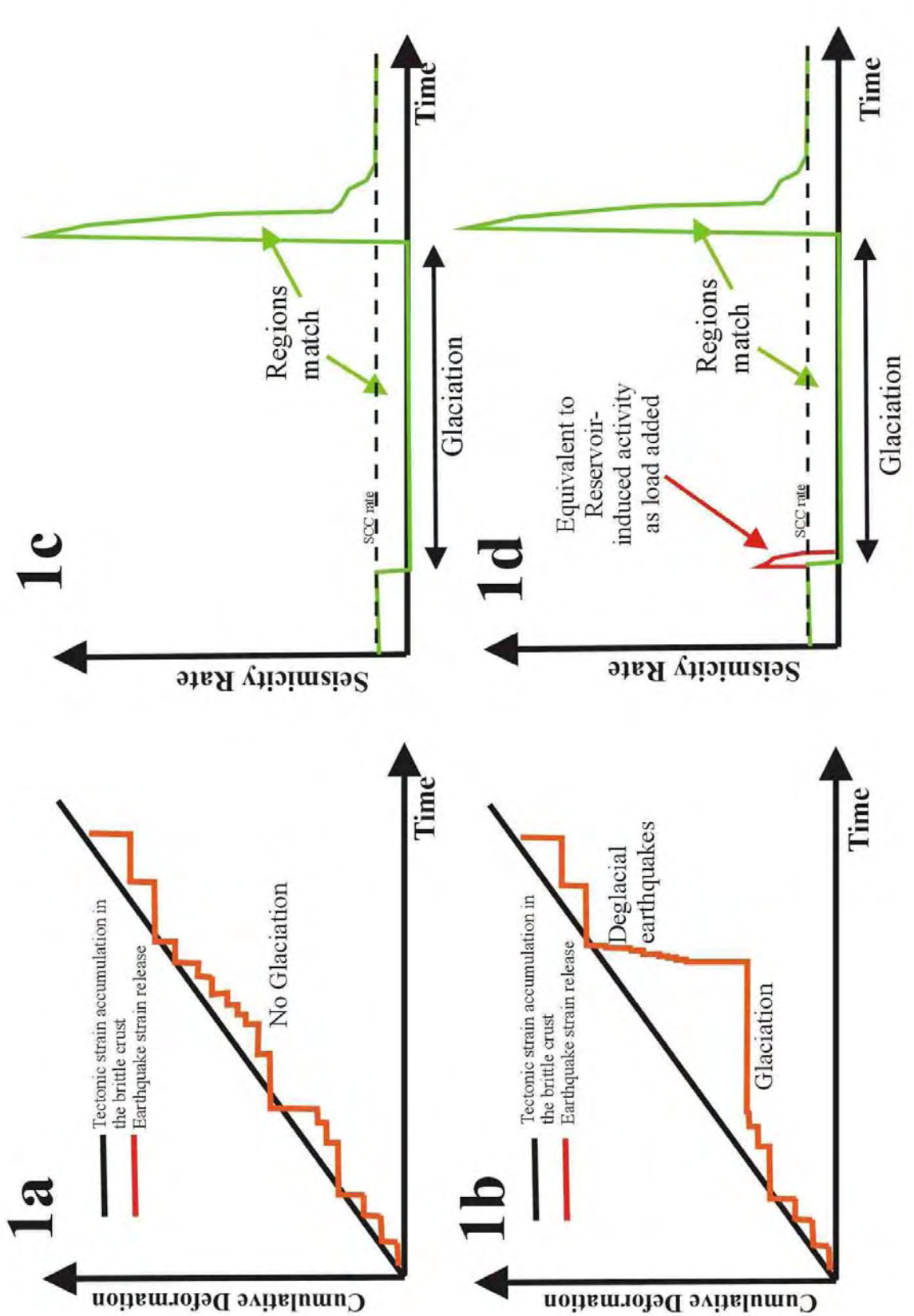

Figure 1. Cartoon representation of concepts used.

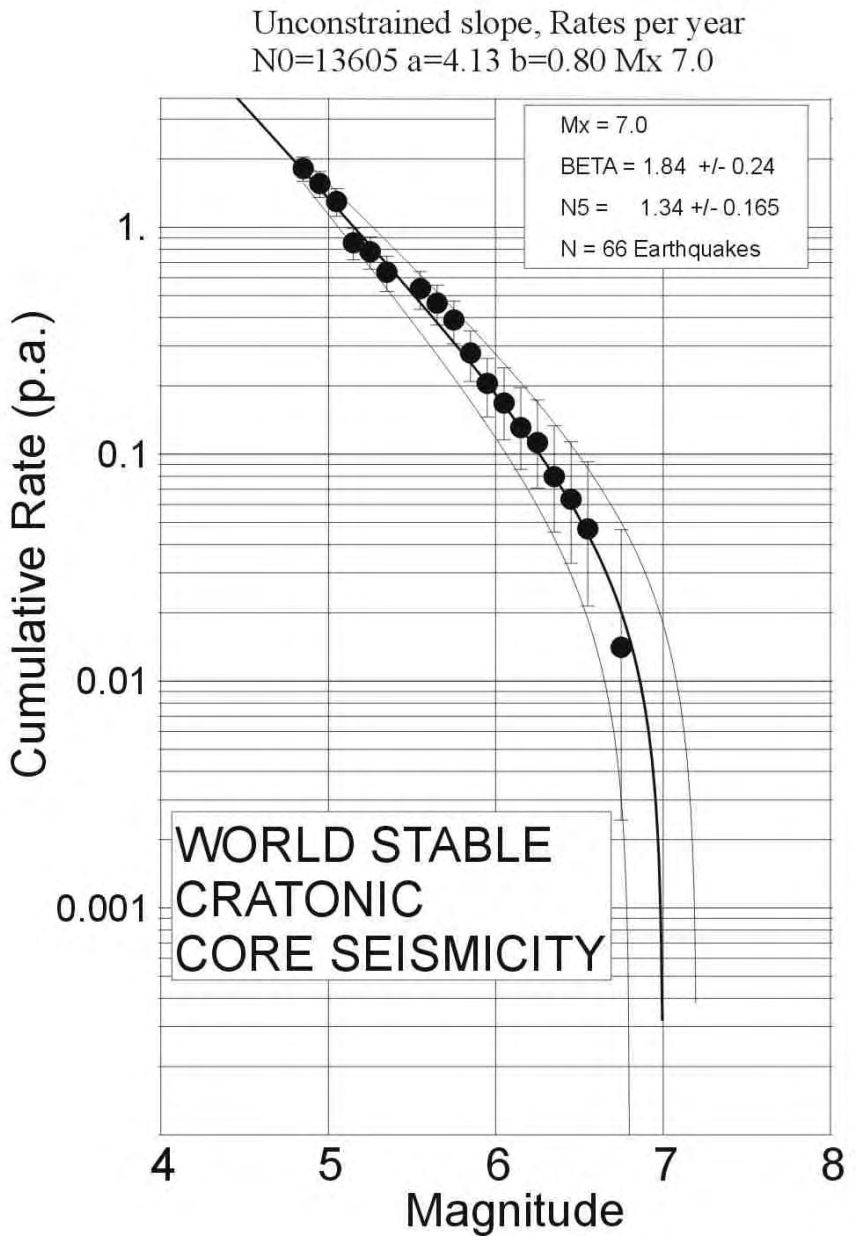

Figure 2. Magnitude-frequency curve for the worldwide Stable Craton Core seismicity (from Fenton et al., 2005)

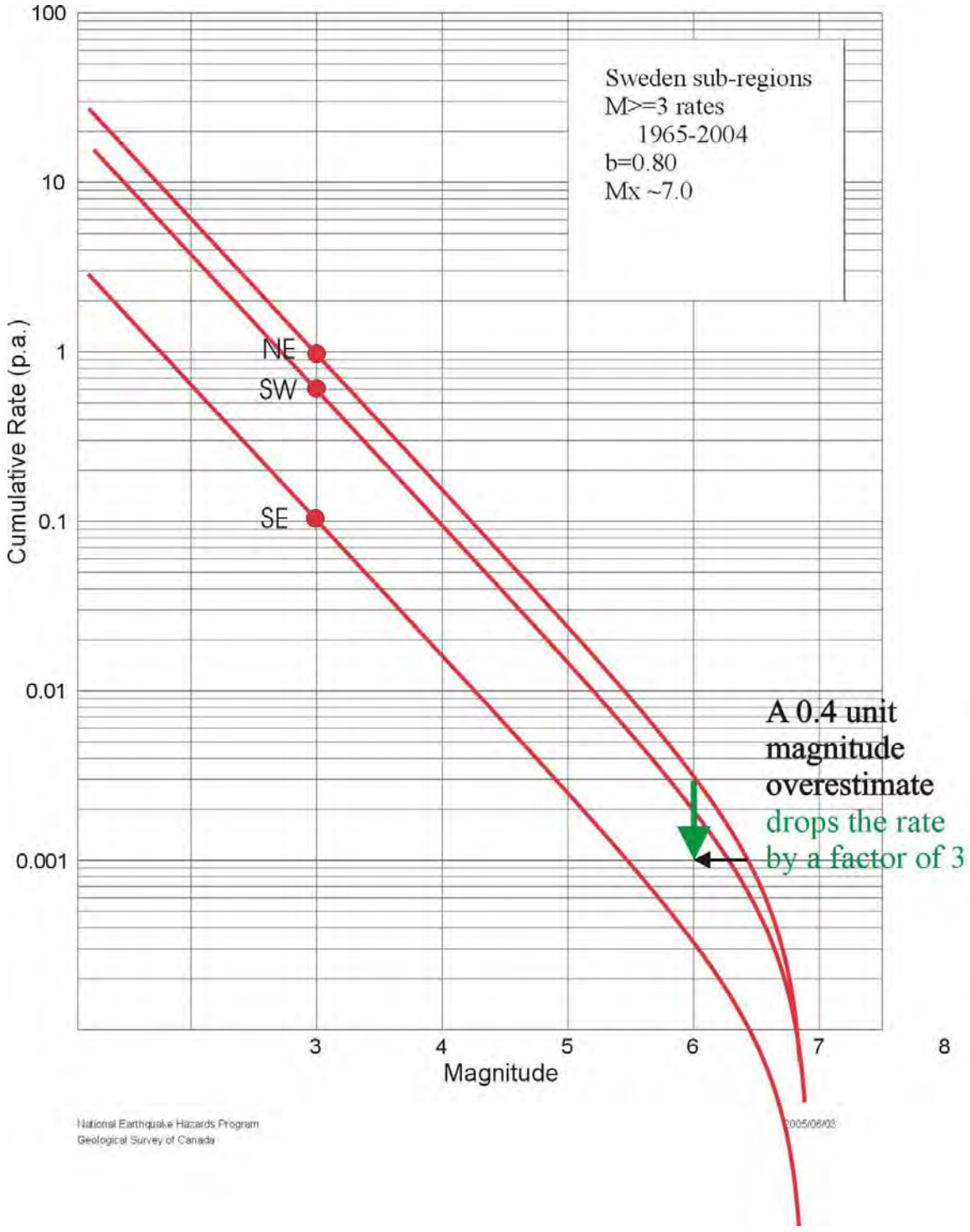

Figure 3. Magnitude-frequency curves for three subsets of Swedish seismicity, 1965-2004

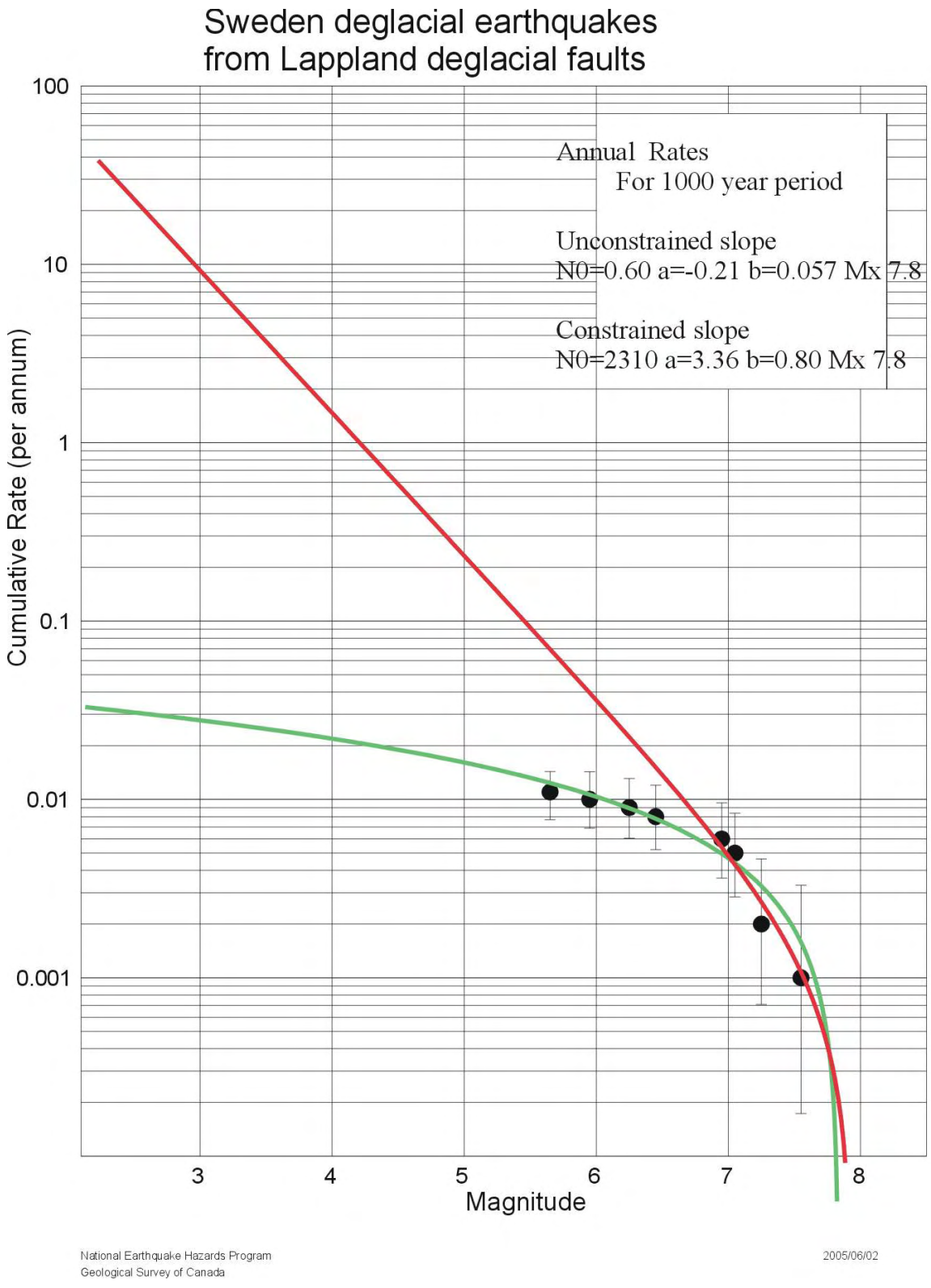

Figure 4. Magnitude-frequency curves for deglacial faults in Lappland (data from Dehls et al., 2000)

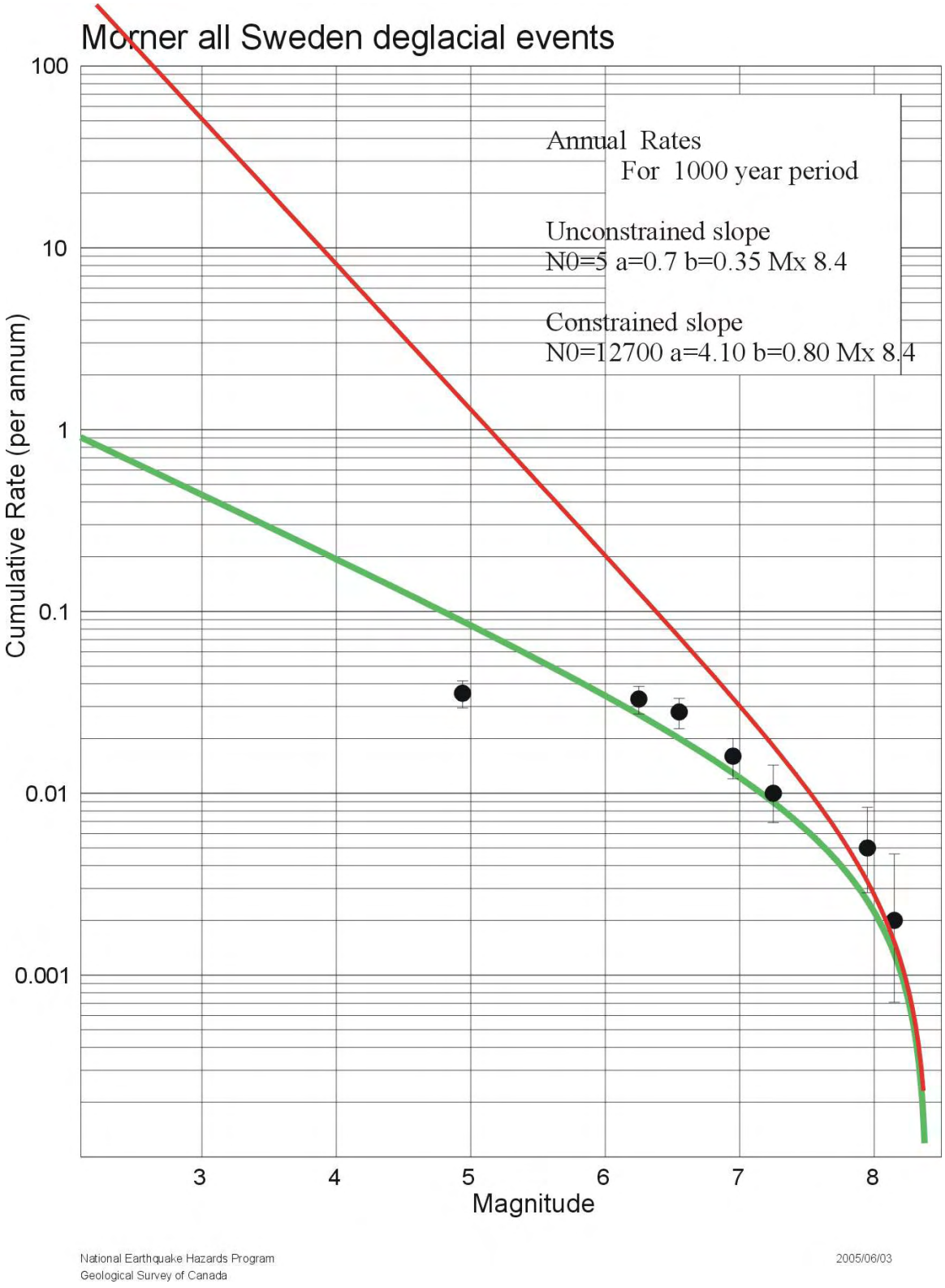

Figure 5. Magnitude-frequency curves for deglacial faults in Sweden (data from Morner, 2003)

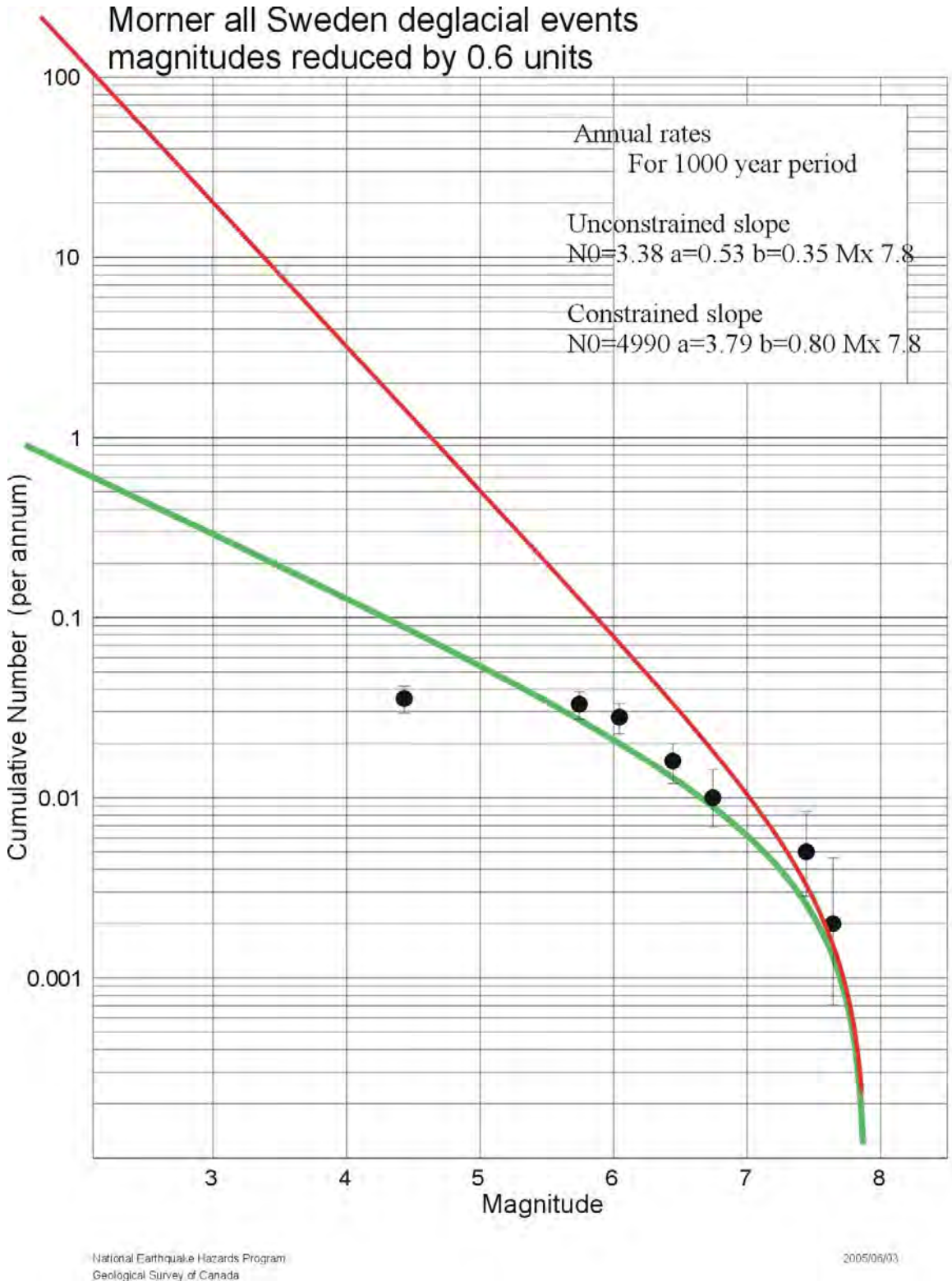

Figure 6. Magnitude-frequency curves for deglacial faults in Sweden after reducing the magnitudes by 0.6 units (otherwise, same data as Fig.5)

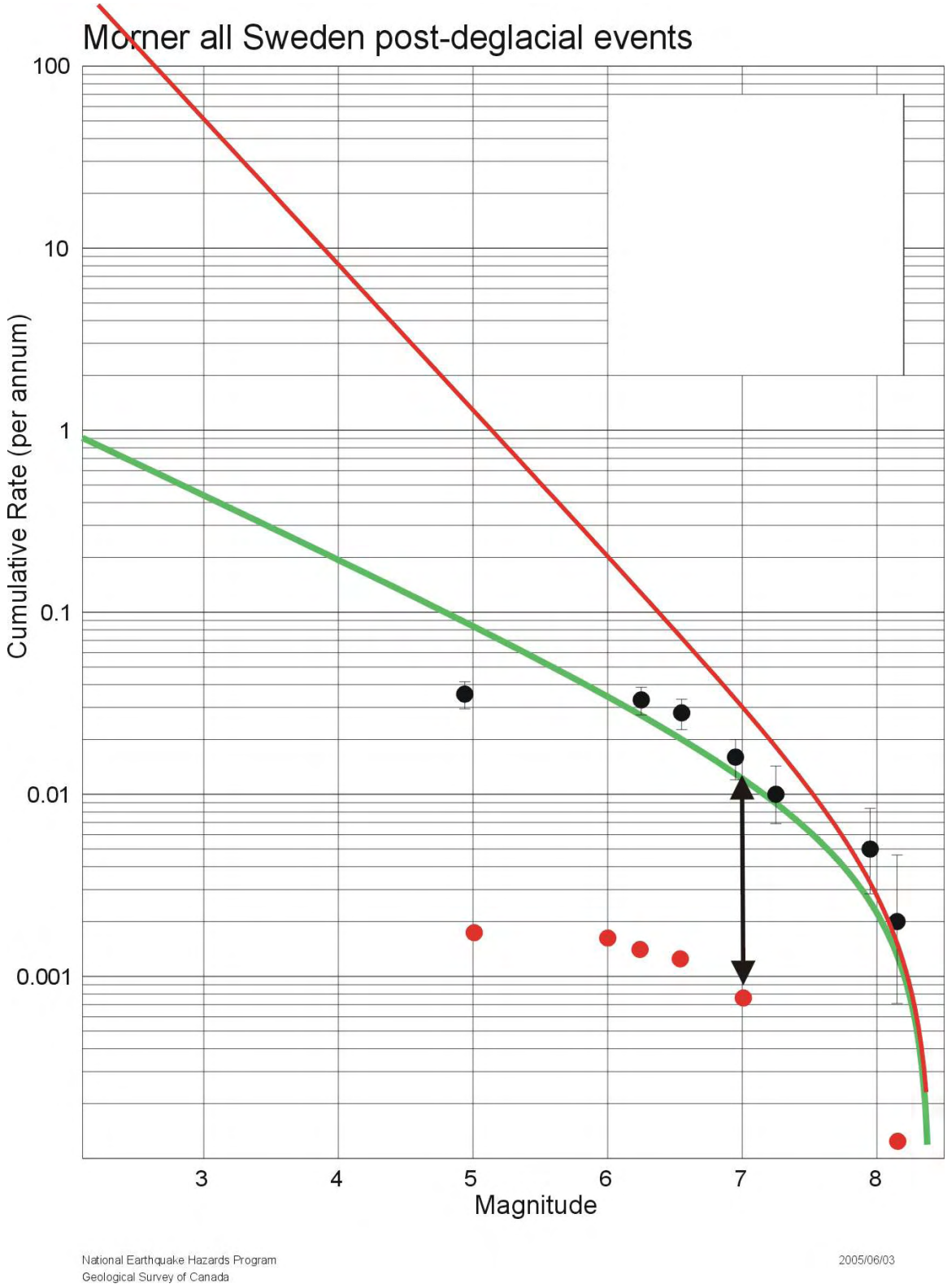

Figure 7. Magnitude-frequency values (red dots) for post-deglacial faults in Sweden. Double-ended arrow shows factor of 15 lower rate relative to Figure 5.

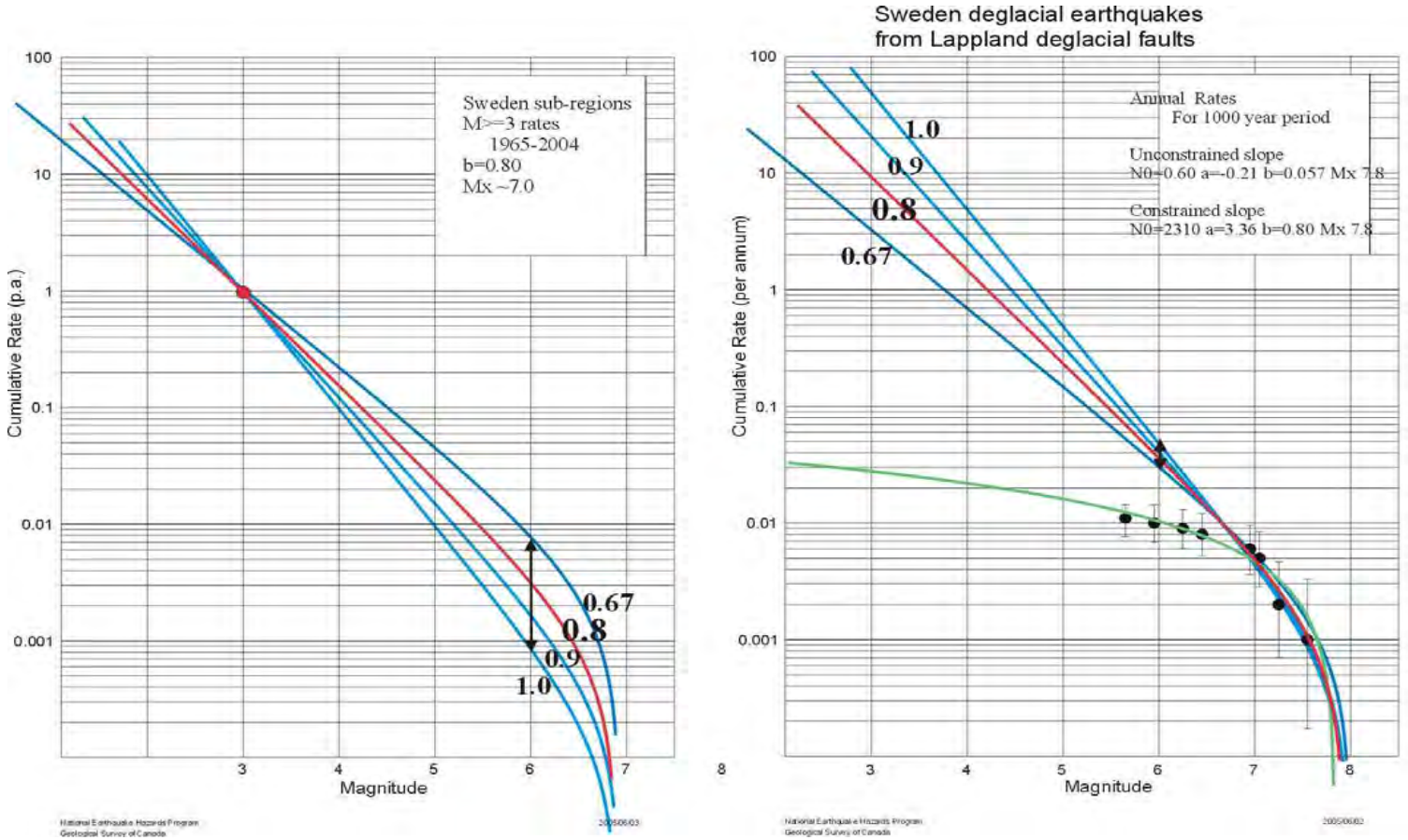

Figure 8. Extrapolations of Sweden seismicity data for the NE region (from Fig. 3) and deglacial earthquake data (from Fig. 4) together with b-values alternative to b=0.8 fitted to the data. Note the relatively large errors at M=6 from the current seismicity extrapolation, and also that the b-values producing the larger estimates differ between the extrapolations.

Figure 9. Spreadsheet showing calculation of deformation rate from the SCC magnitude-frequency curve.

Appendix 6

SSI Elicitation Report

Earthquakes in SE Sweden during a new glacial cycle

Hilmar Bungum

NORSAR

June 20, 2005

Introduction

The present report summarizes my response to two specific questions from SSI during an elicitation process involving five experts that met with SSI (Swedish Radiation Protection Agency) for a two-day meeting in Stockholm May 17-18, 2005. SSI's purpose with the meeting was to present the elicitation methodology and to discuss the questions with the experts.

The elicitation questions are as follows:

(1) What will be the frequency of moment magnitude 6.0 or greater earthquakes per unit area (e.g. per 100 sq. km) in the middle and south of Sweden (Forsmark and Oskarshamn) during a glacial cycle (appr. 100 000 a) assuming conditions similar to the Weichel glaciation? Give an uncertainty distribution for this quantity for each area. Assume a maximum moment magnitude of 7.6 and a seismogenic thickness of 30 km.

(2) Given a magnitude 6.0, and 8.0 earthquake occurring at a point 10 km from a repository in a granitic type of rock, give an uncertainty distribution for the maximum displacement (slip or shear) in an existing fracture in the repository (a disc of 1 km^2 x 50 m?). Your uncertainty distribution should include the possibility that no displacement occurs within the repository.

Besides the meetings in Stockholm, five working days have been allocated for answering these questions, which is supposed to be based on available data and studies and not to imply any independent research work. The report includes first a discussion of possible approaches and methodologies, followed by justified answers, with uncertainty bounds.

It has been indicated from SSI that Question 1 is the most important one and that Question 2 may be covered less thoroughly.

Approaches and models, Question 1

There is a fundamental difference between the two elicitation questions in that the first one is asking for a prediction of the occurrence of earthquake during the next 100,000 years, which most likely will another glaciation cycle, whereas the second one is addressing the estimation of maximum displacement from given magnitude earthquakes at a distance of 10 km from a repository, irrespective of time.

There are three different approaches to this question that need to be considered in terms of what one could base the desired predictions on:

1. Modeling the stress effects related to a new glacial cycle, based on calibrated assumptions;
2. Contemporary seismotectonics, adjusted with assumed additional stress effects from a new glaciation;
3. Postglacial seismicity: What happened during the last glacial cycle, documented essentially through the mapped postglacial earthquakes.

The final model will potentially be determined based on a combination of these approaches, and I will discuss them all in the following.

1. Modeling stress effects

The modelling of glaciation cycles and associated rebound patterns and stress effects are now in a mature state, the theories are well established, the boundary conditions are well understood and the models are well calibrated empirically (Lambeck and Purcell, 2003; Lambeck, 2005). Even so, a quantitative description of the deglaciation process and its relation to fault stability has been rather elusive (Lund, 2005). There are reasons to believe that this in part is related to the fact that the Fennoscandian crust is subjected to a large number of simultaneously acting sources of stress and that the nature and distribution of weakness zones is similarly complex (Byrkjeland et al., 2000; Bungum et al., 2005).

In a specific study of the continental margin region of western Norway, Lambeck and Purcell (2002) have concluded that they find no evidence from their modeling that the crust is currently unstable as a result of past glacial action. Other studies (Hicks et al., 2000; Bungum et al., 2005) have indicated, however, based essentially on stress inferred from earthquake fault plane solutions combined with the occurrence pattern, that a region that includes the coastal parts of northern Norway still may be influenced by flexural effects from the postglacial rebound, in contrast to other regions.

Lambeck (2005) has for the purpose of this project made a numerical analysis of glacial load stresses for Forsmark and Oskarshamn, in part similar to an earlier study for Finland (Lambeck and Purcell, 2003). The study is making a very sensible assumption with respect to future glaciation cycles, namely that they will be similar to past cycles, which means that the last interglacial at 130,000 to 120,000 years ago is equated with the present interglacial, or the Holocene.

Figs. 1 and 2 are both from the Lambeck and Purcell (2005) report, where the former is showing the deviatoric stress components at the two sites and the latter is showing the change in Fault Stability Margin (ΔFSM) predicted for a depth of 5 km, indicating the styles of preferred faulting should failure occur. The model assumes an in-plane stress state of (-10,0) MPa and an azimuth of the ridge push axis of 45°W. I interpret the results from this study as follows:

1. The deviatoric stress during a glaciation cycle is highly sensitive to the character of the ice margin movements (partly because the stress at a given site is not only determined from the load right above that site), and since the details here for a future cycle are not known it will not be possible to separate, within acceptable uncertainty bounds, between the two sites.

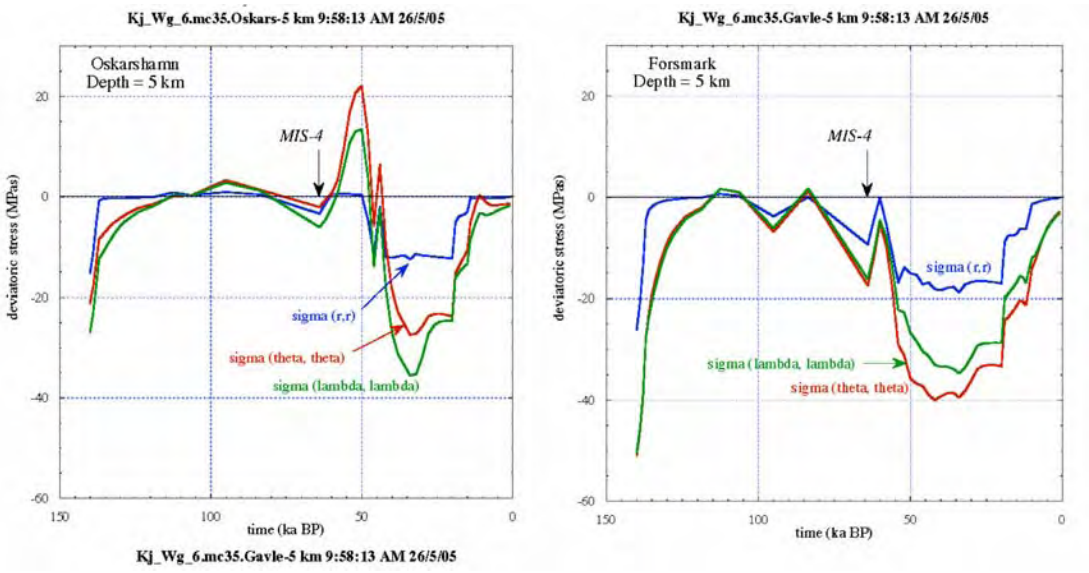

Fig. 1. The deviatoric stress components at Oskarshamn (left) and Forsmark (right), where r is the radial direction (positive outwards), θ latitude (positive south) and λ is longitude (positive east). During the early Weichselian the stress fluctuations at the two sites are small because the ice margins at that time lie to the north of both sites. The first glaciation reaches Oskarshamn at MIS-4 (~64,000 ypb), followed by large and frequent fluctuations of the ice front. From Lambeck (2005), fig. 7.

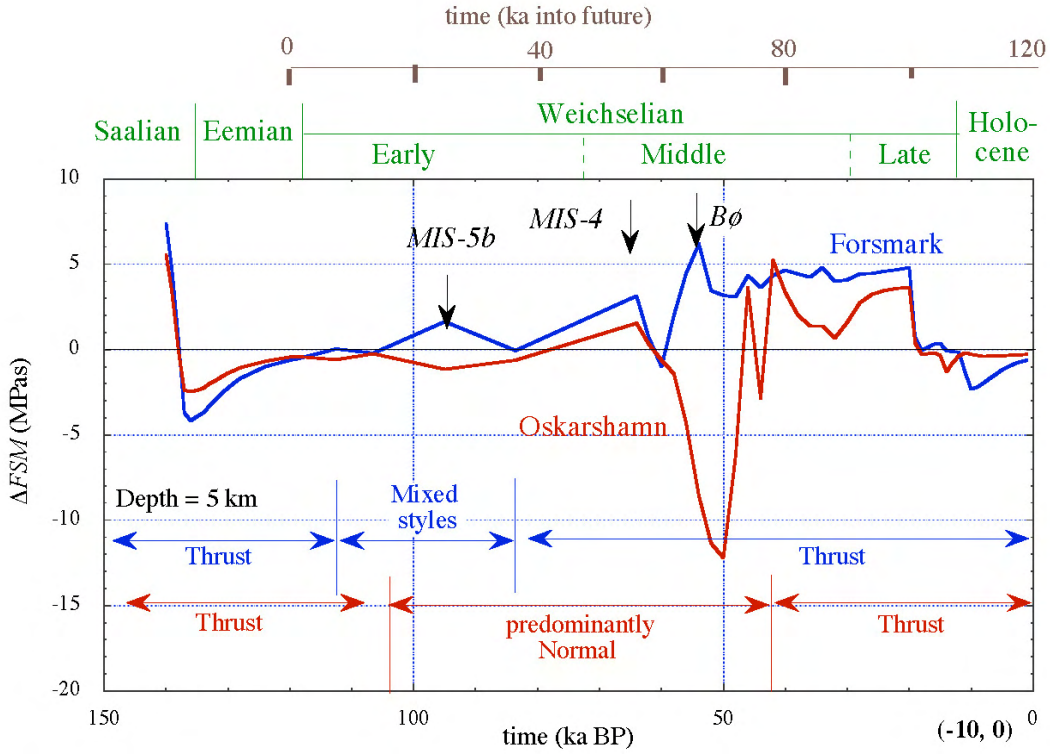

Fig. 2. ΔFSM (Fault Stability Margin change) predictions for a depth of 5 km for Forsmark and Oskarshamn indicating the styles of preferred faulting should failure occur. The model assumes an in-plane stress state of (-10,0) MPa and an azimuth of the ridge push axis of 45° W. From Lambeck (2005), fig. 10.

2. While the exact timing of the predicted stresses are quite uncertain due to the sensitivities to the ice margin movements and the corresponding uncertainties, the magnitudes of the stress variations can be assumed to be more representative for what happened during the last cycle and thereby also during the next one.

3. The ΔFSM predictions indicate strongly that major destabilisation and corresponding failure will occur. While increased in-plane stresses will reduce somewhat the FSM values but without removing the failures, such changes will have a stronger effects on the mode of faulting at different times during the cycle. Largely, however, reverse faulting should be expected.

The overall conclusions that I draw from this review is that we have to expect a major destabilisation and associated active faulting also during the next glaciation cycle, of the type that was experienced last time, but with considerable spatio-temporal uncertainties.

The major problem and challenge here is, however, how this seismicity will be distributed, where the basic supporting data will have to be taken from the last glaciation cycle, like what is done for the modeling discussed in the above. Before that, however, I will visit briefly the contemporary seismotectonics.

2. Contemporary seismotectonics

The present seismotectonics in Fennoscandia has been well studies and is also fairly well understood, even though it is still being discussed, as already referred to, how much influence that still remains from the glacio-isostatic rebound. My opinion is, as already stated, that this influence is minor, but not nil (Bungum et al., 1991; 2005).

The seismicity of Fennoscandia is seen in Fig. 3, based on the Fencat catalogue, while Fig. 4 shows magnitude-frequency distributions for an area in south-western and south-eastern Sweden, the latter containing the Forsmark and the Oskarshamn sites. While there are many more regional studies available, in particular for the coastal areas of Norway where the seismicity is highest, one of the few that is addressing all of Fennoscandia is the GSHAP study (http://www.seismo.ethz.ch/GSHAP/; Grünthal et al., 1999), which numerically delineates the seismic potentials of the different parts of this region.

A similar study that covers Norway, UK and the North Sea, is the one reported on by Bungum et al. (2000). From the latter study (see also Bungum et al., 2005) it was found that in a large region covering most of Scandinavia, the Norwegian margin and the North Sea (size about 2.3×10^6 km^2) the frequency of occurrence was following the Gutenberg-Richter relation logN=4.32-1.05M, corresponding to logN=0.99-1.05M for an area of 100 km^2. This corresponds to one M5 earthquake or larger every 18,000 years, or every 9 years if the entire region is used. This corresponds quite well to the 17 (give or take 2) M≥5 earthquakes in Fig. 2 for the same region, where a time span of about 150 years is covered (with exception of the 1759 Kattegat earthquake).

For the south-eastern part of Sweden where Forsmark and Oskarshamn are located the present activity is clearly lower, as shown by the two Fencat plots in Fig. 4, roughly indicating one M3 earthquake every year within an area of size only a little above 100,000 km^2, corresponding to about 1000 years per M3 event within 100 km^2. With that rate and a b-value of 1 it would take about 100,000 years to reach an M5 event.

This is almost an order of magnitude lower activity rate than for the large window that is dominated by the seismically more active regions in Fennoscandia. For indications of M6 return times, multiply the M5 return times by ten. The most important factor with respect to the long term seismic potentials is, however, not the microseismicity levels but rather the maximum magnitude (e.g., Bungum et al., 2005), which largely controls the moment release,.

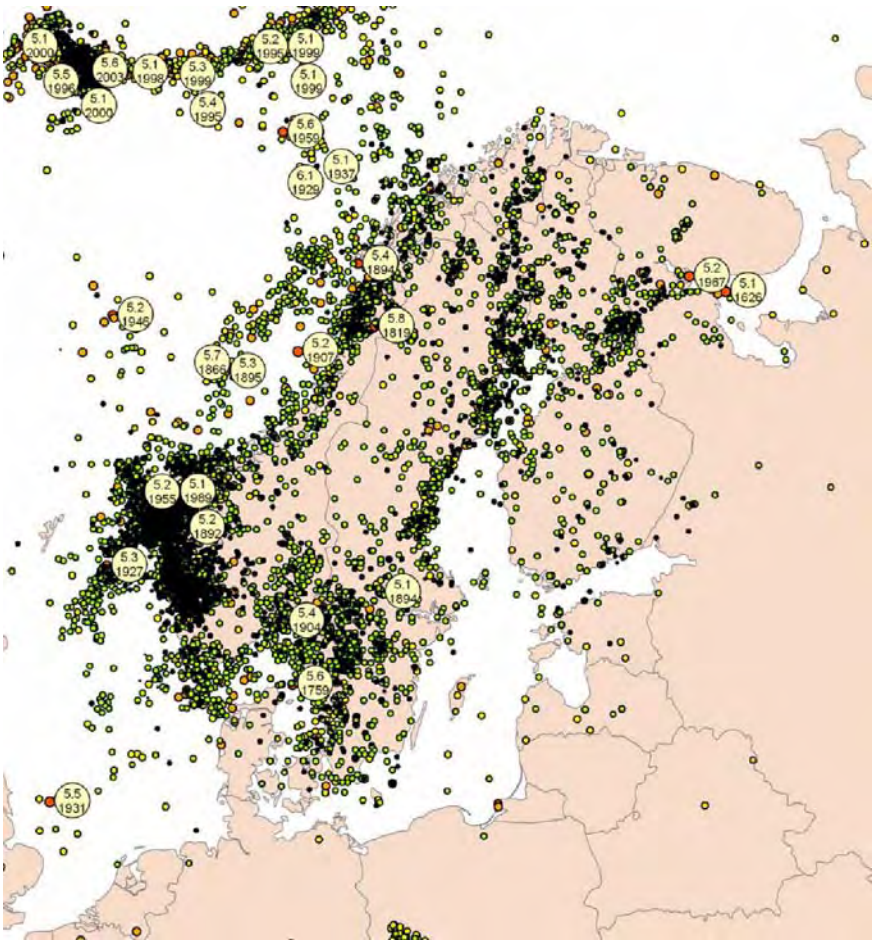

Fig. 3. Spatial distributions of earthquakes in the Fencat catalogue from University of Helsinki (http://www.seismo.helsinki.fi/). Magnitudes larger than M5 are displayed with year of the event. From Munier (2005), fig. 1-1.

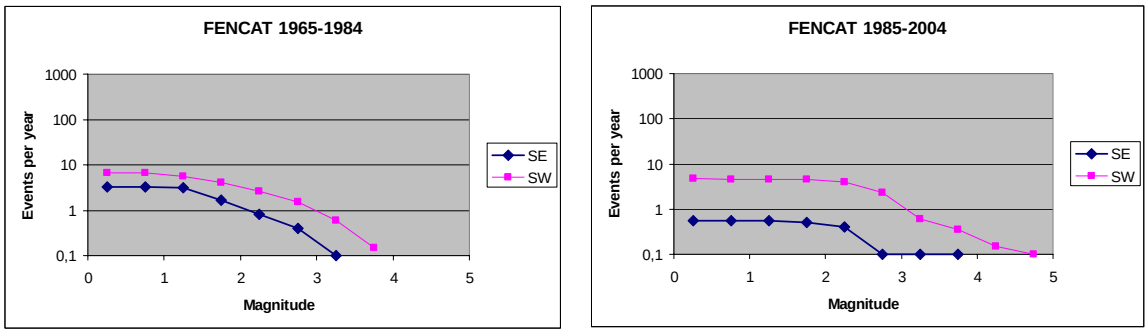

Fig. 4. Magnitude-frequency distributions for the Fencat catalogue within two smaller regions in SW and SE Sweden as defined by Munier (2005), where also the data behind these graphs are taken from. The two plots cover two consecutive 20-year intervals, both normalized to one year.

These numbers are only intended as very coarse indications of the present activity levels, to be compared later with what could be estimated as representative for the most seismically active periods more immediately following the deglaciation.

3. Postglacial seismicity

It was concluded above that the Holocene postglacial seismicity is the best assumption that is available to us as a basis for prediction models for what could be expected during the next 100,000 years in Fennoscandia, and thereby also for Forsmark and Oskarshamn. This postglacial seismicity has been documented in a large number of publications and I do not aim at reviewing these at this stage.

One of the most complete overviews of well-documented postglacial earthquakes with undisputed bedrock manifestations is the one published by Olesen et al. (2004), containing altogether 12 events over an area of roughly 400 x 400 km in Lapland (a similar table in Stewart et al., 2000, is based on the same work, the Norwegian NEONOR project, Olesen et al., 2000). The magnitudes here, ranging up to M_W 7.6 for the Pärve fault, are based on the (global) relations of Wells and Coppersmith (1994). Five of the magnitudes are independently determined by Bungum et al. (2005), based on Bungum and Lindholm (1997), with values up to 8.1. Arvidsson (1996) has similarly high values. Both Arvidsson (1996) and Bungum et al. (2005) have tuned their parameters specifically to the region studied.

A summary of these events and their moment magnitudes and seismic moments is provided in Table 1.

No.	Fault	Olesen et al. (2004)	Bungum et al. (2005)	Arvidsson (1996)	Seismic moment (Olesen et al.)
1	Stuoragurra	7,3	7,7		1,10E+20
2	Nordmannvikdalen	6,0			1,23E+18
3	Berill	6,1			1,74E+18
4	Suasselkä	7,0	7,4		3,89E+19
5	Pasmajärvi-Venejärvi	6,5			6,92E+18
6	Vaalajärvi	6,1			1,74E+18
7	Pärve	7,6	8,1	8,2	3,09E+20
8	Lainio-Suijavaara	7,1	8,0		5,50E+19
9	Merasjärvi	6,3			3,47E+18
10	Pirttimys	6,5			6,92E+18
11	Lansjärv	7,1	7,9	7,8	5,50E+19
12	Burträsk-Bastuträsk	7,1			5,50E+19
	Sum seismic moment				6,44E+20

Table 1. List of Lapland postglacial earthquakes with moment magnitudes from different authors. The seismic moments in the last column are calculated from the Olesen et al. (2004) magnitudes. The region is about 400 x 400 km.

It is well known, needing no additional justification in this short note, that earthquake activity rates and thereby also seismic potentials are expressed most properly through the moment rates and the total seismic moments released over a given time, relating directly to the released energy. Following Hanks and Kanamori (1977), moment

magnitude is defined as $M_W=2/3*\log(M_0)-6.06$ provided that seismic moment is defined in Nm.

Following this, a useful way to express the level of the documented postglacial seismicity in Lapland is therefore to start with the total amount of seismic moment released, as given in the last row of Table 1, and to convert this moment release into a magnitude-frequency distribution with the same moment release and a b-value of 1.0 (as a default value). The results are given in Table 2 for different combinations of the magnitude range within which the moment is released.

No.	M_W low	M_W high	a-value	N for M≥6	N for M≥5
1	0,0	7,6	7,68	48	480
2	0,0	8,2	7,43	27	270
3	6,0	7,6	7,75	56	560
4	6,0	8,2	7,41	26	260

Table 2. Magnitude-frequency relations $\text{Log}(N)=a-1.0*M_W$, corresponding to the release of the total seismic moment from Table 1. The four models are based on different magnitude intervals over which the moments are integrated, with corresponding a- and N-values.

What is seen from Table 2 is that the seismic activity rate needed to produce a certain seismic moment is very sensitive to the maximum magnitude, where I have used the range of values for the Pärve fault in Table 1, from 7.6 to 8.2. This is, as is well known, caused by the fact that the moment release is dominated by the largest events and therefore highly sensitive to maximum magnitude. On the other hand we also see that it makes very little difference if we integrate down to magnitude 0.0 or if we stop at 6.0. In the following I will use M6 as the lower value since Table 1 has no events below that level. For the high value I prefer 8.2, partly because that is a possible magnitude for the largest observed earthquake and partly because we should judge this value not only as the largest one observed but also as the maximum magnitude that could occur during the next 100,000 years.

I have now established a recurrence relation for an area of the size of 400 x 400 km, covering the time period that was needed to produce the events in Table 1. This time period is highly uncertain, and while the few datings that are available are of the order of 8000-9000 ybp, estimates of the time period range from a few hundred years to a few thousand years. I am inclined towards the latter estimate, based on the irregularities of the ice front and the fairly strong fluctuations that are documented, consistent with the modelling discussed above. If we assume that the moment release has taken place over 2-3000 years this will correspond to 100 years per M6 event or 10 years for M5, which actually is quite close the present activity level for Norway, as documented above. This may appear to be surprising at first glance, but it does not mean that the two areas have the same moment release, since this depends strongly on what the maximum magnitude is.

It is seen from the above that I have based my assessment of postglacial seismicity on what has been documented from the Lapland region, not using the observations and claims by Mörner (2004). The reason for this is that I find these claims problematic in the sense that they are not accompanied by similar observations of deep-seated basement-related faults.

Conclusions, Question 1

I will base my conclusions on the moment rate assessments above, and I have on that basis defined a high, a median and a low model, as follows:

1. The high model is assuming that the postglacial Lapland activity is representative also for SE Sweden and that it represents 20,000 years (no area scaling, time up-scaling by 5).
2. The best estimate (median) model is assuming that the postglacial Lapland activity is representative of an area the size of 320,000 km^2 and 50,000 years (area down-scaling by 2, time up-scaling by 2).
3. The low model is assuming that the postglacial Lapland activity is representative of an area the size of 800,000 km^2 and 100,000 years (area down-scaling by 5, no time scaling).

These models give results as shown in Table 3, with predicted values for 100 km^2 and 100,000 years, while the observed Lapland values are for a much shorter time period.

Region		a-value	N(M6)	N(M5)	N(M3)
Lapland	Observed	4,21	0,016	0,16	16,1
Predictions	High	4,90	0,080	0,80	80,3
Southeast	Best estimate	4,21	0,016	0,16	16,1
Sweden	Low	3,51	0,003	0,03	3,2

Table 3. Three models for answers to Question 1, where values are scaled to an area of 100 km^2 and moreover representing the entire 100,000 years time period. The a-value is the one in the Gutenberg-Richter relation log(N)=a-M (assuming b=1), and the N-values are those corresponding to magnitudes 6, 5 and 4, respectively. Note that the Lapland values represent only a few thousand years (at most) while the predictions for SE Sweden values represent 100,000 years.

	a-value	N(M6)	N(M5)	N(M3)	N-factors
m+3σ	6,07	1,19E+00	1,19E+01	1,19E+03	73,100
m+2σ	5,14	1,39E-01	1,39E+00	1,39E+02	8,550
m+σ	4,68	4,74E-02	4,74E-01	4,74E+01	2,924
m	4,21	1,62E-02	1,62E-01	1,62E+01	1,000
m-σ	3,74	5,55E-03	5,55E-02	5,55E+00	0,342
m-2σ	3,28	1,90E-03	1,90E-02	1,90E+00	0,117
m-3σ	1,40	2,50E-05	2,50E-04	2,50E-02	0,002

Table 4. Uncertainty distribution for the predicted seismic activity at Forsmark and Oskarshamn during the next 100,000 years, based on the values in Table 3. The a- and N-values are defined like those in Table 3, and the last column shows the ratios between the N-values.

The uncertainty distributions for these predictions are addressed through the b-values, which we can assume to be normally distributed (so that the N-values will be log-normally distributed). It turns out, even if this was not intentional, that the high and

the low values in Table 3 are equally spaced (±0,705) from the best estimate, which I chose to consider as a median value. I furthermore chose to consider this span between high and low to cover ±1.5σ, corresponding to σ=0.47 and a range of variation as given in Table 4. It is assumed that the distribution is truncated abruptly at +3 sigmas, due to reasons tied to physical limitations. The -2σ level is slightly below the contemporary seismicity in SE Sweden as inferred from Fig. 3.

It should be noted when considering these uncertainties, which are basically epistemic in nature, that sigma values of about 0.3 (corresponding to a factor of 2 in N) is quite common when assessing observed seismicity for logic-tree based seismic hazard analysis purposes, assuming much more predictable recurrence conditions.

Approaches, models and conclusions, Question 2

The second question is of a totally different nature than the first one, which addresses the expected occurrence rate of earthquakes above a certain magnitude level over 100,000 years. The second question is more generic and concerns the effects of individual earthquakes of magnitudes 6 and 8 in terms of displacement at an existing fracture at a distance of 10 km.

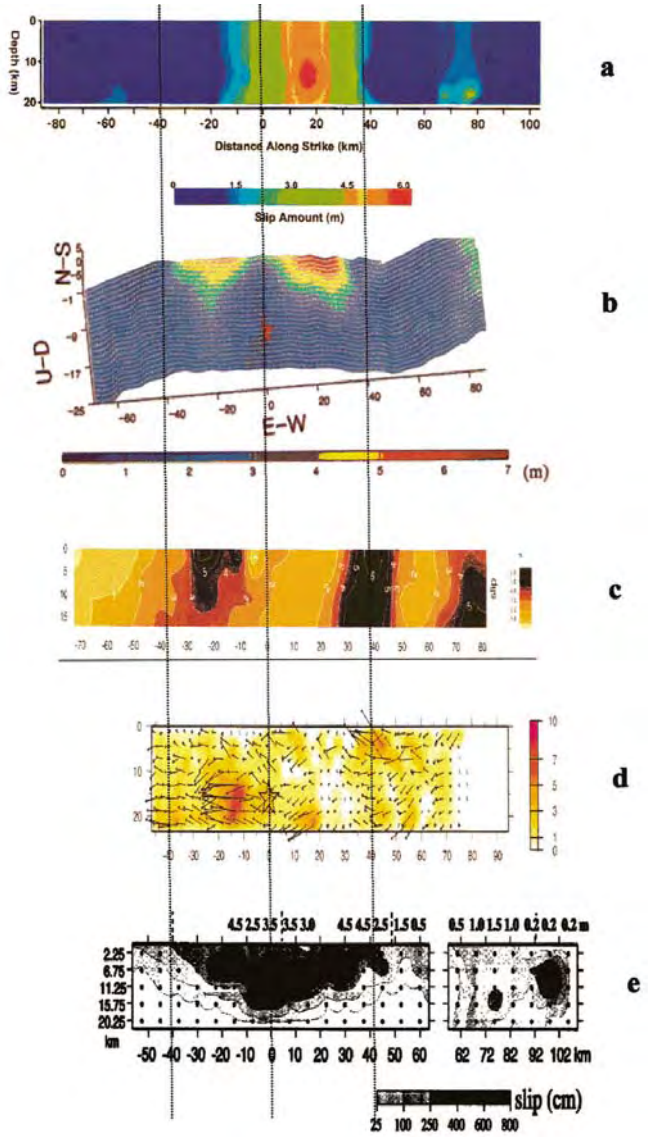

Fig. 5. Finite-fault inversions for the distribution of slip on the rupture of the M 7.4 1999 Izmit, Turkey, earthquake. (a) Gülen et al., 2002, BSSA, 92, 230-244, fig. 13; (b) Li et al., 2002, BSSA, 92, 267-277, fig. 10; (c) Bouchon et al., 2002, BSSA, 256-266, fig. 3; (d) Sekiguchi & Iwata, 2002, BSSA, 92, 300-311, fig. 6; (e) Delouis et al., 2002, BSSA, 92, 278-299, fig. 12. The five solutions are not only very different, they are also to some extent mutually exclusive, for example through the fact that both Bouchon et al. and Sekiguchi & Iwata both invoke supershear rupture, while Delouis et al. state that no supershear motion is needed to explain the data.

From Beresnev (2003), fig. 4.

I start by noting that estimating the slip distribution at the primary fault is by itself a very difficult task, and even more so the slip at fractures that are offset from the main fault. Fig. 5 shows five inversions from one of the best studied earthquakes of all, the 1999 Izmit, Turkey, earthquake. Beresnev (2003) finds that the five slip distributions have in fact very little in common in terms of slip distribution patterns and location of individual asperities, leading in turn to very different geological interpretations. The only consistent feature is the maximum value of slip, which however is largely constrained by the seismic moment.

Irrespective of the problems with slip inversion (beyond the level of average slip) it is clear that the variation of stress drop and thereby also slip and energy release along the primary fault plane is considerable, which clearly will have downstream effects also in terms of slip on fractures away from the principal trace. This uncertainty in the primary slip model is important, and any prediction model that intends to delineate the off-trace effects will easily underestimate the associated variability unless the variability on the primary fault is also taken into consideration.

No modeling or simulation is contributing real knowledge unless the modeling results or the basic model components or parameters can be empirically calibrated. To this end the results shown in Fig. 6 are useful, even if they are based on observations of surface ruptures. The Californian earthquakes used there are mostly around magnitude 7 and above, including the M7.6 Landers 1992 earthquake that 'jumped' twice across previously mapped faults, producing a 70 km long irregular fault trace. Even so, the frequency of occurrence of displacements is down to 0.001 at a distance of 8 km from the principal trace, with no observations beyond that distance.

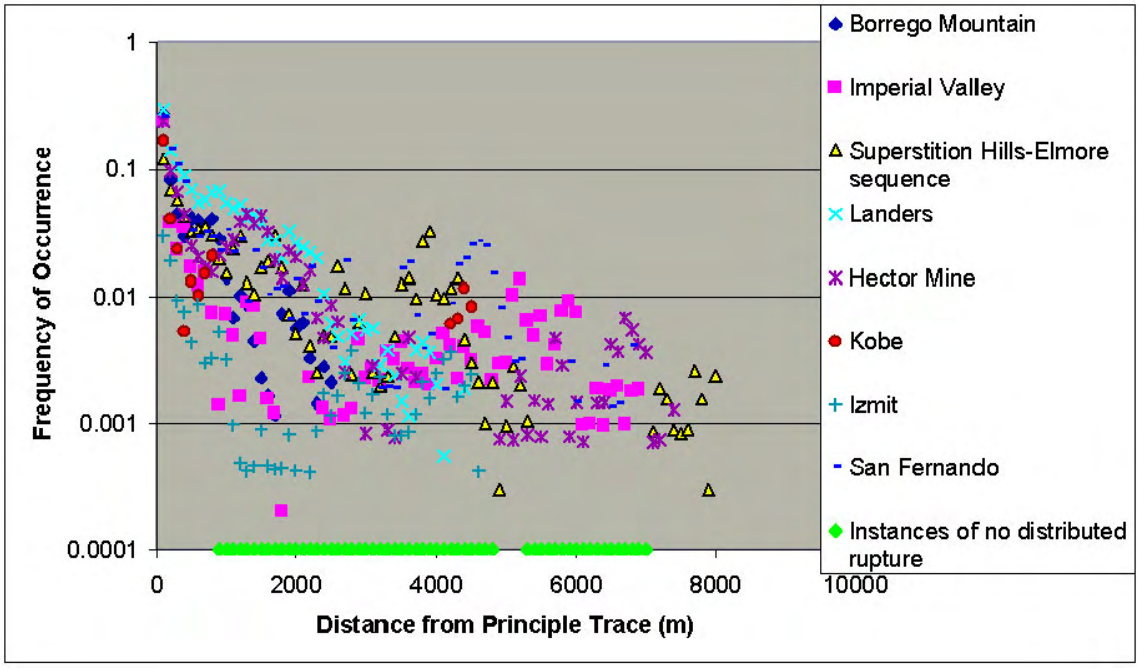

Fig. 6. Frequency of earthquake displacements within 50 m cells as a function of distance from the principal trace. From Petersen et al. (2004), fig. 4.

The problems related to Question 2 have been addressed thoroughly through a number of SKB reports over the last years (La Pointe et al., 1997; 1999, 2000, 2002; Bäckblom and Munier, 2002). The methodology developed is stochastic, including the

earthquake occurrence model, and the relations between magnitude, displacement and fault dimensions are based on regressions (Wells and Coppersmith, 1994) where the uncertainties are incorporated through a Monte Carlo approach. These relations are, however, based on average estimated parameters for each earthquake, and the approach therefore does not include the uncertainty discussed above with respect to the slip distribution on the primary faults.

Even so, the SKB approach can be considered state-of-the-art. There is, however, a major source of uncertainty related to the earthquake model used, which seems to be quite dependent on the contemporary seismicity. The detailed regional variations in the seismicity predicted for the next 100,000 years are in my view questionable, and in any case they are quite different from the model presented in this report.

A useful summary of the SKB model predictions relating to Question 2 is provided in Fig. 7. For M6 at 10 km the maximum induced slip is about 1 mm, and thereby largely negligible, but for M8 the slip is 10 cm and thereby far from negligible. However, these simulations are done for a fracture radius of 1000 m, which appears to be fairly conservative (large fracture dimensions produce more slip).

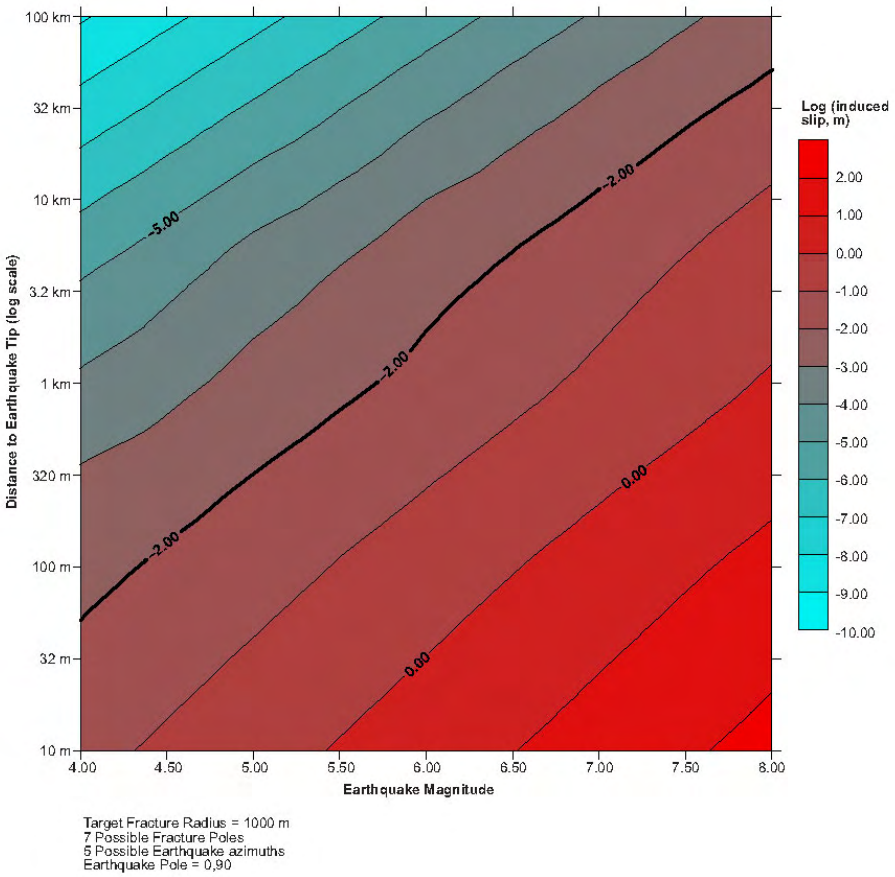

Fig. 7. Maximum induced slip as a function of magnitude and distance, based on combinations of fracture orientation and azimuth, but for a constant fracture radius of 1000 m. From La Pointe et al. (2000), fig. 2-5.

A different and more applicable approach for the problem at hand is the one used in Fig. 8, showing that less than 20% of the simulations will produce slip larger than 10 cm for an M8 earthquake at a distance of 10 km. A slip of 10 cm is considered to be

the level at which damage to a canister may occur, and the diagonal line in Fig. 8 therefore represents the separation between damage (lower right) and no damage.

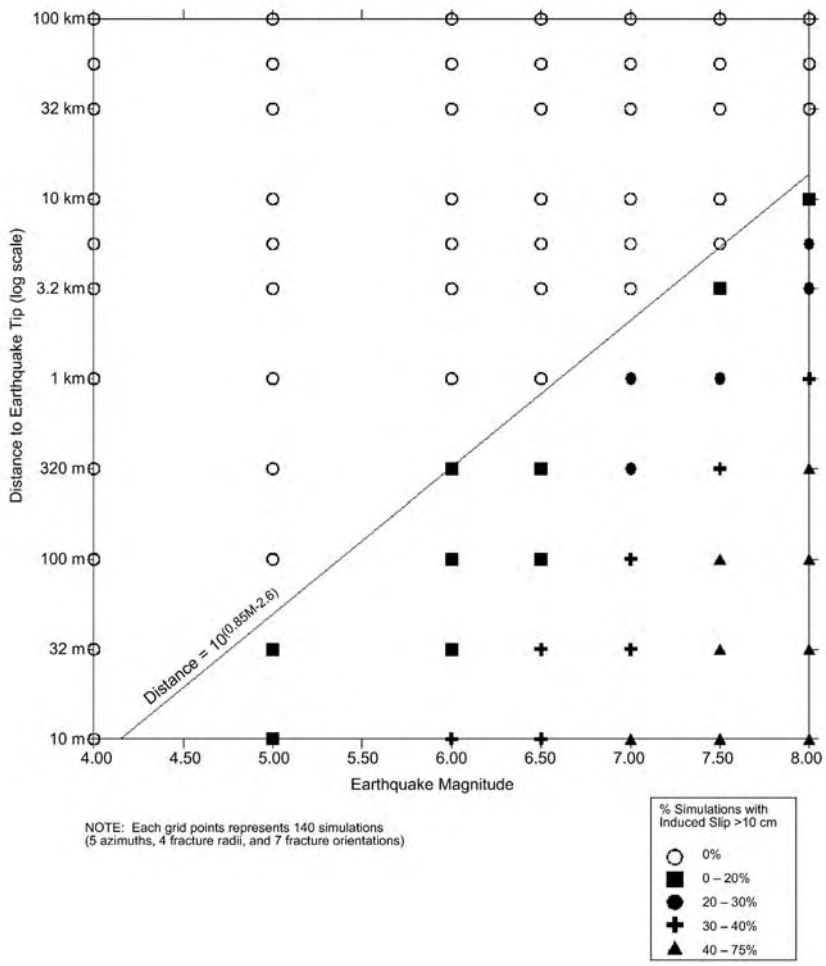

Fig. 8. Percent earthquakes causing induced slip greater than 10 cm as a function of magnitude and distance, based on combinations of fracture orientation, azimuth and radius. From La Pointe et al. (2000), fig. 2-1.

A realistic assessment of the uncertainty distributions for these estimates require an in-depth knowledge and understanding of the modelling methodology and an assessment of the basic relations used and the range of variation applied to the parameters. I have already noted that the earthquake model behind these simulations may be questionable, and likewise I would expect that similar questions may be posed with respect to the rock mechanical assumptions in the model. It will, however, be beyond the scope of this elicitation to address these questions in more detail.

While for example the energy radiation from a rupturing fault includes uncertainties that are aleatory and therefore appears to behave randomly there will also be uncertainties in these simulations that are epistemic. A better separation between these types of uncertainties in the simulations would have been useful.

As for the expected slip values I can not give clear recommendations with respect to their uncertainty distribution, and for the same reason. On a general basis, however, I note that simulations like those used here often do not catch the complete range of uncertainties, even if I will not claim this to be the case here. There are reasons to

expect the slip amplitudes to be lognormally distributed, and what is often found in such cases is that there is a basic randomness in the processes involved that corresponds to a standard deviation of the order of 0.2-0.3 $\log_{10}$ units. With the additional uncertainties in the present case a more realistic sigma value may be of the order of 0.4-0.5 for the uncertainty variation around an estimate that appears to be in the range 1-10 cm. Like for the seismicity the distribution should be truncated at +3σ.

Closing remarks

I have based my model for the seismicity expected for the next 100,000 in SE Sweden and not on the contemporary seismicity but rather on the paleoseismic observations documenting postglacial earthquakes in the Lapland region, distributed in different ways in time and space. The stress effect modeling has been used essentially as a support for expected activity well above the present level, and as an indicator against a model that contains much regional variation, including between the two sites at Forsmark and Oskarshamn. The contemporary seismicity in SE Sweden and Norway correspond roughly to -2σ and -1σ in the uncertainly distribution, respectively.

My model for the expected slip is essentially based on SKB modeling and therefore does not really include any independent evaluation, except for my reflections and recommendations on uncertainties and their distribution.

References

Bäckblom, G. and R. Munier (2003): *Effects of earthquakes on the deep repository for spent fuel in Sweden based on case studies and preliminary model results*. SKB Report TR-02-24, 115 pp.

Beresnev, I.A. (2001): What we can and cannot learn about earthquake sources from the spectra of seismic waves. *Bulletin of the Seismological Society of America*, 91, 397-400.

Bungum, H., A. Alsaker, L.B. Kvamme and R.A. Hansen (1991): Seismicity and seismotectonics of Norway and surrounding continental shelf areas. *Journal of Geophysical Research*, 96, 2249-2265.

Bungum, H., C. Lindholm and J. I. Faleide (2005): Postglacial seismicity offshore mid-Norway with emphasis on spatio-temporal-magnitudal variations. *Marine and Petroleum Geology*, 22, 137-148.

Bungum, H., C.D. Lindholm, A. Dahle, G. Woo, F. Nadim, J.K. Holme, O.T. Gudmestad, T. Hagberg and K. Karthigeyan (2000): New seismic zoning maps for Norway, the North Sea and the U.K. *Seismological Research Letters,* 71(6), 687-697.

Byrkjeland, U., H. Bungum and O. Eldholm (2000): Seismotectonics of the Norwegian continental margin. *Journal of Geophysical Research*, 105, 6221-6236.

Grünthal, G. and the GSHAP Region 3 Working Group (1999): Seismic hazard assessment for Central, North and Northwest Europe: GSHAP Region 3. *Annali di Geofisica*, 42(6), 999-1011.

Hanks, T.C. and H. Kanamori (1977): A moment magnitude scale. *Journal of Geophysical Research*, 84, 2348-2350.

Hicks, E., H. Bungum and C. Lindholm (2000): Stress inversions of earthquake focal mechanism solutions from onshore and offshore Norway. *Norwegian Journal of Geol*ogy, 80, 235-250.

La Pointe, P.R., T. Cladouhos and S. Follin (2002): Development, application, and evaluation of a methodology to estimate distributed slip on fractures due to future earthquakes for nuclear waste repository performance assessment. *Bulletin of the Seismological Society of America*, 91, 397-400.

La Pointe, P.R., T. Cladouhos and S. Follin (2002): *Calculation of displacements on fractures intersecting canisters induced by earthquakes: Aberg, Beberg and Ceberg examples*. SKB Report TR-99-03, 103 pp.

La Pointe, P.R., T.T. Cladouhos, N. Outters and S. Follin (2002): *A methodology to estimate earthquake effects on fractures intersecting canister holes*. SKB Report TR-97-07, 61 pp.

La Pointe, P.R., P. Wallmann, A. Thomas and S. Follin (2002): *Calculation of displacements on fractures intersecting canisters induced by earthquakes: Aberg, Beberg and Ceberg examples*. SKB Report TR-99-03, 103 pp.

Lambeck, K. (2005): *Glacial load stresses*. Note for SSI, Stockholm, May 2005, 13 pp.

Lambeck, K. and A. Purcell (2003): *Glacial rebound and crustal stress in Finland*. POSIVA Report 2003-10. Posiva Oy, Finland, 84 pp.

Lund, B. (2004): Effects of deglaciation on the crustal stress field and implications for endglacial faulting: A parametric study of simple Earth and ice models. SKB Report TR-05-04, 68 pp.

Mörner, N.-A. (2004): Active faults and paleoseismicity in Fennoscandia, especially Sweden. Primary structures and secondary effects. *Tectonophysics*, 380, 139-157.

Munier, R. (2005): *Contemporary seismicity in southern Sweden based on the Fencat catalogue*. Note for SSI, Stockholm, May 2005, 10 pp.

Olesen, O., L.H. Blikra, A. Braathen, J.F. Dehls, L. Olsen, L. Rise, D. Roberts, F. Riis, J.I. Faleide and E. Anda (2004): Neotectonic deformation in Norway and its implications: a review. *Norwegian Journal of Geol*ogy, 84, 3-34.

Olesen, O., J. Dehls, H. Bungum, F. Riis, E. Hicks, C. Lindholm, L.H. Blikra, W. Fjeldskaar. L. Olesen, O. Longva, J.I. Faleide, L. Bockmann, L. Riise, D. Roberts, A. Braathen and H. Brekke (2000): *Neotectonics in Norway, Final report*. Geological Survey of Norway, Report No 2000.002, 120 pp.

Petersen, M., T. Cao, T. Dawson, A Frankel, C. Wills and D. Schwartz (2004): Mapping fault rupture hazards for strike-slip earthquakes. *Proceedings, 13th World Conference on Earthquake Engineering*, Vancouver, B.C., Canada,

Stewart, I.S., K. Sauber and J. Rose (2000): Glacio-seismotectonics: ice sheets, crustal deformation and seismicity. *Quaternary Science Rev*iews, 19, 1367-1389.

Wells, D.L. and K.J. Coppersmith (1994): New empirical relationships among magnitude, rupture length, rupture width, rupture area, and surface displacement. *Bulletin of the Seismological Society of America*, 84, 974-1002.

Appendix 7

Frequency of Earthquakes Mw≥6.0 During a Glacial Cycle in Central and Southern Sweden

James H. Dieterich
Riverside, California USA

Introduction and Summary

This report was prepared for the expert elicitation panel convened by *SSI*. It reviews the factors, data, methods, and judgments employed in arriving at an appraisal of earthquake occurrence resulting from a cycle of glaciation. The question considered is: *"What will be the frequency of moment magnitude 6.0 or greater earthquakes per unit area (e.g. per 100 sq. km) in the middle and south of Sweden (Forsmark and Oskarshamn) during a glacial cycle (approximately 10^5a) assuming conditions similar to the Weichel glaciation? Give an uncertainty distribution for this quantity for each area."*

This report does not address either the probability, or the characteristics, of a renewed cycle of glaciation – both are used as given conditions in the following analysis. The central question for this elicitation is that of predicting the seismic response of a stable craton to the loading and unloading stresses associated with a cycle of glaciation. This question touches on several poorly understood topics for which no established analysis methodologies exist. Furthermore, there is an absence of critical data on both the seismic behavior of the Earth's crust through a cycle of continental glaciation and the current state of stress in this region. Consequently, considerable uncertainty must attach to judgements on the expected frequency of earthquakes.

Stress perturbations are widely understood to be associated with increased seismic activity and glacial loading calculations indicate that stress changes of up to 40 MPa would occur for a repeat of the Weichel glaciation. Those stress changes are much larger than the stresses associated both with the occurrence of aftershocks (Toda and others, 1998), and with induced seismicity associated with the filling large reservoirs (by direct loading from the weight of water, or though changes of effective stress). Hence, a significant seismic response to glaciation appears to be quite plausible.

The method of analysis developed for this report employs the glacial stressing histories at Forsmark and Oskarshamn supplied by Kurt Lambeck. The analysis was designed to provide a framework for assessing the seismic response under circumstances where input parameters are highly uncertain. It gives preferred values of 24 and 42 earthquakes, M≥6, occurring within 100km of Forsmark and Oskarshamn, respectively, as a consequence of glaciation. The extreme limits of the possible seismic response are 0.8 and 142 M≥6 earthquakes at Forsmark, and 1.4 to 247 M≥6 earthquakes at Oskarshamn. These large uncertainties reflect the current state of limited knowledge.

Method of Analysis

The analysis is based on a calculation of the stress relaxation (expressed as seismic moment) required to keep the glacial stresses from exceeding a fault failure stress. Because fault slip criteria are defined in terms of total stress, one must estimate, or make assumptions, about the initial stress state as well as the changes of stress changes due to glaciation to carry out such calculations. Unfortunately initial stress state is particularly difficult to assess or constrain. Earthquake focal mechanisms and regional stress observations compiled for the World Stress Map (Reinecker, and others, 2004) generally indicate the principal horizontal compressive stress is oriented roughly NW-SE in this region. The prevalence of strike slip focal mechanisms further suggest the least compressive horizontal compressive stress is oriented NE-SW, with the intermediate principal stress vertical. Two deep boreholes at the Siljan Ring structure indicate a similar stress state (Lund and Zoback, 1999) and further suggest the current stresses are near the failure stress in the depth range sampled (to about 6km). However, the magnitudes of the stress components thoughout the entire seismic depth range and their spatial variations are poorly understood and allow a wide range of seismic responses to the glacial stresses.

A comprehensive treatment of the elicitation question would be to directly evaluate the effects of the uncertain initial stresses, and it might employ a large number of model simulations that sample the parameter space that describes the range of permissible initial stress states and fault failure conditions. In such an approach weights would be assigned to the different stressing models (perhaps through an elicitation process) to arrive at an evaluation, with uncertainties, of likely earthquake activity. An analysis of this type represents a substantial undertaking that is well beyond the scope of this evaluation.

The approach used here is to first obtain a reference value for the seismic moment using a single highly idealized model of stress and failure conditions during a glacial cycle. As implemented the reference model employs only the stress changes due to glaciation, and it yields the maximum possible seismic response to a glacial cycle. The actual response may be much less than this idealized upper-limit value. To obtain a more realistic preferred estimate of the seismic response, multiplying factors for the upper-limit result are then introduced. These factors incorporate estimates of the effects of various uncertain and non-ideal stress and failure conditions that could not be included in the reference model.

Upper-Limit Model

The analysis for idealized upper-limit response employs the following steps.

1) Define the reference stressing models for stress state and stressing histories at Forsmark and Oskarshamn.

2) Impose a fault failure criterion that limits the maximum stresses, and calculate stress relaxation, by fault slip, needed to keep total stress at or below the failure limit.
3) Find the moment release equivalent to the stress relaxation for a specified volume.
4) Calculate earthquake rates from the moment release using moment magnitude and magnitude frequency relationships.

Step 1: Stressing history. The stress tensor may be represented as an initial stress state at the onset of glaciation, to which are added the changes of stress with time due to glaciation. This analysis uses the histories of glacial stress change at Forsmark and Oskarsham as supplied by Kurt Lambeck. It is assumed that tectonic stressing, which is small compared to glacial stressing, will not affect that component of seismicity arising from glacial stressing. Possible pore fluid changes, which alter the effective normal stress in the failure condition, are not treated directly, but contribute to the total uncertainty estimate described below.

The occurrence of sparse, but widely distributed seismicity indicates that at least some parts of southern Sweden currently have stresses near the fault failure limit. For the reference calculation, the initial stress is assumed to be uniformly at the failure limit everywhere. During glaciation it is further assumed that the stress state at the beginning of every time step is at the failure limit, with principal stress orientations that coincide with the principal axes of the stress change tensor during the time step. With these assumptions, the model employs only the stress changes due to glaciation.

Step 2: Stress relaxation due to fault slip. The analysis employs the Coulomb failure criterion to determine amount of stress relaxation due to fault slip, if any, which occurs during a time step. The Coulomb failure criterion is

$$\tau = \tau_0 + \mu(\sigma - P_f) \qquad (1)$$

where τ and σ are the shear and normal stress, respectively, acting on the fault surface, τ_0 is the cohesion, μ is the coefficient of friction, and P_f is the pore fluid pressure. The reference calculation is independent of the values of τ_0 . The reference calculation uses a preferred value of $\mu = 0.60$. In the way the analysis is formulated, the cohesion term does not enter these calculations. The borehole stress data of (Lund and Zoback, 1999) indicate a coefficient of friction of 0.5 to 0.6 if the observed stresses are assumed to be at the failure limit.

A complete analysis of the problem would entail estimation of the total stress tensor, including the changes of orientation of the principal stress axes, and assumptions about the orientations of potential fault planes that might form or be activated by the stresses. The simplified analysis assumes optimally oriented fault planes exist for all possible rotations of the principal stresses during glaciation.

Figure 1 illustrates the principles employed in computing stress relaxation due to fault slip, if any during, during a stressing increment. Assuming mean stress is constant during

slip, the shear stress relaxation $\Delta\tau$ is given by the path from point B to C. The shear stress relaxation ΔS from point B to C is

$$\Delta S = (\Delta\tau - \mu\Delta\sigma)\cos(\phi), \qquad (2)$$

where $\Delta\tau$ and $\Delta\sigma$ are the changes in change in shear and normal stress for the stress increment AB, prior to slip, and $\phi = \tan^{-1}\mu$. If the stress at B falls on or below the failure curve ($\Delta S \le 0$) then fault slip does not occur during that stressing increment.

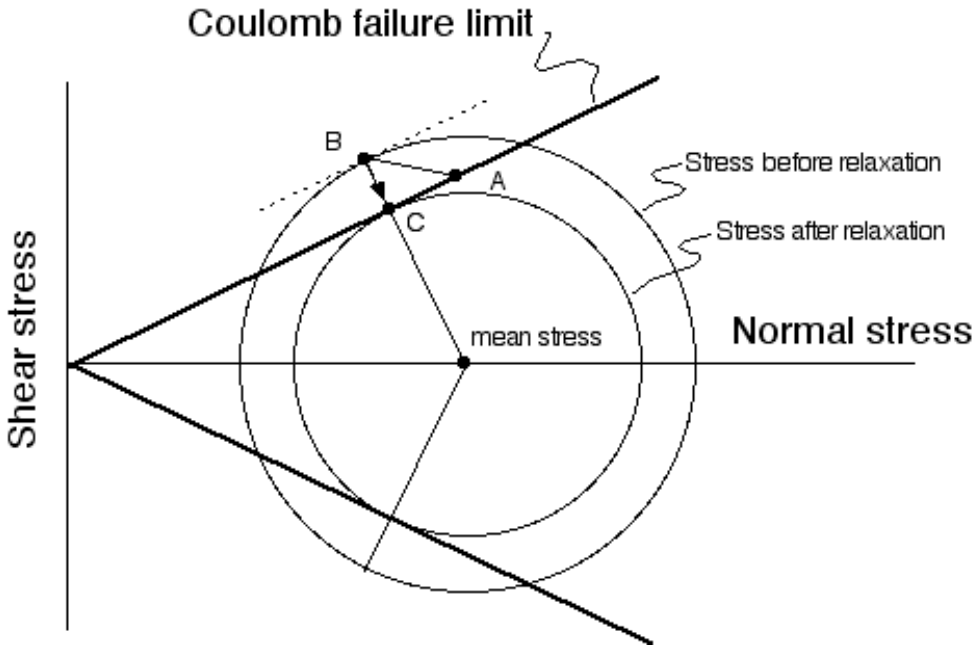

Figure 1. Mohr circle construction for stressing conditions during a time step. At the start of the time step (point A) stresses are assumed to lie somewhere along the failure curve at the failure limit. Assuming no slip occurs, the stresses at the end of the step will be as some point B, which may or may not exceed the failure stress. If stresses lie above the failure stress fault slip will relax the stresses to point C. This stress path assumes the mean stress remains constant during slip.

The solutions for stress release (in 5000a intervals) are illustrated in Figure 2. The letters on the plots indicate the mode of faulting (SS=strike slip, N=normal, T=thrust) required by the stress changes during the stressing interval. These indicate that considerable switching of the principal stress axes occurs during the glacial cycle. Stress changes in which the stress falls below the critical stress during the stressing interval have negative sign. Because no slip can occur, the negative stress changes are not counted for the sum of total stress release for the entire glacial cycle.

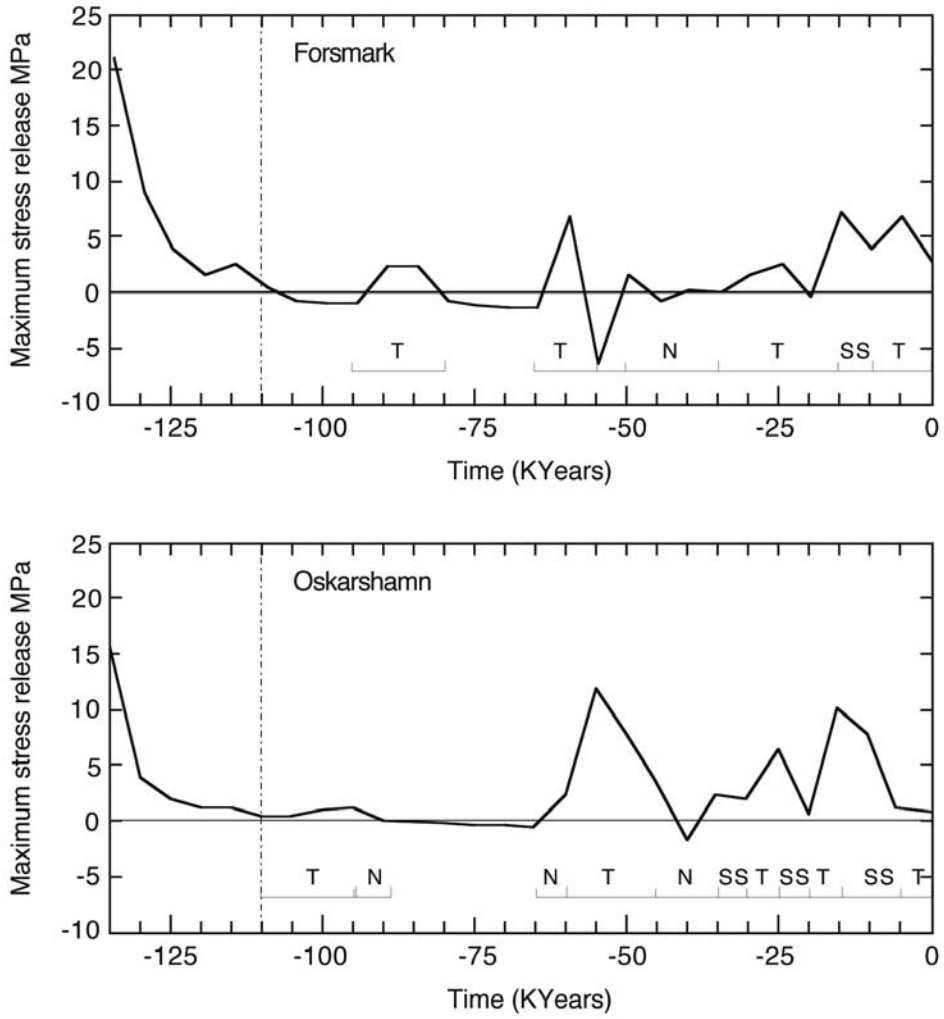

Figure 2. Stress release (in 5000a increments) at Forsmark and Oskarshamn for the idealized base-line seismicity calculation. Letters indicate mode of faulting (SS=strike slip, N=normal, T=thrust).

Step 3: Find total moment release in the reference volume. Seismic moment is defined as

$$Mo = GAd, \tag{3}$$

where G is the elastic shear modulus, A is fault area and d is fault slip. From Hooke's law the relation between shear stress change and displacement for a uniform deformation over some length L is

$$d = \frac{L\Delta\tau}{G} . \tag{4}$$

Hence, moment is simply stress change integrated over the volume. For the uniform stress change employed here,

$$Mo = \Delta\tau AL\,. \qquad (5)$$

For the reference calculation, volume is defined as a region with a 100km radius, centered on Forsmark or Oskarshamn, with an assumed seismogenic depth of 30km.

Step 4: Find the total number of earthquakes from moment release. This calculation employs the relationship between seismic moment and earthquake magnitude

$$M = \frac{2}{3}\log_{10} Mo - 10.7\,, \qquad (6)$$

(Hanks and Kanamori, 1979) with the Gutenberg–Richter magnitude and frequency relationship

$$\log(N) = a - bM\,, \qquad (7)$$

to solve for the rate term a in equation (7). In equation (7) N is cumulative number of earthquakes $\geq M$. For this analysis, the frequency relationship is truncated at the maximum magnitude $M_{\max} = 7.6$, and b=1.0. (These values were specified for the elicitation.)

Reference calculation for maximum response. Table 1 summarizes the results for the reference calculation of seismic response to the cycle of glacial loading. It is emphasized that the results in Table 1 represent a baseline for the maximum possible seismicity from which the preferred estimate of seismic response is derived.

Table 1. Reference calculation for number of earthquakes M≥6.0 due to glacial stressing. Volume = 94,2478 km^3 (100km radius to a depth of 30km)

M≥	Forsmark	Oskarshamn
6	121	206

Preferred Model of Seismic Response

The preferred estimate of seismic response to glaciation takes into consideration a variety of uncertain factors that are expected to modify the actual seismic response from that of the idealized model. These effects are brought into the analysis though the use of a multiplying parameter β where

$$Mo_{SEISMIC} = \beta Mo_{MAX}\,, \qquad (8)$$

Mo_{MAX} is the maximum moment release of the reference calculation described above, and $Mo_{SEISMIC}$ is the preferred estimate of expected seismic moment release. Assuming independence of the various uncertain effects that may modify the reference result, a β–factor for each effect may be independently calculated or estimated then combined to give the total effect. That is,

$$\beta = \beta_S \beta_P \beta_M \,, \tag{9}$$

where, β_S, β_P, and β_M are factors relating to the stress/failure conditions, parameter uncertainty, and model physics, respectively. These are discussed below. Table 2 gives the values for these factors. The preferred values of seismic response are obtained using β at the 0.5 fractile.

Table 2. β-factors used to scale the reference model to the preferred model. β at the 0.50 fractile is used to obtain the preferred seismic response. The upper and lower limits of the final combined β (bottom row) correspond to the 0.001 and 0.999 fractiles, respectively.

	0.50 fractile	0.10 fractile	0.90 fractile
β_S	0.20	0.03	0.46
β_P	1.00	0.50	1.50
β_M	1.00	0.50	1.75
β	**0.20**	Lower limit =0.007	Upper limit=1.21

Factor β_S may be viewed as a measure of the efficiency with which the crust in the vicinity of Forsmark and Oskarshamn converts stress changes from glaciation into seismic moment. The reference calculation assumes β_S=1.0. For the reference calculation to hold in practice, four rather restrictive conditions must be satisfied. The preferred value of β_S=0.2 given in Table 2 was obtained by combining individual β–values associated with each of those four conditions. Those sub-factors are designated as β_{S1}, β_{S2}, β_{S3}, and β_{S4} in Table 3, and are discussed below.

1. The reference calculation assumes the initial stresses acting on the seismogenic faults are everywhere at the failure stress. In other words the faults that become active during glaciation must be incipiently active at the start of the glaciation. Otherwise, some interval of stressing must first occur to bring the fault stresses up to the failure limit before stressing begins to be converted to fault slip. Sparse but widely scattered seismicity in southern Sweden and borehole data indicate that at least some portions of the crust are currently at or near the failure stress. However, the data are insufficient to establish that the crust is everywhere at the critical stress. Hence, one must admit the possibility of some significant of stress heterogeneity, relative to the failure stress. Additionally, the complex cycles of stressing (and associated deformation) with previous glacial cycles may have left

the region in a somewhat chaotic stress state. The assigned estimate of β_{S1}=0.80 reflects my judgement that a modest level of stress heterogeneity probably exists.

2. The reference calculation assumes the optimally oriented fault planes for during each glacial stressing increment are also the optimally oriented fault planes for the total stresses (the sum of initial stress, and all previous stresses). To satisfy this condition, the maximum and minimum principal stress axes from glacial loading must exactly coincide with the principal stress axes of the initial condition. Rotation or switching of the principal stress axes during glacial loading cannot occur. Otherwise only a portion, if any, of the glacial stressing increment can be converted to seismic moment. For example, if the glacial stressing axes are reversed with respect to the initial stress axes, then glacial stressing will counteract the initial stress and move the faults away from failure, even though the reference model indicates slip would occur. The letters in Figure 2, which indicate the mode of faulting, show that the glacial stressing is very complex and involves numerous switches in the orientations of the principal stresses. This switching must drastically reduce efficiency with which the stress changes can be converted to seismic moment. A few highly idealized simulations were conducted with different hypothetical background stresses and switching of glacial stress axes. Those simulations suggest values of β_{S2} the range of around 0.2 to 0.6. For this report a preferred value of β_{S2}=0.4 is used.
3. The reference calculation, assumes that optimally oriented faults, capable of producing M≥6.5 earthquakes actually exist at every step in the computation. They may not. Slip of misoriented faults can occur, but it will not be as efficient as optimally oriented faults in converting a stressing increment to seismic moment. It view of the frequent changes of stress orientation during a glacial cycle, it would seem unlikely that optimally oriented faults exist for all the stress orientations that operate during glaciation. Additionally, faults large enough to be capable of generating earthquakes M≥6, at distances sufficiently close to Forsmark and Oskarshamn to be of importance, cannot be said to exist with certainty. For these effects I have assigned a preferred value of β_{S3}=0.70.
4. Finally, the reference calculation assumes stress relaxation is occurs entirely in the form of seismic moment. However, aseismic fault slip and bulk deformation can occur in seismic regions. For this report a value of β_{S4}=0.90 is used.

Table 3. Sub-Factors for β_S
These subfactors are multiplied with one another to arrive at the values of β_S in Table 2.

	0.5 fractile (preferred value)	β-factors used to estimate β_S at the 0.10 fractile	β-factors used to estimate β_S at the 0.90 fractile
β_{S1}	0.80	0.50	0.90
β_{S2}	0.40	0.20	0.60
β_{S3}	0.70	0.45	0.90
β_{S4}	0.90	0.70	0.95

Multiplying factor β_P incorporates the uncertainties associated with the parameters employed in the calculations. The reference calculations use μ=0.6, $M_{max} = 7.6$, and

b=1.0. The latter two values were specified for the elicitation. However, the use a narrow range of values for μ, b and M_{max} in alternative calculations of maximum moment release indicates considerable sensitivity to uncertainty in these parameters. At the 0.1 and 0.9 fractiles, β_P is assigned values of 0.5 and 1.5, respectively. The preferred value β_P =1 employs the parameter values used in the reference calculation.

Multiplying factor β_M provides a simple estimate of model uncertainty. The preferred value is β_M=1.0 with values of 0.5 and 1.75 at the at the 0.1 and 0.9 fractiles, respectively. This range of values allows for the possibility of models or processes that were not treated in this analysis, which could however alter the results. These might include pore pressure changes, which would alter the fault failure condition; the use of alternate failure criteria; and interactions with the free surface, which would alter the assumed stress relaxation paths.

Preferred estimate of seismic response. Table 4 gives the preferred estimates of seismic response at Forsmark and Oskarshamn including estimates of uncertainty. The value at the 50% fractile is the preferred result and represents the estimate at which the actual seismic response is equally likely to be larger or smaller. The limiting values of seismic response (0.001 and 0.999 fractiles) were directly obtained using the limiting values of β in Table 2. The seismic response estimates at the other fractiles were estimated by interpolation. The number of earthquakes in Table 4 scales directly by the volume of crust considered, which was taken to have a radius of 100km and a depth of 30km.

Table 4. Predicted seismic response at Oskarshamn and Forsmark with estimated distribution of uncertainties. The preferred values (**in bold**) are those at the 0.5 fractile. The data give numbers of earthquakes M≥6 due to glacial stressing occurring within 100km of Oskarshamn and Forsmark.

Fractile	Oskarshamn, M≥6	Forsmark, M≥6
0.001	1.4	0.8
0.05	4	2.4
0.25	21	12
0.50	**42**	**24**
0.75	83	47
0.95	206	118
0.999	247	142

There are no obvious points of reference with which to rigorously test these results. One test of consistency however, is to compare current levels of seismicity in southern Sweden with the predicted seismicity rate for the final interval of the glacial stressing model, which is comparable to the present time. The average of the predicted seismicity at Forsmark and Oskarshamn for that interval is 0.17 M≥3 earthquakes per year for region within a radius of 100km. For this elicitation Raymond Munier, and Björn Lund assembled earthquake data from the Helsinki earthquake catalogue and Hilmar Bungum assembled the data from NORSAR catalog. The two data sets, which probably have

different levels of completeness and span different time intervals, give quite different levels of seismicity for the SE region of Sweden. The Helsinki catalog indicates about 0.03 earthquakes M≥3/a for a region with a radius of 100km, and the NORSAR catalog indicates about 0.3 earthquakes M≥3/a. Hence, predictions of seismicity for the final stressing stages of the preferred model appear to lie within the uncertainty of current rates for southern Sweden. The SW region has somewhat higher levels of activity than the SE region and both catalogs indicate rates of about 0.4 earthquakes M≥3/a. In summary, the model appears to be broadly consistent with current earthquake rates, but the discrepancies in SE region rates, and the relatively10small numbers of recorded earthquakes at levels of catalog completeness currently prohibit more robust tests.

Conclusion

As any reader of this report may fairly conclude, this analysis employed numerous assumptions, simplifications and approximations. In part these were necessitated by the limited time allotment and restricted scope available for this effort. And in part these reflect the limited state of information and knowledge to be applied to this question. These limitations are reflected in the wide uncertainty bands of the predicted glacial response. It is my opinion that a more comprehensive analysis and study of this question would clarify many issues and could provide a more reliable prediction of the glacial response with narrower uncertainties.

References

Hanks, T.C.,and H. Kanamori, 1979, *J. Geophys. Res.*, **84–B5**, 2348-2350.

Lund, B, and M. Zoback, 1999, Orientation and magnitude of in situ stress to 6.5 km depth in the Baltic Shield, *Int. Jour. of Rock Mech. and Mining Sci.*, **36**,169-190.

Reinecker, J., O. Heidbach, M. Tingay, P. Connolly, and B. Müller (2004): The 2004 release of the World Stress Map (available online at www.world-stress-map.org)

Toda, S., R.S. Stein, P.A. Reasenberg, J.H. Dieterich, and A. Yoshida, 1998, Stress transferred by the 1995 Mw=6.9 Kobe, Japan, shock, *J. Geophys. Res., 103*, 24,543-24,565.

Appendix 8

Glacial load stresses: Can existing faults or other zones of crustal weakness be reactivated during glacial cycles?

Kurt Lambeck.

Elicitation issue 1.
What will be the frequency of moment magnitude 6.0 or greater per unit area (of 100 km^2 in middle and southern Sweden (Forsmark and Oskarshamn) during a glacial cycle assuming conditions similar to the Weichsel glaciation?

1. Introduction.

The scientific questions underpinning the elicitation question can be reduced to three broad questions:

1. What is the evolution of the state of stress in the crust during a glacial cycle or what is the incremental stress induced in the crust by the ice loading and unloading?
2. What is the background stress regime in the crust in Sweden? In the absence of glaciation what stress differences occur due to long-term tectonic processes or due to the inherited structure of the crust and upper mantle?
3. How does the crust respond to the background stress fields and how will it respond to the super positioning of these fields with the deviatoric glacial loading/unloading stresses. Will existing faults or other zones of weakness be reactivated? Are there classes of faults that are preferentially reactivated? How large will be the resulting earthquakes?

Then, if these questions can be answered it becomes possible to consider answers to the specific question of the elicitation, for example:

4. What is the likelihood of fault reactivation at specified localities during past and future glacial cycles?
5. What is the probability of such occurrence of at least one large earthquake occurring at a particular locality during the last glacial cycle?

The answer to the first three general questions has not been formally addressed for specific locations in Sweden and there is no single body of work from which the answers can be extracted. This is in large part because to answer them requires information from various disciplines that do not naturally cross paths. The first scientific question requires knowledge of the past glacial history of Scandinavia as a whole and not just for the final stages of the last ice sheet but also for the entire cycle. (Glacial cycles are defined here as the interval between successive interglacials, times when climate conditions were similar to those of the past ten or so millennia and which repeat at about 110,000 year intervals.) It also requires an ability to predict the behaviour of the next glacial cycle. (Glacial cycles, as defined here, have occurred for about one million years and the average duration of the interglacial phase is of the order of 10,000 years. Thus we assume that it is inevitable that a new onset of glaciation can be expected at some time in the future unless the physical processes currently operating are disrupted.)

Beneath a growing ice load the load stresses are distributed through the effectively elastic lithosphere and into the underlying viscous mantle. Beneath the growing load the crust subsides and on the flanks the crust is deflected upwards, in part because of the flexural response of the 'elastic' layer to the load and in part because the viscous mantle material beneath the area of loading is displaced sideways. The magnitudes and rates of this deformation are controlled by the elastic and viscous properties of the lithosphere and mantle. The stress field generated by the load and the deformation will be approximately proportional to the second spatial derivative of the deformation. Thus in evaluating the stress field a first step is to evaluate the displacement field. This latter is observed at the Earth's surface, both from geological data on time scales of 10^3 to 10^5 years and from geodetic data on time scales of 10^0 to 10^2 years so that models for the earth response to glacial loading can be experimentally tested.

To answer the first question postulated above requires a formulation of the equations governing the response of a planet to changes in surface loads as well as rheological properties of the planet. The theory is well established and the relevant rheological parameters are usually inferred from the observations of the surface response itself. That is, for a quantified ice load what rheology is required to satisfy the observed surface response. But the complexities lie in the detail for the response at any one location and time will be a function of the global changes in load, not just the load at the point in question, and it will be a function of the history of loading because of the viscous behaviour displayed by the Earth. That is, the deformation and stress today is a function of the anterior evolution of the load. A detailed evaluation of this deformational response entails a detailed knowledge of the rheological properties, including the mapping of zones of potential weakness, information that is mostly unavailable and in consequence the models usually rest on simplifying assumptions about the structure of the crust.

The widespread occurrence of earthquakes in the Earth's crust indicates that this layer is stressed even in regions that have not been glaciated or which lie away from the world's tectonically active zones. An ancient continent like Australia, for example, is subject to large earthquakes even though there has been no active tectonics for a hundred million years and more anywhere within its borders. Thus the crust can be considered to be generally close to a critical stress state such that relatively small changes in stress orientation or magnitude may reactivate deformation on zones of weakness. Thus knowledge of the background stress field is required, upon which the glacial-loading stress field is superimposed. Thus the second question requires knowledge of the tectonic processes operating on the Earth as well as of the past processes that have shaped the planet. These past processes have shaped the topography and internal density distribution of the crust and mantle and any departures from hydrostatic equilibrium (from the condition of lateral uniformity of crust and mantle) will create a background stress field. On-going processes such as the drivers of plate tectonics will superimpose regional deviatoric stress fields in the upper layers of the Earth. In the case of Scandinavia, does the sea-floor spreading occurring at the Atlantic Ocean Ridge produce a regional stress field over Scandinavia over and above the stresses created by topography and internal density anomalies? To answer these questions requires access to crustal stress/strain

information that usually comes from a range of field observations of near-surface conditions.

The third question requires knowledge of the strength of the crust and mantle. When and where will brittle failure occur in the cold upper layers of the Earth? Are there zones of weakness where failure is likely to be focussed during increasing stress during a loading cycle? How are the stresses rearranged once failure occurs? It is at this stage that the usual theory exhibits its limitations. The available models all assume that the lithosphere and mantle can be represented by the equations of continuum mechanics and once failure occurs they are no longer valid. Thus they can provide a useful description of conditions up to the time of failure but not beyond. At this point one turns to the seismic evidence, to determine from the field record of seismic activity the frequency with which earthquakes occur in different tectonic settings and to extrapolate to new stress regimes. Does present seismicity define zones that are likely to be reactivated during future stress cycles? Under what stress conditions does this reactivation occur today and how will the frequency of reactivation be altered in response to a modified stress field?

I have attempted to provide answers to the first of the three general questions using models and procedures that have been developed previously for not necessarily related purposes. Only some of these results have been published to date. They include results from a similarly focussed study of crustal stability in Finland (Lambeck and Purcell, 2003) but use a new ice sheet model for the last glacial cycle that is based on an inversion of shoreline data spanning the past 140,000 years (Lambeck et al., 2005). The procedures have been applied specifically here for the localities of interest, Oskarshamn and Forsmark, and for the last glacial cycle. The results for the deviatoric stress regime should be representative of the last cycle and they indicate that large stress differences can develop depending on the location of the site relative to the ice margin and centre of ice loading, on the dimensions of the ice load, and on the thickness of the ice. If the past ice-cycle is a guide to the future then these results can be used as an indicator of future change in crustal stress regime. The second question is answered by a simplified model in which the background stress is driven by 'ridge push'; consistent with a body of field data that suggests a compressive regime across much of Scandinavia (e.g. Zoback, 1992; Lund and Zoback, 1999). We assume that the present-day observed stress state is largely free from residual glacial-cycle deviatoric-stresses, as indicated by model calculations (Lambeck and Purcell, 2003), and that it therefore can be used for extrapolation to past or future background states. The third question is partly addressed by calculations of the degree the crust is stabilized or destabilized by the evolving glacial load-stress, using a parameter known as the change in fault stability margin ΔFSM (Johnston, 1987; Wu and Hasegawa, 1996). This parameter determines whether stress on a potential fault shift towards or away from a failure limit but, because the failure limit is usually unknown, it does not predict whether failure actually occurs. To establish this latter condition it should be possible to compare the model calculations against palaeo-fault data: if faults occurred in the past and the magnitude of displacement can be determined then the comparison with the model-predicted stress conditions would determine the failure limit. In the case of the Oskarshamn region there may be some evidence that suggests that some of the late glacial shorelines have been displaced subsequent to their formation (N.-O.

Svensson) but this needs to be substantiated with further fieldwork. In the absence of that the calibration can be done using the faults from northern Sweden although this requires an assumption of uniformity of crustal properties across Sweden.

2. Evolution of the stress field induced by the last glacial cycle.

2.1 Background

The stress calculation for loading of the earth by a time-dependent surface load, the ice sheet, involves several steps:

(i) definition of the surface load, in this case of the cyclic exchange of mass between the ice sheets and the oceans,
(ii) establishment of an appropriate earth rheology,
(iii) evaluation of the displacement and strain fields at and within the surface of the planet, and
(iv) evaluation of the incremental stress field.

(i) The surface load assumed for this study is the past ice load over Scandinavia, Arctic Russia, and the Barents-Kara Seas. Because of a broad regional influence of the North American ice sheet on the Scandinavian crust the ice model is supplemented with loads of other ice sheets and, for the sake of completeness, the changing water load in the ocean basins and adjacent seas. As Scandinavia lies on the broad bulge around the larger Laurentide ice sheet the contribution from the latter is not wholly negligible and results in a spatial asymmetry of the stress field around the Scandinavian load (Lambeck and Purcell, 2003). Also, for the early part of the cycle, Scandinavia lies on the broad bulge that formed around the arctic Russian ice and this introduces a temporal asymmetry in the stress fields for the stages 5 and 4 glacials and the last glacial when there was no or only very little ice over arctic Russia.

The derivation of the ice load for the LGM and post-LGM interval has been previously described and is the outcome of an inversion of sea-level data across northern Europe for earth-rheology and ice-thickness parameters (Lambeck et al., 1998a). The most recent iteration of this inversion is used (Lambeck and Purcell, 2003). The ice load for the pre-LGM starting with the penultimate glacial maximum (the Saalian) is also based on a combination of ice-margin information and simple glaciological models constrained by the inversion of shoreline location and sea level data (Lambeck et al., 2005). This pre-LGM load history focuses on the interval from the Late Saalian (~ 150,000 -140,000 years ago), the penultimate glacial maximum, through to the Early Middle Weichselian (~ 60,000 years ago). These latter characterise the onset of the glaciation over Scandinavia, culminating in the first post-Eemian large-scale glaciation of Sweden. The model includes an approximate ice history for the Middle Weichselian period from ~ 60,000 years ago to the Last Glacial Maximum at ~ 20,000 years ago with a short interglacial period, the Bø, following stage 4, but does not include well-developed Jæren and Ålesund intervals. Thus the results presented here will not contain all of the rapid fluctuations in the ice advance and retreat that occurred during the latter part of Middle Weichselian (MIS-3). Overall, the ice model used for the past 150,000 years exhibits all of the characteristics of the last glacial cycle and can be expected to also cover likely changes in any future cycle.

Because of the viscoelastic response of the earth the isostatic rebound at any time is a function of earlier changes in the ice sheet. Thus to model the rebound for the last glacial cycle an earlier cycle has been introduced in which the total ice volume is consistent with the global sea-level fluctuations inferred from the marine oxygen isotope record of Waelbroeck et al. (2002) and in which the ice has been distributed between the component ice sheets in the same ratios as for the last glacial cycle. In so far as the 'memory' of the previous cycle contributes less than 20% to the sea level signal of the next cycle, an uncertainty in the early ice sheet of 50% introduces an uncertainty of less than 10% in the predictions for the next cycle.

(ii) The rheology of the Earth's mantle is assumed to be linear. This is largely for mathematical convenience but it is also consistent with the field evidence. This means that, for the time and stress scales considered, the earth response is approximated by a linear rheology quantified by effective parameters that describe the observed rebound phenomenon on these time scales. The parameters are estimated from the rebound observations themselves. Strategies have been developed that ensure that the ice sheet and rheological parameters are adequately separated although some correlation may still occur (Lambeck et al., 1998a,b; Lambeck 1999). That is, different combinations of earth and ice parameters may describe equally well the observed deformation field and predict equivalent stress fields. For the following calculations an elastic lithosphere over a viscoelastic mantle is assumed with elastic moduli estimated at seismic frequencies and mantle viscosity parameters described in Lambeck and Purcell (2003). Calculations with a range of model parameters that are consistent with the observed fields indicate that the uncertainty introduced by this choice is O (10%).

In the model results used below, the adopted effective lithospheric thickness is 80 km and it includes the crust and part of the upper mantle. Thus on the time scales and stress levels of glacial cycles it is this layer that acts as an elastic layer that is subject to negligible stress relaxation. The mantle viscosity immediately below the lithosphere is 4×10^{20} Pa s.

(iii) The theory for the deformation of the Earth under ice and water loads is well established and theory and solutions have been independently checked. The model is for a spherical, radially stratified earth model, with a linear Maxwell visco-elastic response so that the Love Number formulation can be used (Peltier, 1974; Cathles, 1975). This has the advantage of maintaining a gravitationally consistent description of the ice-water load, and of allowing analysis of detailed load geometries through harmonic decomposition of the load and super positioning of the responses to each harmonic component. The theory used here (Nakada and Lambeck, 1987; Lambeck and Johnston, 1998; Lambeck et al., 2003) is recognised as being both complete and accurate (Mitrovica and Milne, 2003). The displacement field includes the horizontal and radial displacement. The radial displacements can be tested against the geological field evidence for sea-level change or the geodetic evidence for radial surface displacement. The horizontal displacements are not recorded in the geological data and the geodetic observations are not yet adequate for reliable results. Thus the two components are

related by the theory of continuum mechanics. This has the consequence that certain classes of earth models cannot be adequately tested.

(iv) The stress calculations associated with the glacial loading and unloading also follow established theories for linear viscoelastic bodies using the standard formalism relating stress to strain rate with appropriate boundary conditions. The latter include zero traction at the outer surface of the earth and the normal stress at the surface determined by the load. The normal stress at iso-density surfaces within the earth is specified by the buoyancy force due to the displacement of more (or less) dense material during deformation. The results used here have been checked against those developed by Wu and Hasegawa (1996) (see also Wu et al., 1999: Johnston et al. 1998). The background stress field includes the hydrostatic field plus, for some of the results discussed below, an assumed plate-tectonics stress field. The complete deviatoric stress tensor is calculated as a function of depth. For the calculation of the stress, but not the strain field, we assume incompressibility in the lithosphere as this facilitates considerably the solution through the property relating the radial displacement gradient to the displacement as a function of position (e.g. Johnston et al. 1998). The full deviatoric stress tensor (the departure from a hydrostatic reference state) is defined by six elements τ_{rr}, $\tau_{r\theta}$, $\tau_{r\lambda}$, $\tau_{\theta\theta}$, $\tau_{\lambda\lambda}$, $\tau_{\theta\lambda}$ where r is the radial direction, (positive outwards), θ (colatitude) is the direction in the meridian (positive south – the direction of increasing colatitude), and λ (longitude) is along a latitude circle, (positive eastward). Extensional stresses are defined as positive.

(v) The evaluation of the possible failure mechanisms is done using the Fault Stability Margin (*FSM*) criteria. If σ_1, σ_2, and σ_3 represent the maximum, intermediate and minimum (extensional) principal stress components, then the Fault Stability Margin is defined as (see Fig. 1)

$$FSM = \beta\,[2\tau_0 - \mu(\sigma_1 + \sigma_3)] - (\sigma_1 - \sigma_3)/2$$

where

$$\beta = \sin(\tan^{-1}\mu)/(2\mu) = (1+\mu^2)^{-1/2}/2$$

The cohesion τ_0 and the friction coefficient μ define the failure limit of the material according to Byerlee's law

$$\tau = \tau_0 - \mu\,\sigma$$

where τ is the shear stress on the fault plane and σ is the stress normal to the fault plane (e.g. Johnson 1970; Jaeger & Cook 1979). Typically $\mu \approx 0.6$. In terms of a conventional Mohr representation of stress, the FSM is the minimum distance of the Mohr circle from the failure limit. The position of this limit is usually not known but its slope is defined by μ. In the above definition of the *FSM* the principal stresses represent the total stress field. The change in Fault Stability Margin from the initial stress state $\tau_{i,j}^{(0)}$ is given by

$$\Delta FSM = FSM - FSM^{(0)}$$

where $FSM^{(0)}$ is the value for the pre-load condition (the hydrostatic and plate-tectonic stress fields). The change in Fault Stability Margin is therefore represented by the amount by which the Mohr circle is displaced towards or away from the failure criteria limit when an incremental stress is added to the background stress. With the sign convention adopted here negative FSM correspond to stable conditions. For the results to be consistent with the usual convention, the sign has been changed throughout. Thus negative values of ΔFSM indicate that the Mohr circle has shifted towards the failure

limit and that the incremental stress field enhances the likelihood of faulting for optimally oriented 'virtual' faults. That is, existing faults close to this orientation and for which the background stress is close to critical may be reactivated under the influence of the glacial unloading. Positive values for the Δ*FSM* indicate enhanced fault stability.

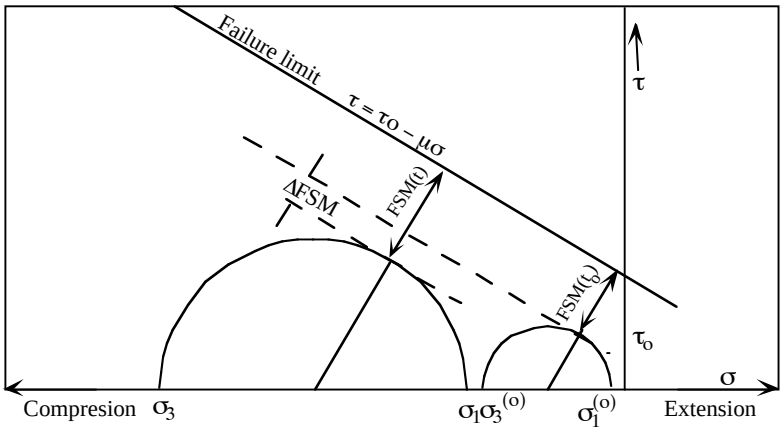

Fig. 1. Definition of the Fault Stability Margin *FSM*. Compressive stresses are negative. $\sigma_1^{(0)}$ and $\sigma_3^{(0)}$ are the maximum and minimum principal stresses of the reference state and σ_1 and σ_3 are the maximum minimum principal stresses of the perturbed state. Δ*FSM* is the change in the Fault Stability Margin. In this case it is positive and the incremental stress stabilises the fault.

2.2 Results

2.2.1 The interval since the Last Glacial Maximum. We calculate here the isostatic rebound and the associated stress field for the last two glacial cycles, starting at the penultimate interglacial at about 240,000 years ago. If we assume that future cycles will be similar to the past cycles then we can use this result as a prediction for future change by equating the Last Interglacial, from 130,000 to 120,000 years ago, with the present interglacial, the Holocene. For the preliminary results given below we present only the stress variation during the past 20,000 years, from the LGM to the present. This permits a comparison to be made with previously published results. For the preliminary results, the only background stress considered is the hydrostatic state $\sigma_i^{(0)}$ (i =1,2,3) = ρgD where ρ is the crustal density, g gravity and D depth in the crust. That is, we assume that before 240,000 years before present the earth was in hydrostatic equilibrium and it is then cyclically loaded and unloaded up to the present. By starting at this early time we ensure that any long-period relaxation times are adequately represented. We calculate the stresses up to the present and any non-hydrostatic components will be today's residual stress from the previous glacial cycles.

Figure 2 illustrates the deviatoric stresses for the Forsmark locality at the surface and at 5 and 15 km depth. The components shown are τ_{rr}, $\tau_{\theta\theta}$, $\tau_{\lambda\lambda}$ and the other components $\tau_{r\theta}$, $\tau_{r\lambda}$, $\tau_{\theta\lambda}$ are small such that the first three components approximate principal stresses. (The largest off-diagonal values occur for $\tau_{\theta\lambda}$ and approach 15% of $|\tau_{max}|$. They are non-zero because of the asymmetry of the ice sheet. The components $\tau_{r\theta}$, $\tau_{r\lambda}$ are non-zero but small, the non-zero values resulting from the changing orientation in space of level

surfaces through time.) The behaviour is similar for the three depths so that it will generally suffice to consider the results at 15 km as being representative for the crust. (The model is effectively that of an elastic layer, of depth-dependent properties, over a viscous mantle. Thus the load is partly supported by the mantle and the concept of zero deviatoric stress on a middle plane does not provide a good approximation. Also, the shear modulus increases with depth and this will also result in a modified depth dependence of stress when compared with standard engineering plate solutions. Only at depths greater than ~ 15 km does the depth dependence become significant.) Note that compressional stresses are negative. All three major components are compressional with the radial (positive outwards) being of least absolute value and if failure were to occur it will be by thrust faulting. Figure 3 gives similar results for Oskarshamn.

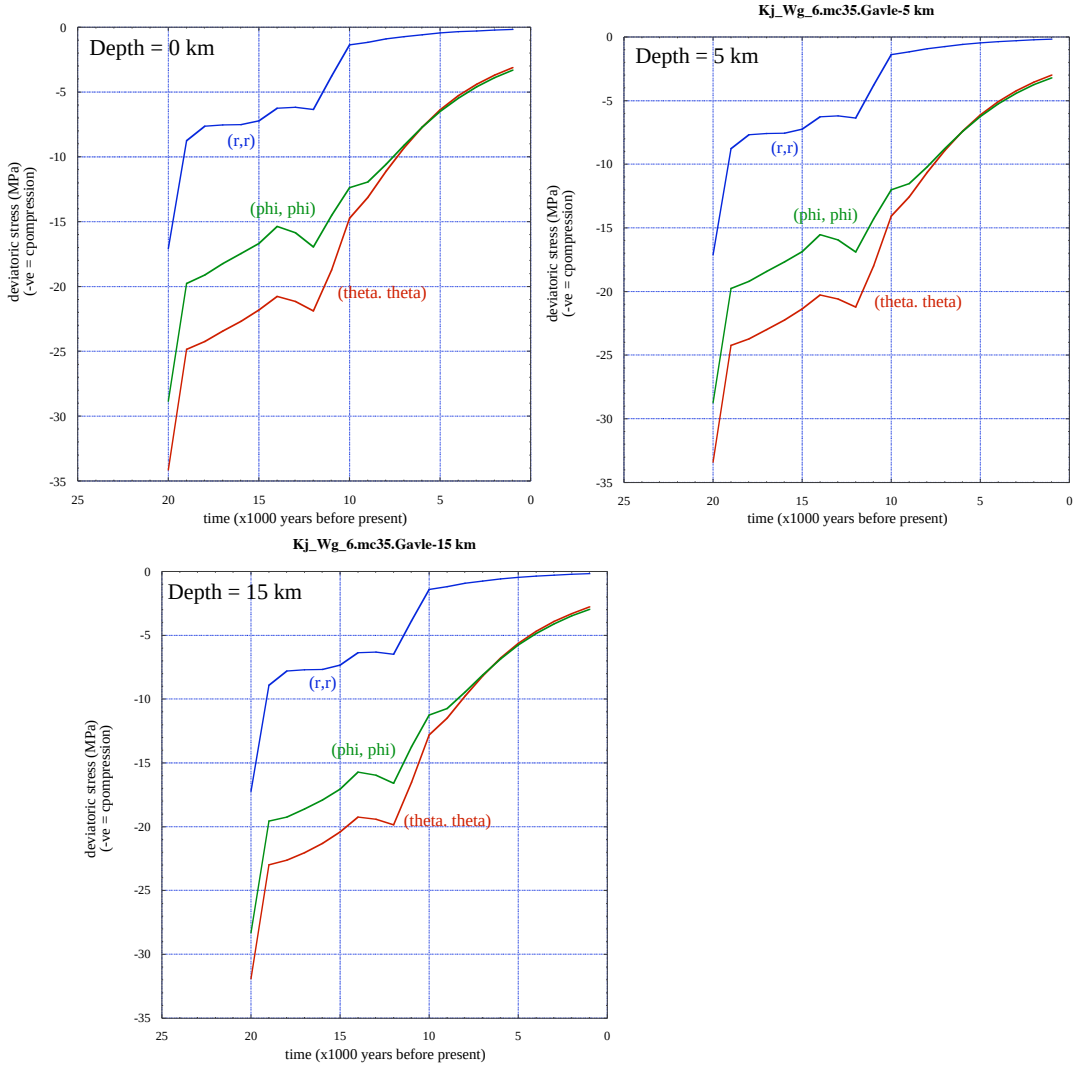

Figure 2. Deviatoric stress at Forsmark from the LGM to the present due to glacial loading and unloading of the last two glacial cycles. (r,r) = τ_{rr}; (phi,phi) = t_{ll}; (theta,theta) = $\tau_{\theta\theta}$,

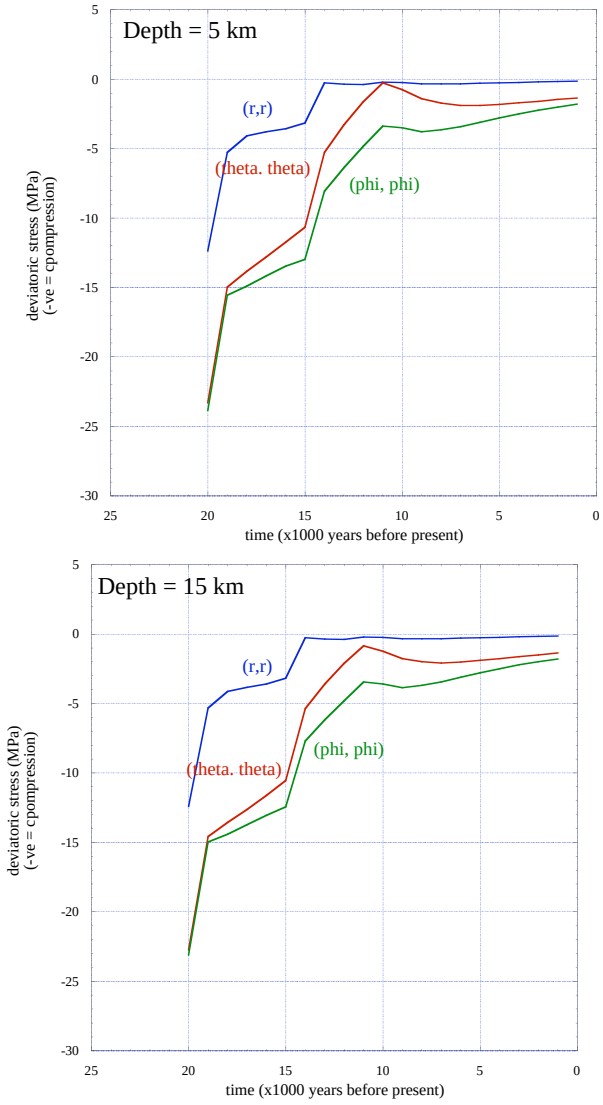

Figure 3. Same as Fig. 2 but for Oskarshamn and at 5 km and 15 km depths only.

At both sites the rapid change in stress at ~ 20,000 years is because in the ice model the ice load has remained approximately constant from ~ 26,000 to 20,000 years ago and is then followed by a rapid collapse over the Gulf of Bothnia causing the late advance of ice over the northern European Plain and down the Baltic to Denmark (Lambeck et al., 2000). The small increase in the magnitude of the stress at ~ 12,000 years is because the ice retreat halted at this time (the Younger Dryas) and a small increase in ice occurred. The stresses given above are the incremental stresses from the ice load cycle. The total stress is the sum of this field and the hydrostatic background field (I have ignored other stress fields for the moment) and this is illustrated in Fig. 4 as the principal stresses at both Forsmark and Oskarshamn for 5 km depth. The patterns are similar but the magnitudes of the stresses differ by a few MPa because of the different ice loads (magnitude and time of retreat) for the two localities.

The change in Fault Stability Margin is illustrated in Fig. 5. Initially the values are positive and the ice stabilises the crust (the Mohr circle is moved away from the failure limit) but at about the time of retreat of the ice from the region (or when the ice has become thin) the sign changes and the crustal stability is reduced. The peak destabilising occurs earlier at Oskarshamn than at Forsmark because of the earlier ice retreat at the first site and the maximum amplitude of $|\Delta FSM|$ is greater at Forsmark because the ice thickness there was greater than at Oskarshamn.

The table below summarizes the principal stresses at three depths including the orientation of the maximum compressive stress. The vertical stress is the least compressive stress at all times. At Forsmark the orientation of the maximum principal stress remains nearly constant over the depth range considered but at Oskarshamn the two horizontal principal stresses change order between 5 and 10 km depth.

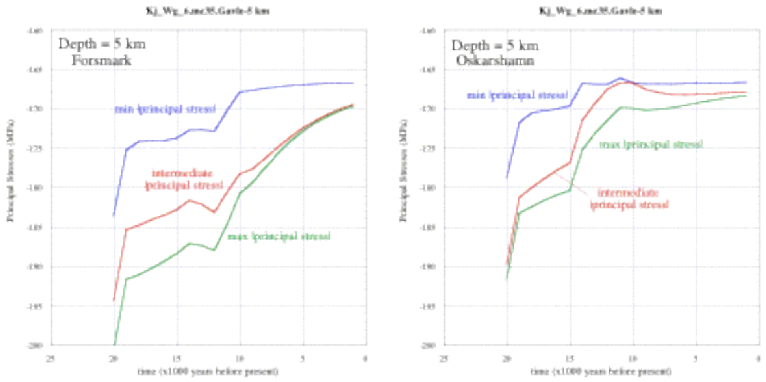

Figure 4. Principal stresses at 5 km depth at the two localities.

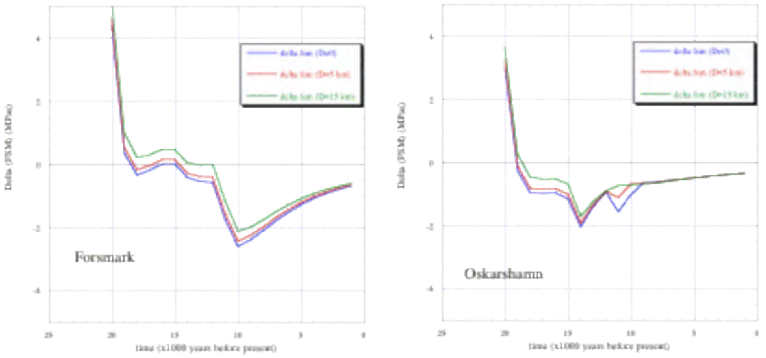

Figure 5. Change in Fault Stability Margin at three depths at the two locations.

Table 1. Principal compressive stresses as function of depth at time of maximum crustal instability.

Site	Time yr before present	Depth km	Max. comp. (M Pas.)	Azimuth (degrees) (- ve=west)	Interm. comp. (MPas.)	Least comp. τ_{rr} (MPas.)
Forsmark	10,000	5	180.8	-17	178.2	167.9
		10	346.6	-19	344.4	334.4
		15	512.5	-20.1	510.4	500.9
Oskarshamn	14,000	5	187.1	-15	181.6	166.7
		10	341.2	77	338.1	333.3
		15	507.3	78	504.8	499.8

2.2.2 Results for extended time series 140 ka BP to present. The above results are illustrated below for the longer time series, from the end of the penultimate interglacial at ~140,000 years ago to the present (the load cycle for the previous glaciation is included hence deviatoric stresses are not zero at the start of the Last Interglacial). The character of the Weichselian ice margin movements of the adopted model at the two localities can be seen from Figure 6 which illustrates the radial stress τ_{rr} at the surface. During the early Weichselian, the stress fluctuations at the two sites are small because the ice margins during the stadials MIS-5d and MIS-5b lie to the north of Oskarshamn and only reach Forsmark during the latter stadial (MIS-5b). The first post-LIg glaciation of the Oskarshamn region occurs during MIS-4 at ~ 64,000 years ago, with the ice being significantly thicker over Forsmark than Oskarshamn. Thereafter the southern margin of the model ice sheet fluctuates rapidly in keeping with the global sea-level oscillations at this time. The adopted model includes major ice retreat at the end of MIS-4, during the Bø Interstadial when the ice retreated from Oskarshamn but not from Forsmark, and some later rapid but small fluctuations of the ice across the southern area, including a major Middle Weichselian Baltic Ice Advance at ~ 45,000 years ago. (The Ålesund interstadial at ~ 37,000 years ago which is sometimes taken to be a time of almost total ice retreat from Scandinavia (Arnold et al., 2002) has not been included in this model. It will introduce a further oscillation at ~ 37,000 to ~ 33,000 years ago similar to that at ~ 45,000 years ago.)

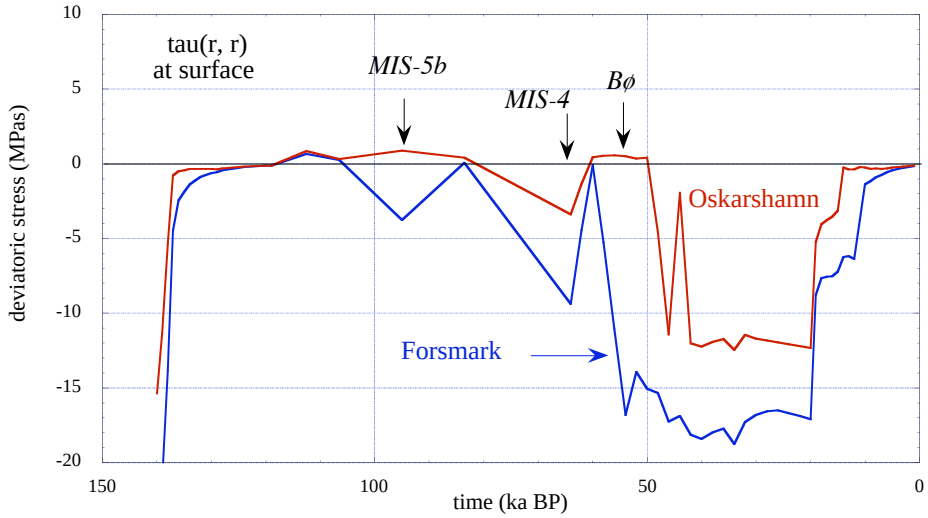

Figure 6. The radial stress component at the τ_{rr} surface at the two sites.

Figure 7 illustrates the major deviatoric stress components τ_{rr}, $\tau_{\theta\theta}$, $\tau_{\lambda\lambda}$ for the two sites. In interpreting such results two factors need to be kept in mind: (i) because the stresses generated by the surface loads are spatially distributed, the stress at any one site is not only a function of the load immediately over the site but also of the loads away from the site, and (ii) because of the viscous memory of the mantle, the stress at any time reflects not only the load at that time but also the earlier loads. In consequence, the deviatoric stresses can fluctuate significantly from one location to another and this is seen in these results, with the predicted stress pattern at Oskarshamn being quite different from that at Forsmark. In particular, extensional deviatoric stresses $\tau_{\theta\theta}$, $\tau_{\lambda\lambda}$ are predicted to occur at Oskarshamn at ~ 50,000 years ago, but not at Forsmark because while the former site is

ice-free it lies on the peripheral bulge of the deformation created by the more northern ice.

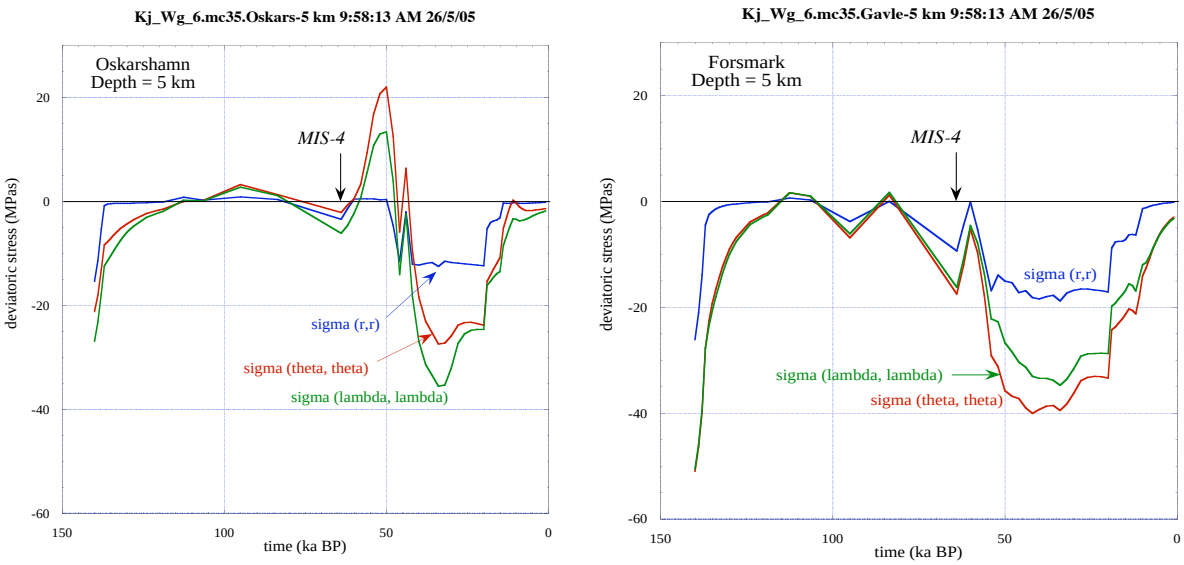

Figure 7. The deviatoric stress components τ_{rr}, $\tau_{\theta\theta}$, $\tau_{\lambda\lambda}$ at (left) Oskarshamn and (right) Forsmark.

Because the work for which the ice model used here has not focussed on the Middle Weichselian period, the ice history for the interval from 60,000 – 30,000 years ago is uncertain and does not include the Ålesund interstadial. Thus predictions of the stress field for this period are correspondingly less certain than for the other periods and may undergo additional oscillations in the period 40,000 to 30,000 years ago. Nevertheless, the ice model captures the main characteristics of the last glacial cycle: the initial ice activity being restricted to the high ground of Norway and Sweden followed by periods of rapid advance of ice from the north and times of ice retreat before the maximum glaciation develops. Thus while the timing of the predicted stresses may be questioned, the magnitudes are representative of what will have occurred during the past glacial cycle and that can be expected to occur during a future cycle.

Figure 8 illustrates the predicted ΔFSM for the two locations. The major destabilisation is predicted to occur at Oskarshamn at ~ 50,000 years ago, corresponding to the time when rapid fluctuations occur in the location of the ice margin and when the stress field at Oskarshamn is determined by the flexural stresses in the peripheral zone of the ice load that extended south to about Forsmark. Any failure at this time would occur as normal faulting with a preferred east-west fault orientation.

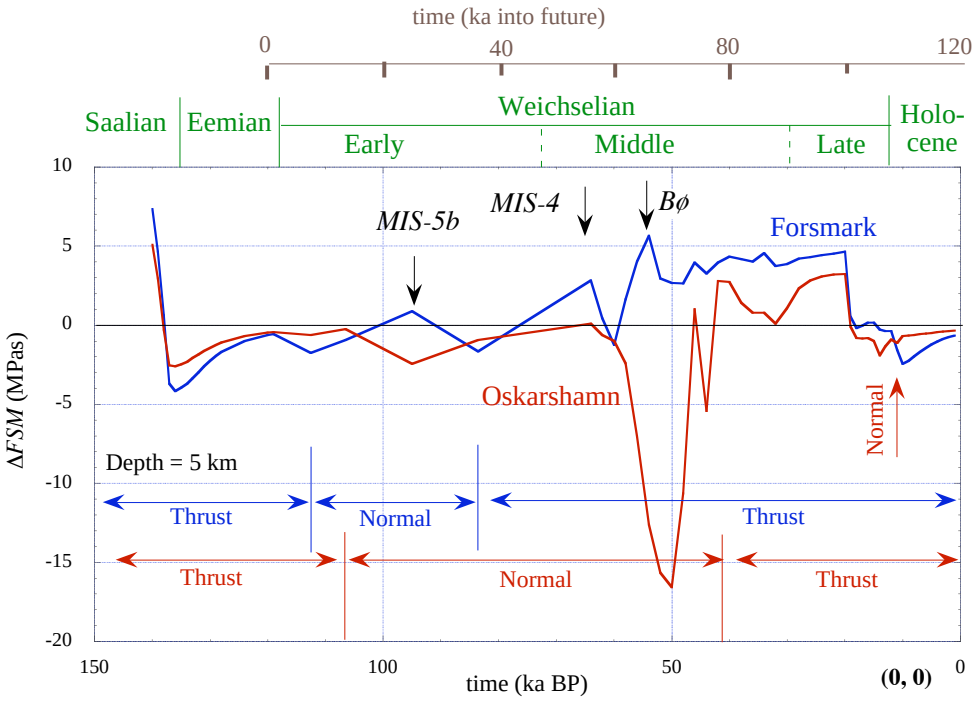

Figure 8. ΔFSM predictions for the Forsmark (blue) and Oskarshamn (red) locations indicating the styles of preferred faulting should failure occur. The predictions are for a depth of 5 km. No in-plane stress has been applied. The time scale at the top of the diagram is the schematic future change assuming that (i) we are near the end of the present interglacial and (ii) that the next glacial cycle replicates the past cycle.

2.3 An answer to the first general question.

The incremental stress regime during a past glacial cycle can be predicted with some confidence once the glacial history has been quantified. This quantification still contains elements of speculation because of the incomplete preservation of the records for the past glacial advances and retreats. But the model adopted here is believed to have the characteristics of a typical glacial cycle with initially slow build up and the peak glaciation coming only late in the cycle. The calculations show that the predicted stress fields vary significantly from location to location, particularly when the ice sheets grow larger and the sites lie close to maximum ice margins. This arises because of the dependence of the flexural stresses in the peripheral bulge zone on both the height and radius of the ice sheet (c.f. Figure 4, Lambeck and Nakiboglu, 1980). Thus Forsmark is an intrinsically more stable site than Oskarshamn, all other factors being the same, because when it lies on the bulge, the ice sheet creating it is relatively small and localised over northern Sweden. But Oskarshamn in on the bulge only when the ice sheet has become correspondingly larger. Were failure to occur at either site during the glacial cycle it would be seen preferentially as normal faulting at the Oskarshamn locality at the time that the ice sheet first reached into southern-central Sweden. How the crust actually responds will depend on the stabilizing influence, or otherwise, of the background stress field.

The most notable result is the large instability that develops at Oskarshamn at the end of MIS-4. This glacial stage is unusual for the last cycle in that it is the first time since the last interglacial that a large ice sheet develops over Scandinavia, one that begins to match the subsequent glacial maximum during stage 2, while at the same time the last of the large Russian ice sheets centred on the Kara Sea (Svendssen et al., 2004), began its retreat. During the retreat of these ice loads, southern Sweden lies on the bulge of both ice loads and the component stress field are both extensional such that their combined effect is to introduce the crustal instability noted in Fig. 8. As the ice sheets retreat the extensional stresses grow until the time of the next ice advance over the area at 50 ka when the load stress exerts a stabilising influence. During this time central Sweden remains beneath the ice and the effects of the two loads tend to cancel out. A similar but smaller amplitude instability develops in southern Sweden during the earlier stadial, MIS-5b.

3. Background tectonic stress field.

3.1. Results

The background tectonic stress comprises several components. One part is topographic stress and this would evolve slowly with time due to erosion and sedimentation. It has been demonstrated that this can be a significant component along the Norway margin but it has not been previously considered for Sweden. These stresses will typically be of the order ρgh where ρ is the crustal anomaly, g gravity and h the elevation. Another component is the non-hydrostatic stress resulting from density anomalies in the crust and upper mantle. These will be comparable to the topographic anomalies because of the general state of isostasy reached in the crust. We do not consider these components here because for both localities the topographic variations are relatively small. The third component is the plate tectonics stress.

This stress field can be inferred from the present-day stress orientation measurements on the assumption that these stresses now dominate the largely relaxed glacial-load stresses. Such measurements (Stephansson, 1989, 1993; Claus et al., 1989) show considerable variability probably due to topographic stresses and to internal crustal structures including faults. Stress indicators from depths of 300 m or greater show greater consistency and point to a mainly NW-SE direction of maximum compression (Zoback, 1992; Lund and Zoback, 1999). Thus I assume that the principal tectonic stress is one of compression, with the maximum stress orientation being NW-SE. I do not specify the stress magnitude since this is largely unknown but also because it is only the stress difference that is important in defining the ΔFSM (Wu & Hasegawa, 1996). Estimates of ~ 5-10 MPa for the stress drop on some of the palaeo faults of Sweden (Arvidsson 1996) suggest that an appropriate value for the maximum stress difference for the plate-tectonic stress is of this amplitude and I adopt 10 MPa.

The background stress field modifies the Mohr circle construction in Fig. 1 in two ways: the centre of the Mohr circle shift along the principal stress axis and the radius of the circle is modified. Beneath the ice a compressive regional stress field shifts the Mohr circle to higher (negative) values and the radius increases such that the two modifications compensate and the ΔFSM estimate remains unchanged, provided that the deviatoric in-

plane stresses are less than the principal load stresses as will generally be the case for large ice sheets (c.f. Fig. 2). Only near the margins of the ice sheet will the effects of a compressive regional stress field modify the Δ*FSM* estimates in any significant manner. In particular, where the incremental (glacial load) stress field is extensional the effect of the in--plane stress is to drive the crust to a state of greater stability and to change the potential style of faulting from normal to thrust. Hence we can expect that the southern Sweden results will be more sensitive to the choice of in-plane stress parameters than the central Sweden results.

This is illustrated in Figure 9 for the two sites and for σ_H^{max}-σ_H^{min} = -10 MPa with a NW-SE orientation for the maximum horizontal stress axis σ_H^{max}. The results are for 5 km and are representative of upper crustal depths.

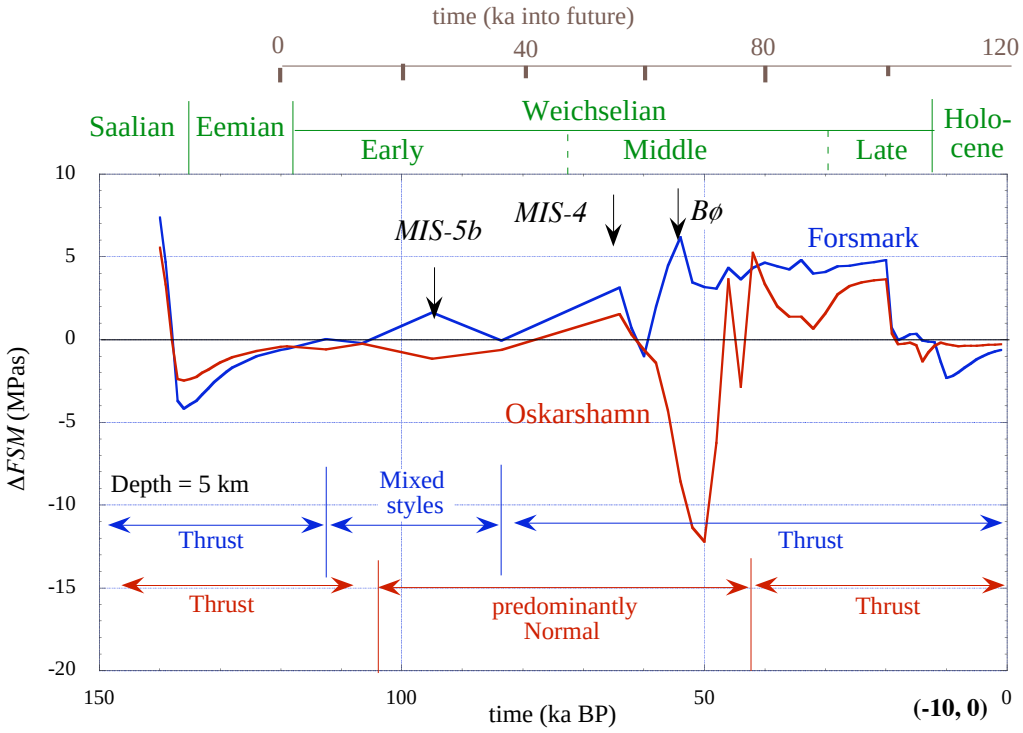

Figure 9. Same as Figure 8 but with an in-plane stress state of σ_H^{max}-σ_H^{min} = -10 MPa and with the maximum stress direction from NW to SE.

This result differs from the zero in-plane stress case primarily during the Middle Weichselian interval and then at the Oskarshamn site only, with the crust moving towards a more stable state and the possibility of failure by normal faulting is now decreased to a short time interval only, from 56,000 to 44,000 years ago.

3.2 An answer to the second general question.

A consensus opinion on the background stress field would be that it is compressive with the axis of maximum in-plane stress oriented normally to the Atlantic Ridge axis. There is also a consensus that the stress drops for large Scandinavian earthquakes is of the order -10 MPa, which suggests that the crust in compression is able to support stresses up to

about this limit. The effect of the in-plane stresses is to stabilize the crust in two important ways: (i) the stress state moves away from the failure limit when compared with the zero in-plane stress state, and the nature of faults with preferred orientation changes from normal to thrust (compare Figures 8 and 9). The total stress state again is spatially variable and the maximum departures from stability occur at Oskarshamn for the same reason as for the zero in-plane case.

4. The state of stress in Northern Sweden after the last glaciation.

The predictions discussed above indicate that substantial stress differences can develop in the crust during a glacial stress cycle and that there is a potential for reactivation of existing faults or zones of weakness. If this has occurred at either locality it should be seen mainly at times when particular combinations of ice sheet margin, ice thickness and site location occur. Such conditions are most likely to occur when the site lies near the edge of a large ice sheet and of the two locations considered, the Oskarshamn region is more likely to be subject to earthquake triggering than the Forsmark area, all other factors being the same. The most probable time of occurrence during the last glacial cycle is prior to the LGM but if surface faulting had occurred the surface evidence will have been largely erased by the last part of the glacial advance and retreat. These Middle Weichselian stresses are larger than during the last phase of deglaciation because at this latter time there is not the contribution from an eastern ice load.

Where unambiguous postglacial faulting has occurred is in northern Sweden with the well-known post-glacial faults (Lagerbäck, 1990, 1992), the largest of which Pärvi Fault with an estimated moment magnitude of 7.6 according to Olesen et al. (2004) or 8.1-8.2 according to Bungum et al. (2005) and Arvidsson (1996). To establish an empirical relationship between moment magnitude and the Δ*FSM* estimates, the stress state for northern Sweden has been calculated using the same procedure as for the Forsmark and Oskarshamn sites. Results are shown in Figure 10 for three fault locations; Lansjärv, Lainio and Pärvi for the same in-plane force case as in Fig. 9.

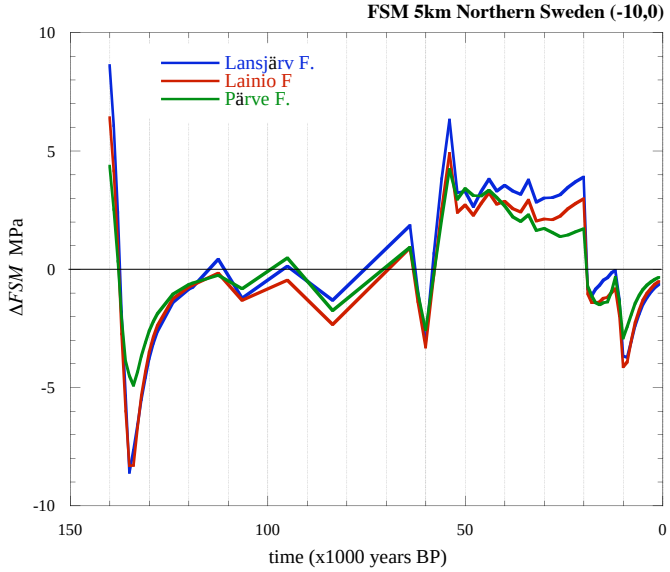

Figure 10. Predicted Δ*FSM* values at three of the northern Sweden faults for the case with in-plane horizontal stress and at 5 km depth.

As the three sites all lie well within the ice margins at all times of major glaciation, these results are largely unaffected by the choice of in-plane stress provided that the deviatoric stress of the latter is less than the incremental load stresses at these sites. The results indicate that the maximum departure from stability occurs after the retreat of the ice from the region, particularly at the end of the glacial maxima at 9000-10,000 years (calibrated) before present, consistent with estimates of the age of the faults (Lagerbäck, 1979, 1992), and at the end of the penultimate interglacial, but also at the end of the MIS-4 glaciation. Thus the faults can be expected to be reactivated several times during any one glacial cycle and as there have been at least 8 major cycles since the onset of the present glacial pattern, it would not be surprising if the earthquake zones represent major zones of weakness as a result of repeated faulting.

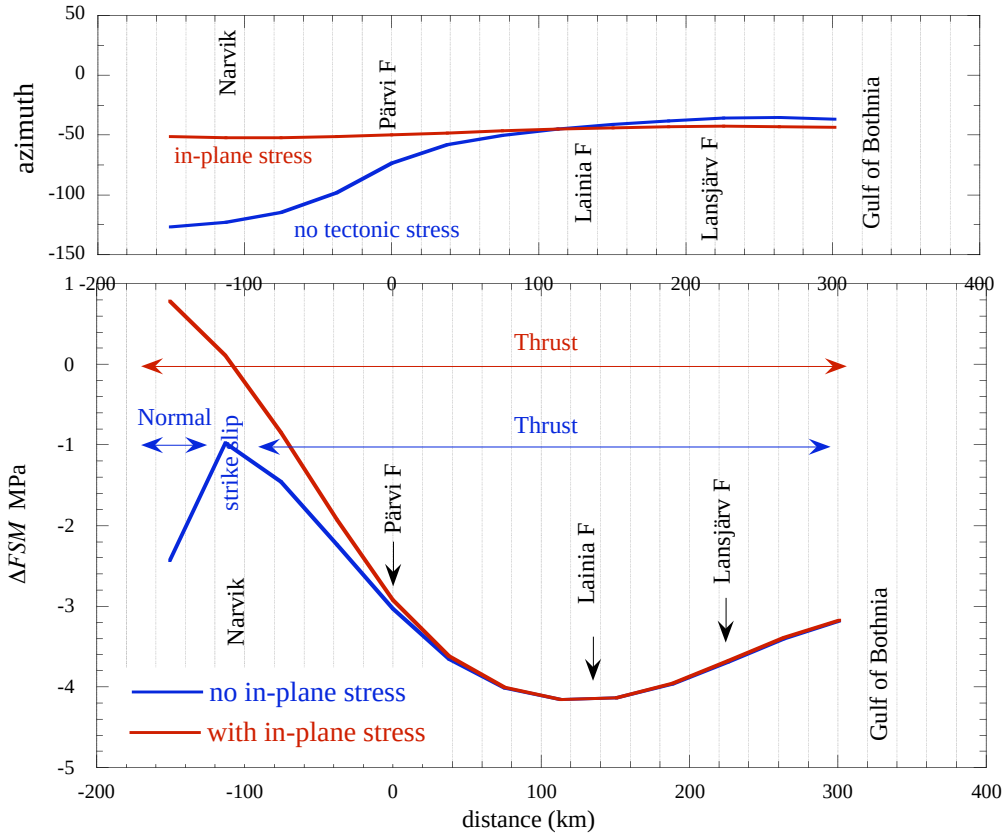

Figure 11. Predicted Δ*FSM* values at 10,000 years ago along a section from the Norwegian shelf near Lofoten to the Gulf of Bothnia for the two in-plane stress states (blue zero in-plane stress, red, deviatoric stress of –10 MPa) and at 5 km depth. The top part of the figure indicates the predicted orientation of the maximum horizontal stress vector for the two cases.

The change in ΔFSM along a section across northern Sweden and Norway at 10,000 years ago is shown in Figure 11 for the two background stress states. Only at the margins of the former ice sheets, in this case at the Norwegian margin, do the two cases differ in both the magnitude of the ΔFSM and in the style of faulting. The value ranges between -3 and -4 MPa over the area encompassed by the faults with failure occurring by thrusting. Only at the Atlantic coast does the preferential fault mechanism change, rotating from thrust through strike slip to normal. The orientation of the maximum principal horizontal stress is also indicated in Figure 11. For the zero in-plane stress condition this azimuth rotates from ~-36° at Lansjärv to about -73° at Pärvi fault but when the in-plane force is introduced this rotation is much less significant (~ 10°) and within observational noise.

Generally these model predictions for the northern Swedish region are consistent with the field evidence for the faults and styles of faulting, suggesting that the model predictions should also be realistic for the southern and central Sweden localities discussed above. In one regard the situation in northern Sweden differs from that in southern-central Sweden in that the topographic relief, including that of the Norwegian shelf is more important and the background stress may need to be modified to take this into account. In addition, there may be a long-term evolution of this stress if erosion and sedimentation has been significant. The erosion-sedimentation stress is primarily that predicted by elastic plate theory since the time constants here are probably longer than for the glacial loading cycle; thus, at the surface, extensional stress will occur at the locus of unloading and compressive stress at the centre of sediment loading across the shelf. Some simple models for this stress field have been considered in the context of studying the stability of the shelf margin during glacial loading (Lambeck and Purcell, 2002) which indicate that this incremental stress field may amplify the instabilities for sites closer to the coast such that if this effect was included for the above transect it would drive the crust further from stability at sites such as Pärvi than at Lansjärv. Estimates for this contribution are of the order of 0.2 MPa for an average plateau erosion of 10m and fjord deepening of 40 m per glacial cycle with offshore deposition of 50% of the material eroded at any time (Lambeck and Purcell, 2002). This is less than the uncertainty in the glacial stress estimates and this contribution can probably be ignored. It is, however, interesting to note that the Pärvi fault is larger than the ones to the east, although the stress calculation suggests that the deviatoric glacial-rebound stresses are the largest and this may be a consequence of these additional incremental stress fields.

5. The response of the crust to glacial loading at Forsmark and Oskarshamn.

The results for northern Sweden indicate that failure can occur with earthquakes of seismic moments up to 7.6 at a time that ΔFSM ~ -4 MPa. On the assumption of uniform rheology and distribution of faults between this region and the Forsmark and Oskarshamn areas (I am not aware of evidence that would allow me to avoid this assumption) then, with Figure 9, we would infer that failure is likely to occur at the Oskarshamn locality, if there are zones of weakness with preferred orientation. In contrast, failure is not predicted for the Forsmark site. Comparing the Oskarshamn and northern Sweden results (Figures 9 and 10) indicate that the maximum departure from stability occurs at the former site with ΔFSM values of the order of –10 MPa during the special load

configuration of MIS-4 whereas such values are approached in northern Sweden only at the end of the intense penultimate glaciation. Thus major failure would be predicted to have occurred at that time, and at the end of earlier major glaciations, with reactivation having occurred at the end of the last glaciation. In contrast, the last opportunity for failure at Oskarshamn would have occurred before the last glacial maximum and, in a region where the ice was probably warm-based, the morphological evidence for surface faulting can be expected to have been largely removed.

6. Response to Elicitation issue 1.

6.1 Preamble

The results for northern Sweden suggest that one can have confidence in the principles of the model stress calculation and on the inferences of when the crust approaches more stable or less stable states. Different parameters for the earth structure and rheology will change the magnitudes of the stress estimates but I would not expect a change in the overall stress regime. The biggest uncertainty resides in the assumptions about the ice history. Future glacial cycles are likely to exhibit the same cyclic behaviour of the ice sheet growing and retreating with successive advances extending further south. The early part of the cycle is unlikely to produce large deviatoric stress fields. Sites where (i) the ice is not very thick and (ii) that do not lie near the margin of 'large' ice sheets are unlikely to be subject to large negative ΔFSM values. Forsmark satisfies these criteria, Oskarshamn less so.

The Northern Sweden earthquakes indicate that moment-magnitude 7.6 earthquakes do occur when ΔFSM values are ~ -5 MPa. Such values are predicted for Oskarshamn but not for Forsmark. Based on the mapping of the northern area, there is > 100 km between faults with ~ 12 faults in an area 400x400 km. Thus the probability of an earthquake occurring in a unit area of 100 km^2 of northern Sweden in the immediate post-glacial period is ~1/130 (or ~1 in 4 for an area of radius of 100 km).

ΔFSM values of –5 MPa can be reached at Oskarshamn at least once during a typical glacial cycle. The faults that will be preferentially reactivated at such times are normal faults. If such faults exist then there is a potential for crustal failure. By analogy with the Northern Sweden evidence, the probability of such failure occurring once in any unit of 100 km^2 is 1/130. This assumes that every unit of area has a similar distribution of zones of weakness and has had a similar glacial-stress cycle. The present background seismicity at Oskarshamn appears to be relatively low, suggesting that there are no zones of particular weakness in the area and that any present energy release occurs preferentially away from the area. Thus the above estimate of 1/130 is likely to be an upper limit. If I use the current density of earthquakes as a measure of stability (crust twice as stable as half the number of earthquakes) then I would place a lower limit (3σ) at 1/400. Because I do not have knowledge of the structural geology and cannot assess whether there is a probability of there being unmapped faults, I would place an upper limit (3σ) at 1/100.

In contrast to Oskarshamn, Forsmark is an area that is less likely to be destabilized at any time during glacial cycles unless future glaciations are more intense than that of the Late

Saalian. Perhaps as a corollary, the location is also one where current seismic activity is low compared with other regions. The Late Saalian glaciation appears to have been the most intensive one since the onset of the 100,000-year cycle about 800,000 years ago. Thus the probability of such an intense glaciation occurring again is taken at 1/8.

6.2 Inference:

Oskarshamn: Some seismic activity at the level of moment-magnitude 7.6 may be triggered by glaciations in southern Sweden during a full glacial cycle at times of particular ice geometries. Such geometry is predicted to occur about once in a glacial cycle. At that time, the probability of at least one earthquake of such magnitude occurring in a unit area of 100 km^2 is about 1 in 130 within a cycle of 100,000 years. For areas where the current seismicity is low, this probability will be reduced. My assessment that 1/130 is a reasonable estimate for the probability, with limits of 1/400 and 1/100 (3σ estimates).

Forsmark: Seismic activity at the level of moment-magnitude 7.6 is unlikely to be triggered by glaciations in central Sweden during a full glacial cycle. In addition, current background seismicity is low. Thus probabilities will be less than that for Oskarshamn. I place the probability of an earthquake of moment-magnitude 7.6 occurring in a unit area of 100 km^2 at about an order of magnitude less.

7. References.

Arnold, N.S., van Andel, T.,Valen, V., 2002. *Quat. Res.*, **57**, 38-48.
Arvidsson, R., 1996. *Science*, **274**, 744-746.
Bungum, H., Lindholm, C., Faleide, J.I., 2005. *Mar. Petrol. Geol.*, **96**, 2249-2265.
Cathles, L.M., 1975. *The Viscosity of the Earth's Mantle*, Princeton University Press.
Claus, B., Marquardt, G., Fuchs, K., 1989. In *Earthquakes at North-Atlantic Passive Margins: Neotectonics and Postglacial Rebound*, pp. 277-287. eds S. Gregersen et al., Kluwer.
Jaeger, J.C., Cook, N.G.W., 1979. *Fundamentals of Rock Mechanics*, Methuen.
Johnson, A.M., 1970. *Physical Processes in Geology,* Freeman, Cooper and Co.
Johnston, A.C., 1987. *Nature*, **330**, 467-469.
Johnston, P., Wu, P., Lambeck, K., 1998. *Geophys. J. Int.*, **132**, 41-60.
Lagerbäck, R., 1979. *Geol. Foren. Stockholm Forh.*, **100**, 263-269.
Lagerbäck, R., 1990. *Geol. Foren. Stockholm Forh.*, **112**, 333-354.
Lagerbäck, R., 1992. *J. Geol. Soc. Lond.*, **149**, 285-291.
Lambeck, K., 1999. *J. Geol. Soc.*, **156**, 465-486.
Lambeck, K., Johnston, P., 1998 In *The Earth's mantle: Composition, Structure, and Evolution*, pp. 461-502, ed. I. Jackson, Cambridge University Press.
Lambeck, K., Nakiboglu, S.M., 1980. *J. Geophys. Res.*, **85**, 6403-6418.
Lambeck, K., Purcell, A., 2002. Tech. Rept, Univ. Bergen.
Lambeck, K., Purcell, A., 2003. Tech. Rept 2003-10, POSIVA, Helsinki.
Lambeck, K., Smither, C., Johnston, P., 1998a. *Geophys. J. Int.,* **134**, 102-144.
Lambeck K., Smither, C., Ekman, M., 1998b. *Geophys. J. Int.,* **135**, 375-387.
Lambeck, K., Yokoyama, Y., Johnston, P., Purcell, A., 2000. *Earth Planet. Sci. Lett.*, **181**, 513-527.
Lambeck, K., Purcell, A., Johnston, P., Nakada, M., Yokoyama, Y., 2003. *Quat. Sci. Revs.* **22**, 309-318.
Lambeck, K., Funder, S., Kjær, K., Larsen, E., Möller, P., 2005. *Boreas* (in prep.)
Lund, B., Zoback, M.D., 1999. *Int. J. Rock Mech. Min. Sc.* **36**, 169-190
Mitrovica, J.X., Milne, G.A., 2003. *Geophys. J. Int.*, **154**, 253-267.
Nakada, M., Lambeck, K., 1987. *Geophys. J.*, **90**, 171-224.
Oleson, O., Blikra, L.H., Braathen, J.F. et al., 2004. *Norweg. J. Geol.*, **84**, 3-34.
Peltier, W.R., 1974. *Rev. Geophys. Space Phys.*, **12**, 649-669.

Stephansson, O., 1989. In *Earthquakes at North-Atlantic Passive Margins: Neotectonics and Postglacial Rebound*, pp. 213-229, eds S. Gregersen et al., Kluwer.

Stephanson, O., 1993. In *Comprehensive Rock Engineering, Principles, Practice and Projects*, pp. 445-459, ed. J.A. Hudson, Pergamon Press.

Svendsen, J.I., Alexanderson, H., Astakhov, V.I. et al. (eds), 2004. Quat. Sci. Revs., **23**, 1229-1271.

Waelbroeck, C., Labeyrie, L., Michel, E. et al., 2002 *Quat. Sci. Revs,* **21**, 295-305.

Wu, P. Hasegawa, H.S., 1996. *Geophys. J. Int*., **125**, 415-430; **127**, 215-229

Wu, P., Johnston, P., Lambeck, K., 1999. *Geophys. J. Int*., **139**, 657-670.

Zoback, M.L., 1992. *J. Geophys. Res*., **97**, 11703-11728.

Appendix 9

Large earthquakes during a glacial cycle

Report to the June 2005 SSI expert panel

Björn Lund
Department of Earth Sciences
Uppsala University
Sweden

1 Introduction

This report contains my contribution to the Swedish Radiation Protection Authority (SSI) expert panel elicitation on earthquakes during a glacial cycle. On May 17-18, 2005, SSI gathered a panel of five experts in order both to evaluate an elicitation methodology [*Hora and Jensen*, 2002] and to obtain expert opinion on the likelihood of large earthquakes due to glaciation. It was pointed out by SSI that the numbers resulting from the elicitation process were not going to be used as the basis for a hazard assessment for a nuclear waste repository. The experts were allocated five days of work on the elicitation issues and were then due to meet again for two days, June 20-21, 2005, to present their results and to participate in the actual elicitation.

During the initial meeting, we discussed two proposed elicitation issues and decided to focus on the first issue, with experts addressing the second issue only if there was enough time. The first issue was slightly modified from the original formulation:

Elicitation issue 1 What will be the frequency of moment magnitude 6.0 or greater earthquakes per unit area (e.g. per 100 sq. km) in the middle and south of Sweden (Forsmark and Oskarshamn) during a glacial cycle (approximately 100000 yr) assuming conditions similar to the Weichsel glaciation? Give an uncertainty distribution for this quantity for each area.

Two common assumptions were made:

1. The maximum earthquake moment magnitude should be 7.6 (nominal value for the Pärve fault [*Stewart et al.*, 2000]).
2. A thickness of the seismogenic crust of 30 km.

I have addressed the issue with the following modifications.

1. As a background, non-glacial seismicity rate I have used the references agreed on during the first meeting, which are cast in terms of local magnitudes, not necessarily based on moment magnitudes.

2. I have used a circular area of radius 100 km, i.e. 31415 km^2.

3. The glacial model supplied by Kurt Lambeck [*Lambeck*, 2005] has a time step starting at 106.5 kyr BP, which I used as the starting point for my analysis.

This report contains the basic assumptions underlying my analysis, a description of the method I used and comments on the uncertainties. It should be noted that the five days allocated for this work did not allow a full analysis with proper treatment of uncertainties and modelling verification.

2 Approach to elicitation issue 1

The influence of a large ice sheet on seismogenesis has been discussed using essentially two different lines of thought. On one hand, as discussed by e.g. *Johnston* [1987, 1989], an ice sheet suppresses the seismicity induced by tectonic loading, causing strain energy to accumulate and then be released in a burst at the end of deglaciation. On the other hand, as modelled by e.g. *Quinlan* [1984]; *Wu and Hasegawa* [1996]; *Johnston et al.* [1998]; *Lund* [2005], fault stability during the glacial cycle is affected by the stresses induced in the Earth by the ice load. In this report, I will follow the latter approach but instead of neglecting the tectonic strain release I will allow it as a constant seismic base rate in the calculations that follow. This is not in agreement with the suppression of seismicity observed by e.g. *Johnston* [1987], but is a simple way to incorporate the tectonic strain effect.

As the basis for my work here I have utilized the models of glacially induced stresses provided by K. Lambeck [*Lambeck and Purcell*, 2003; *Lambeck*, 2005] to the expert panel; current seismicity in southern Sweden as reported by the Helsinki bulletin, the Swedish National Seismic Network and the compilation by *LaPoint et al.* [1999]; the maximum magnitude earthquake agreed on in the elicitation question; and a model for the temporal evolution of seismicity by *King and Bowman* [2003]. Using the glacially induced stresses I have estimated the stability of faults during the glacial cycle for different assumptions on the existing tectonic stress field. The resulting temporal variations in fault stability were then used as a basis for estimating the temporal variation in seismicity rate, using a variation on the method proposed by *King and Bowman* [2003] and estimates of the current background rate and the maximum activity rate. Finally, the number of earthquakes of magnitude six or higher were summed over the glacial cycle.

3 Glacially induced stresses

The modelling of the Earth's response to an ice load, i.e. Glacial Isostatic Adjustment, is nowadays rather well understood and developed. Refinements such as fully three-dimensional and high resolution models are still emerging, but the fundamental aspects of lithospheric bending and glacial rebound is well established, see Lambeck's contribution to this compilation. Climate driven ice sheet models [e.g *Näslund et al.*, 2003] and a multitude of empirical data such as shore-line displacements, lake-level data, glacial moraines etc. provide further evidence that there is good reason to believe that a future glaciation will not be fundamentally different to the latest glaciation. For the purpose of estimating crustal stresses during the next glacial cycle we will, therefore, use the stresses estimated from the Weichselian ice sheet model of *Lambeck* [2005]; *Lambeck and Purcell* [2003].

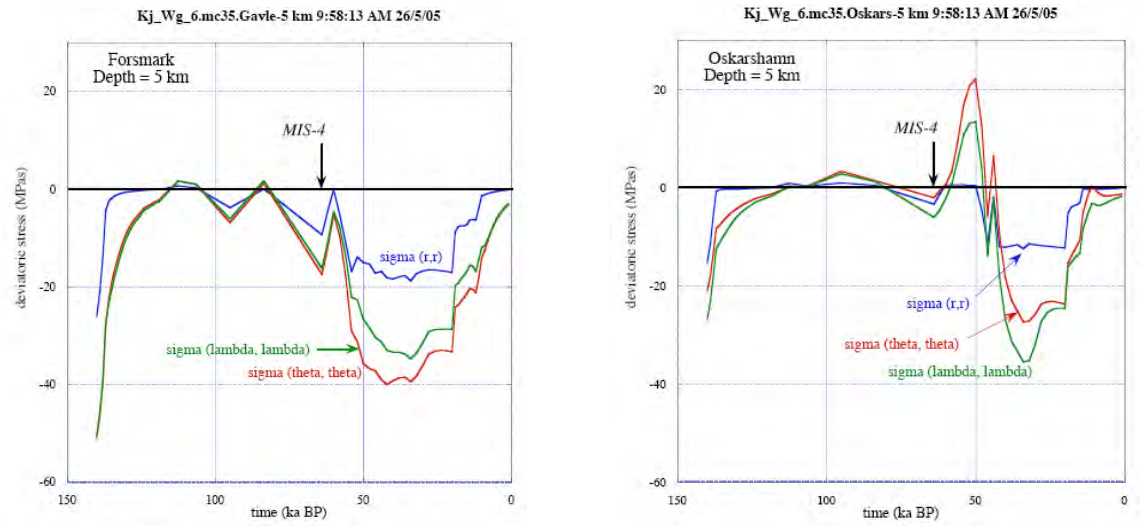

Figure 1: Evolution of the stress field at 5 km depth at Forsmark (left) and Oskarshamn (right). σ_{rr} is the radial (vertical) component, $\sigma_{\theta\theta}$ the colatitude (south horizontal) component and $\sigma_{\lambda\lambda}$ the meridian (east horizontal) component. These stresses only contain the glacially induced stresses. From *Lambeck* [2005], Fig. 7.

Figure 1, from *Lambeck* [2005], shows the evolution of the horizontal and vertical stresses at Forsmark and Oskarshamn during the last interglacial and the subsequent Weichselian ice age. We see the decrease in stress at the end of the previous glaciation, at approximately 135 kyr BP, how Oskarshamn is virtually ice free (the vertical stress, σ_{rr}, is approximately zero) until 65 kyr BP and how there is varying, but increasing each time, ice coverage over Forsmark. The large tensional stresses induced at Oskarshamn are due to the fore-bulge created by the thickening of the ice sheet to the north. Through the final stage of the glaciation both Oskarshamn and Forsmark are covered by thick ice and, thus, show similar behavior. We note that the horizontal stresses are always larger in magnitude than the vertical stress. The reversal in which of the horizontal stresses is the largest between the two sites are due to three-dimensional effects [*Lambeck 2005, personal communication*].

Fig. 1 shows that the glacially induced stresses are very sensitive to the location of the ice margin. In addition, the stresses also depend on the slope of the ice margin and the thickness of the ice. Hence, small variations in the ice model have can have large impact on the stress levels so, due to the inherent uncertainties in our knowledge of the location of the ice front in a subsequent glaciation, I will not treat Oskarshamn and Forsmark as separate sites but instead perform the analysis using the modelled stresses from the two sites as possible variations at a single site in southeastern Sweden.

4 Fault stability during the glacial cycle

The stability of faults in the stress fields created by a glaciation depends on a number of factors in addition to the glacially induced stresses. The background, tectonic stress field, the strength of the crust and pore pressure effects are all vital to an analysis of fault stability [see e.g. *Wu and Hasegawa*, 1996; *Lund*, 2005]. The following analysis will be based on the Coulomb failure function

$$CFF = \tau - \mu(\sigma_n - P) - \tau_0 \tag{1}$$

where τ and σ_n are the shear and normal stresses on the fault plane, μ is the coefficient of friction, P the pore pressure and τ_0 the cohesion. The *CFF* measure is positive when the shear stress on the fault is large enough to cause failure, and negative if the fault is stable. As is customary when analyzing fault stability at depth in the crust, the cohesion will be ignored in the following. Pore pressure effects are very important for fault stability and the addition to the crustal pore pressure from the ice sheet is likely to be varying substantially in time and space due to varying basal pore pressure conditions. In the analysis presented here I have considered a hydrostatic pore pressure in the crust without contribution from the ice sheet, i.e. assuming very low pore pressure under the ice sheet.

The initial stress field, in this case the sum of the lithostatic (overburden) stress, the tectonic stresses and any other contributors to the stress field such as topography or varying layer thicknesses in the Earth, is very important when assessing the likelihood of of fault instability. On the scale of plate tectonics, a glacial cycle of 100 kyr is a short time and we would, therefore, expect the preglacial tectonic stress field to be similar to the current tectonic stress field. Erosion during glaciation affect the topography, and thus the stresses, but this is a relatively small effect. Approximately 10 kyr have passed since the last ice left southern Sweden and any remaining glacially induced stresses are modelled to be very small. I will, thus, consider the initial stress field to be similar to the current ambient stress field.

What the current ambient stress field is, is however not a trivial problem. There are not many stress measurements made below 1 km depth in Sweden, and stresses above 1 km are generally severely affected by local geological conditions. *Slunga* [1991] showed that earthquake focal mechanisms in southern Sweden generally agree on a strike-slip state of stress with a direction of maximum horizontal compression of $\mathrm{N60^{\circ}W}$. *Lund and Zoback* [1999] found a strike-slip regime with the maximum horizontal stress in the direction $\mathrm{N65^{\circ}W}$ in the two deep boreholes in Siljan, central Sweden. A number of authors have found that individual earthquakes in Sweden show large variation in their focal mechanisms, from normal to reverse faulting, with an increasing number of reverse faulting mechanisms in the more northerly parts of Sweden. Magnitudes of the in-situ stresses are even more elusive, an exception being the *Lund and Zoback* [1999] study. In the following, I will use both a strike-slip and a reverse faulting ambient stress field. Since there is so little data, I will assume an initial crustal stress field in failure equilibrium on optimally oriented faults, using laboratory derived coefficients of friction [see *Zoback and Townend*, 2001, for a short review]. The stability analysis below will consider the stability of the most unstable, i.e. optimally oriented, faults in the area. I use a coefficient of friction of 0.6 when constructing the initial stress field and when analyzing fault stability with the Coulomb failure function.

Fig. 2 shows the inferred stability of optimally oriented faults in the Oskarshamn and Forsmark areas for a variety of different initial stress states. Generally, we see that the direction of the maximum horizontal stress, σ_H, has very little effect on fault stability. Comparing with Fig. 1, we also see that in the case of a reverse faulting stress state, stability is enhanced when the sites are ice covered and instability is promoted during phases of rapid deglaciation, both at the end of the previous glaciation and at the end of the Weichsel glaciation. The onset of instability comes earlier at Oskarshamn than at Forsmark, as expected by the deglaciation history. We note that the general collapse of the ice sheet at approximately 19 kyr BP destabilizes faults in Oskarshamn but not in Forsmark, where further deglaciation is necessary before instability occurs.

Turning instead to the strike-slip initial states in Fig. 2, we see that there is some difference between the two initial states, the purple state based on the *Lund and Zoback* [1999] being at all times more stable than the green state. This is due to the difference between the

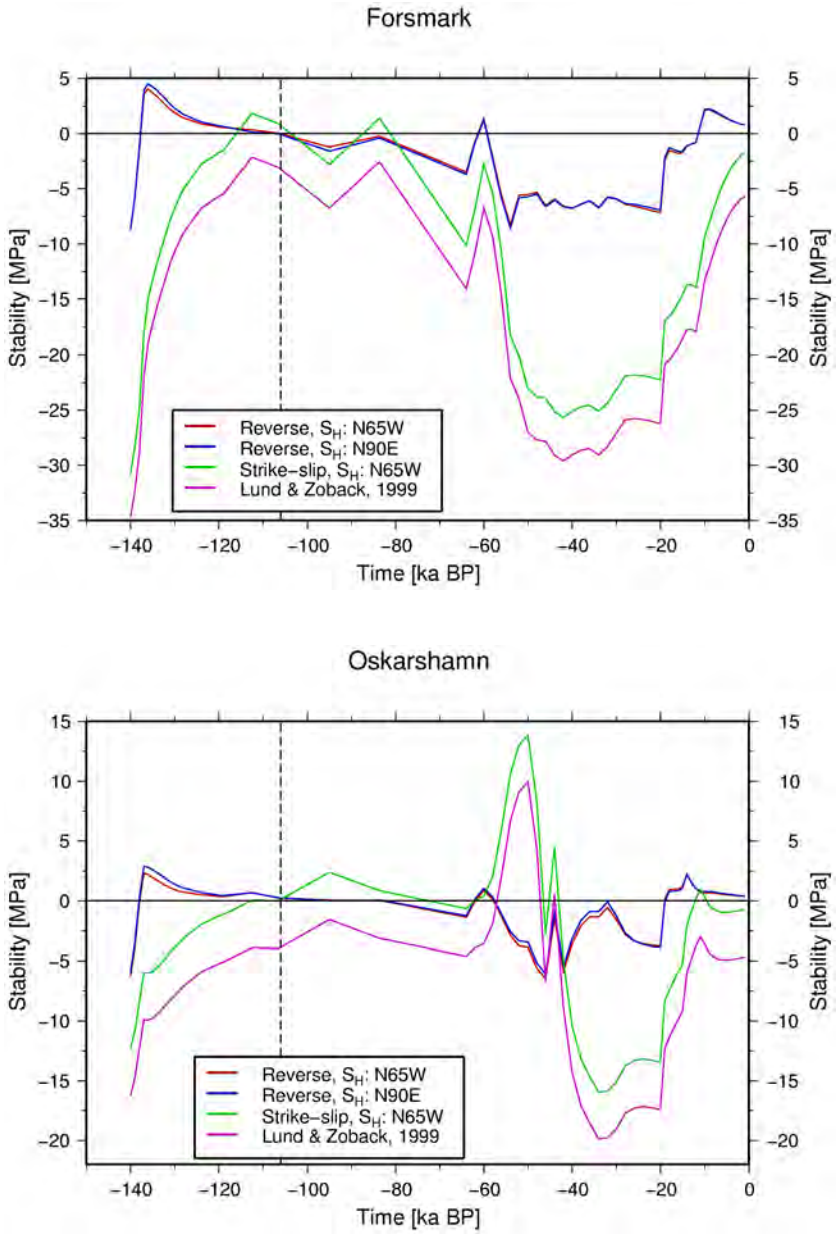

Figure 2: Estimated fault stability at Forsmark (upper) and Oskarshamn (lower) during the glacial cycle. Red, blue and green lines use an initial state of stress in frictional equilibrium (see text) whereas the purple line uses the stress state from *Lund and Zoback* [1999]. Red lines have a reverse faulting initial state of stress, with maximum horizontal stress, σ_H, in the direction $\mathrm{N65^\circ W}$. Blue lines have a reverse faulting initial state of stress with σ_H E-W, approximately parallel to the ice edge. Green lines have a strike-slip faulting initial stress state with σ_H in the direction $\mathrm{N65^\circ W}$.

horizontal stress magnitudes being lower in the *Lund and Zoback* [1999] stress state than for the state constructed to be in frictional equilibrium using a coefficient of friction of 0.6. We also note a large difference between the two sites. As discussed above, the Oskarshamn region experiences a glacially induced tensile horizontal stress during the growth of the ice sheet 60-50 kyr BP. At that time, Oskarshamn is in the fore-bulge of the bending lithosphere and with a strike-slip initial state, fault instability is strongly promoted. During the most heavily glaciated times, faults are stabilized and the deglaciation does not cause any strong tendencies for fault instability, as in the reverse faulting case. At Forsmark, the strike-slip

state has indications of fault instability during the early glacial phase, but for most of the glacial cycle faults in Forsmark are stabilized by the glaciation.

Summarizing, we see that a reverse faulting state of stress causes fault instability at deglaciation in both areas. The combination of high horizontal stresses from the initial stress state and high residual horizontal stresses from the glaciation, after the ice has disappeared, will always cause fault instability at deglaciation. A strike-slip initial state, which is more likely considering the current stress field in southern Sweden, will however not produce similar conditions of fault instability at deglaciation. It is more likely that strong fault instability was present during mid-glacial times. The large difference between Oskarshamn and Forsmark depend on details of the ice model. It is, probably, not unlikely that conditions similar to those modelled for Oskarshamn could occur in Forsmark and I will, therefore, not distinguish between the two sites in the further analysis.

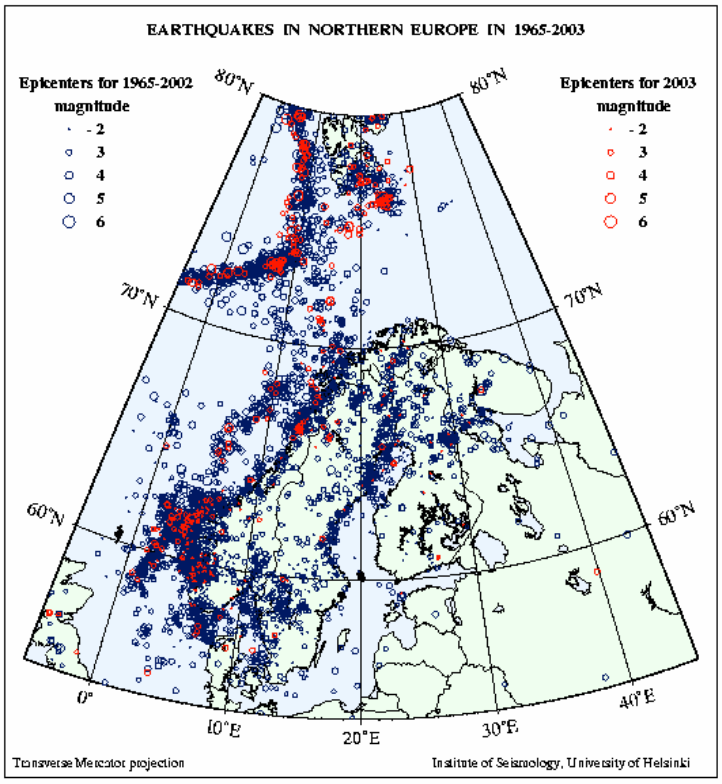

Figure 3: Seismicity of northern Europe, 1965 - 2003, as recorded by the Helsinki bulletin [*Fincat*, 2005]. Note the scarcity of events in southeastern Sweden.

5 Seismicity of southeastern Sweden

The stresses induced by a glaciation will modify the non-glacial seismicity of an area, increasing or decreasing it as faults are moved closer to, or further away from, stability. In order to establish the background seismicity, we have investigated a number of different sources of seismic data for the region of interest. Both Forsmark and Oskarshamn are located in areas of very low seismicity, as is much of southeastern Sweden, see Fig. 3. The Helsinki catalog [*Fincat*, 2005] contains data from region, which is reasonably accurate from approximately 1965. The magnitude of completeness is probably around 2.5, which is very high compared to the maximum recorded magnitude in the region, which is on the order of 3.5 during the time of the catalog. [*LaPoint et al.*, 1999] estimated a magnitude-frequency relation for southeastern Sweden, which they normalized to a circular region of radius 100 km (31415 km^2) and a time of 100 kyr, see TR-99-03 in Fig. 4. In the Figure I have included frequency-magnitude relationships for 40 years of data from the Helsinki catalog [*Fincat*, 2005] for southeastern Sweden (red line), as defined in the note supplied to the expert panel by SKB [*Munier*, 2005]. I also included an estimate based on only 3.2 years of data, scaled to 40 years, from the new Swedish National Seismic Network (SNSN) (purple line) [*Böðvarsson and Lund*, 2003]. We see that the Helsinki and SNSN estimates are lower than the [*LaPoint et al.*, 1999], but since I have not carried out an in-depth analysis of the data, I will use the [*LaPoint et al.*, 1999] data as the current seismicity, and also as the constant tectonic background seismicity. This background rate will produce 2.7 events equal to or above magnitude six in the circular area in 100 kyr [*LaPoint et al.*, 1999].

Elicitation issue 1 was formulated using a maximum magnitude earthquake for Sweden during the glacial cycle. I will use this event, and a Gutenberg-Richter relation based on the event and a b-value of approximately one, as the basis for a model of the seismicity at the

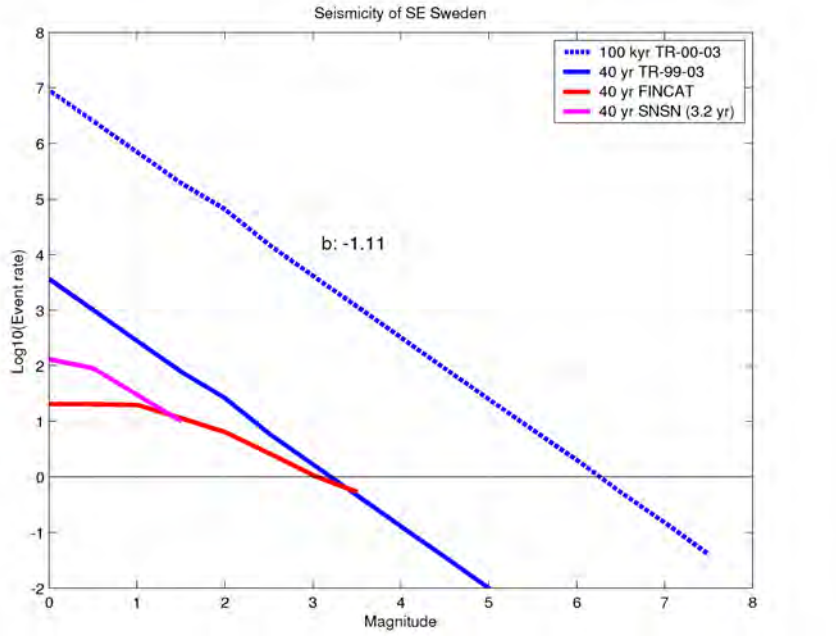

Figure 4: Gutenberg-Richter relationships for various earthquake data sets for southeastern Sweden. TR-99-03 is the [*LaPoint et al.*, 1999] data, FINCAT is the Helsinki bulletin and SNSN the data from the new Swedish National Seismic Network, see the text for details.

time of peak activity during the glacial cycle, whenever that period occurs.

6 Modelling stress evolution

The stability analysis performed above gives an indication of how stable faults are at different times during the glacial cycle. In order to use this information to estimate seismicity levels, I use a model by *King and Bowman* [2003] for earthquake statistics based on Mohr-Coulomb failure stress considerations. They studied the evolution of seismicity between large earthquakes, using the stress field induced by the earthquake together with tectonic stress accumulation with time. The model considers an inhomogeneous background stress field where faults are at or below failure in a random pattern. This background field is then disturbed by the occurrence of a large earthquake, which increases stress in some areas, causing aftershocks, and relaxes stress in other areas. As tectonics reload the fault region, earthquakes are produced in the areas where stress increases. Tectonic strain accumulation is continued until the area is ready for another large earthquake. *King and Bowman* [2003] use a rectangular grid of 300 by 300 nodes to which they randomly assign a Coulomb failure stress. The evolving stress field is added at the nodes and nodes at which the Coulomb stress reaches failure are counted as earthquakes. The magnitude of an event depends on how many failing nodes (N) are connected, all connected nodes are counted as one event with the magnitude determined as $M = N^{0.3}$. The model produces enough earthquakes at each time step to estimate the Gutenberg-Richter relation, which makes it possible to investigate b-value variations.

The *King and Bowman* [2003] model considers an area where large earthquakes and tectonic strain accumulation combine to produce spatially and temporally varying stresses which affect the inhomogeneous background field. This approach is not directly applicable to the situation considered here, which studies two separate sites where stress is only varying in time, with the glacial cycle. However, the model can still be used to generate frequency-magnitude relationships for the stress fields pertaining to different times in the glacial cycle. I generate a grid of randomly distributed CFF-values, mostly below the failure threshold but with enough nodes above the threshold to reproduce the background seismicity Gutenberg-Richter relationship. I then proceed to model the Gutenberg-Richter relationship for the time period of the maximum magnitude event, $\mathrm{M_W}$ = 7.6, by adding the maximum CFF value for the considered scenario to all the nodes, as well as by increasing the area of the model. The increase in grid size for increasing CFF-stress is necessary in order to not underestimate the number of smaller events. I use the following relationship between magnitude and the number of failing nodes: $M = N^{0.46}$. Gutenberg-Richter curves for all other times in the considered scenario can then be generated from the model using appropriate scaling of CFF values and model size. If, however, the glacial stresses are such as to increase the stability of faults, I do not estimate Gutenberg-Richter curves below the background seismicity, but rather let the background stay constant.

Fig. 5 shows the *LaPoint et al.* [1999] reference curve, scaled to 1 kyr, as well as my model results for the background seismicity rate and the 1 kyr time interval of maximum activity. We see that the background model curve agrees very well with the *LaPoint et al.* [1999] curve, and that the maximum curve has a reasonable b-value of 0.92. Note that the maximum activity curve has been scaled to a circular area of radius 100 km, from the area of Sweden (450000 square km). My implementation of the Gutenberg-Richter relationship for the maximum magnitude event implies that as the maximum magnitude increases, the number of smaller events will also increase. Also note that the time of maximum activity is

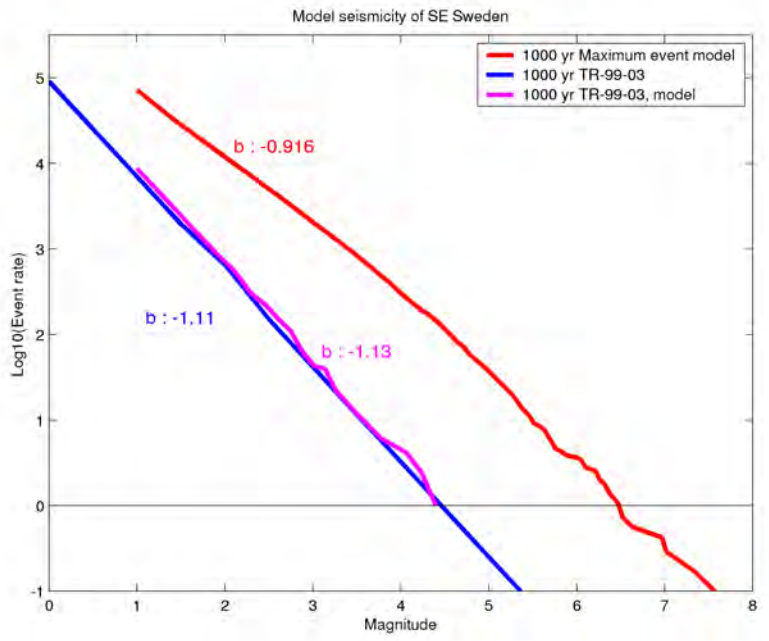

Figure 5: Gutenberg-Richter curves of seismicity for a circular area of radius 100 km and 1 kyr. Blue is the background curve given in *LaPoint et al.* [1999], purple the model based background curve and red the model curve for the time interval when the maximum magnitude event, M=7.6, occurs somewhere in Sweden.

considered to occur when the CFF stress is the largest, without regard to the actual value of that stress. This disregards the large absolute difference between the maximum CFF stresses in, e.g., the Forsmark reverse faulting initial case (max CFF = 2.5 MPa) and the Oskarshamn strike-slip initial case (max CFF = 14 MPa). One could claim that the latter case should experience more, or larger magnitude, seismicity due to the larger stressing rates. I have, however, considered each case in isolation and only assumed that the time of maximum CFF gives the time of maximum activity.

7 Results

I have used two of the results of the stability analysis above in order to estimate earthquake activity during the glacial cycle, using the modelling outlined above. The Forsmark stability analysis for a reverse faulting initial stress state, applied to optimally oriented faults, was used as an illustration of endglacial faulting, i.e. large earthquake activity during the last stages of deglaciation. The Oskarshamn analysis for a strike-slip initial stress field illustrates the consequences if the glacial stresses from a region which is in a strong fore-bulge area are added to a strike-slip stress state. In this case, the resulting seismicity deviates strongly from what is generally thought of as glacially induced seismicity, but which may have been present in southern Scandinavia during mid-glacial times.

The upper row of Fig. 6 shows the modelled seismicity for the Forsmark reverse faulting state. The result is displayed as Gutenberg-Richter curves at different points in time during the glacial cycle. The time axis is directly from the model provided by *Lambeck* [2005], starting at 106.5 kyr in accordance with the given assumption that a glacial cycle lasts approximately 100 kyr. As expected from the modelling procedure, we see that the times of

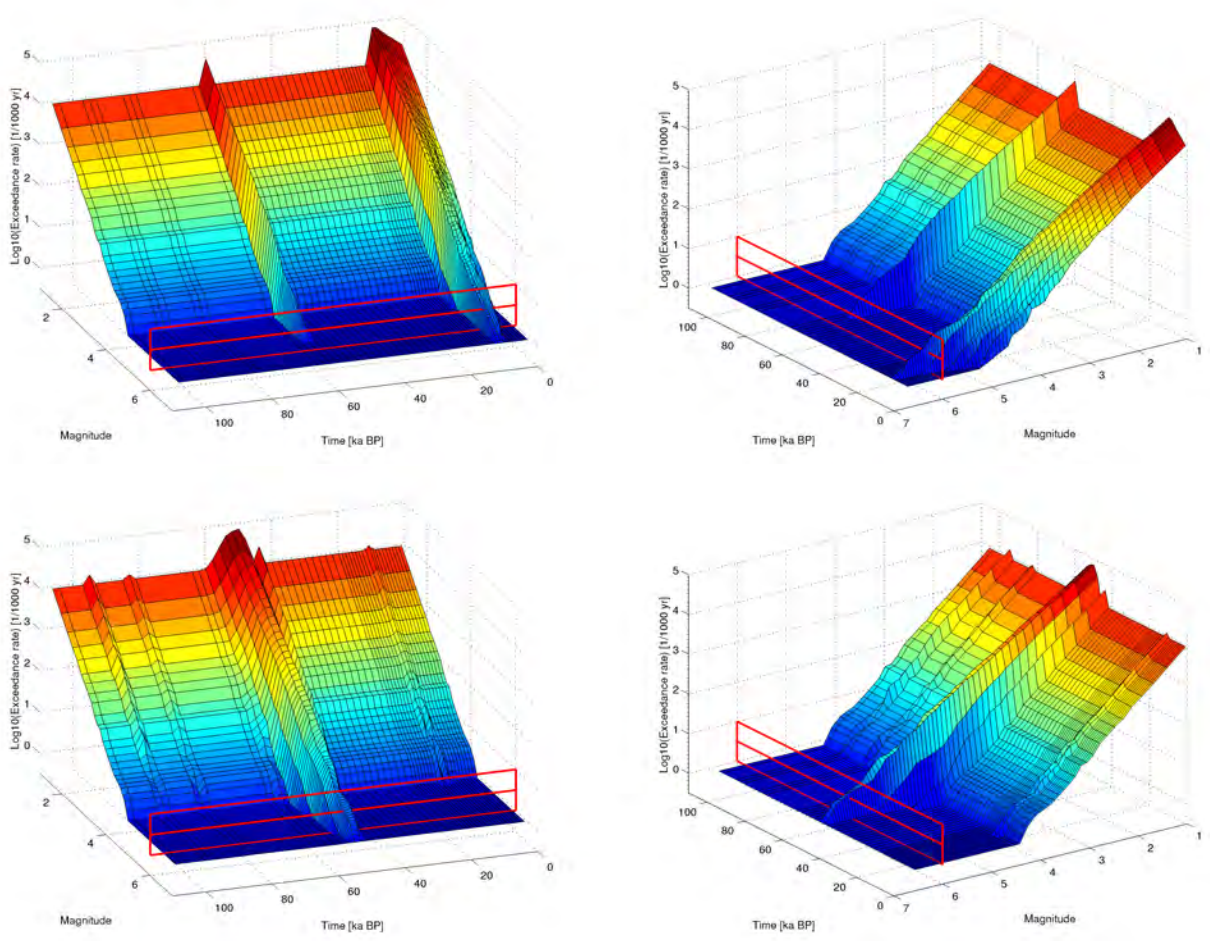

Figure 6: Distribution of seismicity, as Gutenberg-Richter curves, with time during a glaciation. The red grid delineates the M=6 line at N = 1, 3 and 10. Upper) The Forsmark reverse faulting initial state case. Lower) The Oskarshamn strike-slip faulting initial state case.

largest activity coincides with the times of large fault instability, at the end of deglaciation, compare with Fig. 2. There is also a spur of increased seismicity during the deglaciation at approximately 60 kyr BP. The figures show that there are rather few earthquakes of magnitude six or larger generated during the glaciation.

The lower row of Fig. 6 shows the case for the Oskarshamn strike-slip initial state of stress. As in the Forsmark case, the times of increased seismicity follow closely the times of high fault instability, which corresponds to the time around 50 kyr BP when Oskarshamn was in the fore-bulge of the growing ice sheet. We see that this case produces almost no seismicity during deglaciation. Again, there are very few magnitude six or larger earthquakes produced.

In Fig. 7 I plot the distribution of magnitude six or larger events with time, with the cumulative number of such events. We see that the Forsmark reverse faulting case produces approximately 15 magnitude six or larger events, and that the Oskarshamn strike-slip state produces approximately 11 events. The gentle slope in these figures when the seismicity is very low is the background tectonic strain release.

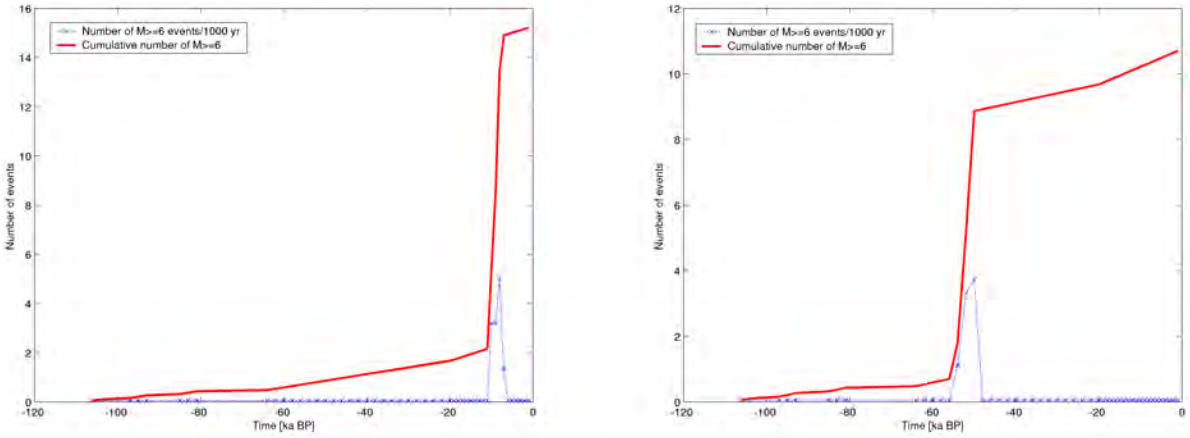

Figure 7: Number of events per time interval (blue) and cumulative number of events (red) as a function of time during the glaciation. Left) The Forsmark reverse faulting initial state case. Right) The Oskarshamn strike-slip faulting initial state case.

8 Discussion of uncertainties

The analysis in this report was performed during five days and a thorough investigation, with parameter variations, would have required substantially more time. Some of the assumptions in this report contain very large uncertainties or simplifications, and the following is a list of some of the these.

- The result is very much governed by the assumption about the maximum magnitude for the largest earthquake that occurs during the glacial cycle. In this model, a larger earthquake implies more smaller earthquakes and, thus, more events of magnitude six or larger.
- Paleoseismic evidence is incomplete, and debated, but there have been no large endglacial faults found in either Forsmark or Oskarshamn. Paleoseismics is not complete enough to constrain the frequency-magnitude relationship, in addition, it is not necessary for a magnitude six event in the thick Swedish crust to rupture to the surface.
- The current earthquake statistics in SE Sweden is poorly constrained due to the very low seismicity.
- The ice load, thickness, steepness and temporal evolution governs the induced stresses and these are likely to show some variation for different glaciations.
- The deviatoric background stress field (tectonics, mountains, etc) is not known well enough.
- Pore pressure effects have a very large impact on fault stability and the glacially induced pore pressure variations are likely to be considerable.
- The applied model for seismicity generation from stress field evolution may not be the most appropriate. This model does not incorporate stress relaxation after an event, which leads to an overestimate of the seismicity.

- The model implementation slightly underestimates the number of smaller events and the model statistics are rather unstable at lower activity rates.

9 Conclusions and parameter distribution

The modelling carried out in this report, with all the approximations and uncertainties discussed above, indicates that there will be a rather limited number of magnitude six or larger events in a circular area with radius 100 km during a glacial cycle such as the Weichselian. Different initial stress fields produce slightly different amounts of events, as do the locations of Forsmark and Oskarshamn with respect to the ice model. I do not consider the location differences to be significant with respect to variations in the ice model, or the repeatability of ice sheets during different glaciations, so I will not consider earthquake rates for the Forsmark and Oskarshamn sites separately. My modelling gives 10 to 15 events of magnitude six or larger, depending on the initial conditions, for a site in southeastern Sweden. The elicitation procedure requires a probability distribution of the earthquake frequency, which I estimate as follows:

Cumulative probability	0	0.25	0.5	0.9	1
Frequency of M >= 6	0	4	12	100	200

References

Böðvarsson, R., and B. Lund (2003), The SIL seismological data acquisition system – as operated in Iceland and in Sweden, in *Methods and Applications of Signal Processing in Seismic Network Operations*, edited by T. Takanami and G. Kitagawa, no. 98 in Lecture Notes in Earth Sciences, Springer Verlag, Berlin.

Fincat (2005), The Helsinki bulletin, Institute of Seismology, University of Helsinki, http://www.seismo.helsinki.fi/bul/index.html.

Hora, S. C., and M. Jensen (2002), Expert judgement elicitation, *Tech. Rep. SSI 2002:19*, Swedish Radiation Protection Authority, Stockholm, Sweden.

Johnston, A. C. (1987), Suppression of earthquakes by large continental ice sheets, *Nature*, *330*, 467–469.

Johnston, A. C. (1989), The effect of large ice sheets on earthquake genesis, in *Earthquakes at North Atlantic Passive Margins: Neotectonics and Postglacial Rebound*, edited by S. Gregersen and P. Basham, pp. 581–599, Kluwer, Dordrecht.

Johnston, P., P. Wu, and K. Lambeck (1998), Dependence of horizontal stress magnitude on load dimension in glacial rebound models, *Geophys. J. Int.*, *132*, 41–60.

King, G. C. P., and D. D. Bowman (2003), The evolution of regional seismicity between large earthquakes, *J. Geophys. Res.*, *108*, 2096, doi:10.1029/2001JB000783.

Lambeck, K. (2005), Glacial load stresses, note to the SSI expert panel, Stockholm, Sweden.

Lambeck, K., and A. Purcell (2003), Glacial rebound and crustal stress in Finland, *Tech. Rep. Posiva 2003-10*, Posiva Oy, Olkiluoto, Finland.

LaPoint, P. R., T. Cladouhos, and S. Follin (1999), Calculation of displacements on fractures intersecting canisters induced by earthquakes: Aberg, Beberg and Ceberg examples, *Tech. Rep. TR-99-03*, Swedish Nuclear Fuel and Waste Managment Co. (SKB), Stockholm, Sweden.

Lund, B. (2005), Effects of deglaciation on the crustal stress field and implications for endglacial faulting: A parametric study of simple Earth and ice models, *Tech. Rep. TR-05-04*, Swedish Nuclear Fuel and Waste Managment Co. (SKB), Stockholm, Sweden.

Lund, B., and M. D. Zoback (1999), Orientation and magnitude of *in situ* stress to 6.5 km depth in the Baltic Shield, *Int. J. Rock. Mech. Min. Sci., 36*, 169–190.

Munier, R. (2005), Eartquake analyses, note to the SSI expert panel, Stockholm, Sweden.

Näslund, J.-O., L. Rodhe, J. Fastook, and P. Holmlund (2003), New ways of studying ice sheet flow directions and glacial erosion by computer modelling – examples from Fennoscandia, *Quat. Sci. Rev., 22*, 245–258.

Quinlan, G. (1984), Postglacial rebound and the focal mechanisms of eastern Canadian earthquakes, *Ca. J. Earth Sci., 21*, 1018–1023.

Slunga, R. (1991), The Baltic Shield earthquakes, *Tectonophysics, 189*, 323–331.

Stewart, I. S., J. Sauber, and J. Rose (2000), Glacio-seismotectonics: ice sheets, crustal deformation and seismicity, *Quaternary Sci. Rev., 19*, 1367–1389.

Wu, P., and H. S. Hasegawa (1996), Induced stresses and fault potential in eastern Canada due to a disc load: a preliminary analysis, *Geophys. J. Int., 125*, 415–430.

Zoback, M. D., and J. Townend (2001), Implications of hydrostatic pore pressures and high crustal strength for the deformation of intraplate lithosphere, *Tectonophysics, 336*, 19–30.

SSI-rapporter 2005

SSI reports 2005

2005:01 Reports from SSI:s International Independent Expert Group on Electromagnetic Fields 2003 and 2004.
SSI's Independent Expert Group on Electromagnetic Fields 190 SEK

2005:02 (SKI 2005:02) International Peer Review of Swedish Nuclear Fuel and Waste Management Company's SR-Can interim report
Budhi Sagar, Lucy Bailey, David G Bennett, Michael Egan, Klaus-Jürgen Röhlig

2005:03 (SKI 2005:06) Granskning av SKB:s SR-Can interimsrapport:SKI:s och SSI:s bedömning av SKB:s uppdaterade metoder för säkerhetsanalys
Benny Sundström och Björn Dverstorp et. al.

2005:04 (SKI 2005:10) Concentrations of Uranium, Thorium and Potassium in Sweden
Bo Thunholm, Anders H. Lindén och Bosse Gustafsson 130 SEK

2005:05 (SKI 2005:32) Säkerhets- och strålskyddsläget vid de svenska kärnkraftverken 2004
SKI och SSI

2005:06 Percutan coronar intervention PCI – en strålskyddsutredning av verksamheten på landets sjukhus
Avdelningen för patient- och personalstrålskydd
Anja Almén, Torsten Cederlund och Britta Zaar 70 SEK

2005:07 Kommentarer och vägledning till föreskrifter och allmänna råd om hantering av aska som är kontaminerad med cesium-137
Avdelningen för beredskap och miljöövervakning
Hans Möre och Lynn Marie Hubbard 80 SEK

2005:08 Large-scale groundwater flow with free water surface based on data from SKBs site investigation in the Forsmark area.
SKI och SSI
Anders Wörman, Björn Sjögren och Lars Marklund

2005:09 Twelve years of cooperation in the field of radiation protection
SSI Internationellt Utvecklingssamarbete, SIUS
Sten Grapengiesser och Torkel Bennerstedt 120 SEK

2005:10 Rapporter från SSI:s vetenskapliga råd om ultraviolett strålning, 2002, 2003 och 2004
Avdelningen för beredskap och miljöövervakning
SSI:s vetenskapliga råd om ultraviolett strålning 250 SEK

2005:11 SSI:s granskning av SKB:s Fud-program 2004
Avdelningen för avfall och miljö
Carl-Magnus Larsson et al. 170 SEK

2005:12 Personalstrålskydd inom kärnkraftindustrin under 2004
Avdelningen för patient- och personalstrålskydd
Stig Erixon, Peter Hofvander, Ingemar Lund, Lars Malmqvist, Ingela Thimgren och Hanna Ölander Gür 70 SEK

2005:13 Review of SKB's interim report of SR-Can: SKI's and SSI's evaluation of SKB's up-dated methodology for safety assessment
Avdelningen för avfall och miljö
Björn Dverstorp och Bo Strömberg et al. 120 SEK

2005:14 Mätningar av naturlig radioaktivitet i och från filter vid några vattenverk
Avdelningen för beredskap och miljöövervakning
Inger Östergren, Gustav Åkerblom och Britt-Marie Ek 70 SEK

2005:15 Radiological Protection in Transition - Proceedings of the XIV Regular Meeting of the Nordic Society for Radiation Protection, NSFS - Rättvik, Sweden, 27-31 August 2005
Redaktörer: J. Valentin, T. Cederlund, P. Drake, I.E. Finne, A. Glansholm, A. Jaworska, W. Paile och T. Rahola 600 SEK

2005:16 Radon Risk Map of Estonia; Explanatory text to the Radon Risk Map Set of Estonia at the scale of 1:500,000
Valter Petersell, Gustav Åkerblom, Britt-Marie Ek, Margit Enel, Voldermar Möttus och Krista Täht.

2005:17 Utveckling, övervakning och åtgärder när det gäller radioaktivt cesium i renar efter Tjernobylolyckan
Birgitta Åhman. 70 SEK

2005:18 Kartläggning av kvalitetssäkringsrutiner för DAP-mätare i svensk sjukvård
Anja Almén, Jan-Erik Grindborg och Wolfram Leitz 70 SEK

2005:19 Utsläpps- och omgivningskontroll vid de kärntekniska anläggningarna 2002-2004
Maria Lüning 300 SEK

2005:20 Expert Panel Elicitation of Seismicity Following Glaciation in Sweden
Stephen Hora and Mikael Jensen 270 SEK

SSI report

STATENS STRÅLSKYDDSINSTITUT, SSI, är central tillsynsmyndighet på strålskyddsområdet. Myndighetens verksamhetsidé är att verka för ett gott strålskydd för människor och miljö nu och i framtiden.

SSI är ansvarig myndighet för det av riksdagen beslutade miljömålet Säker strålmiljö.

SSI sätter gränser för stråldoser till allmänheten och för dem som arbetar med strålning, utfärdar föreskrifter och kontrollerar att de efterlevs. Myndigheten inspekterar, informerar, utbildar och ger råd för att öka kunskaperna om strålning. SSI bedriver också egen forskning och stöder forskning vid universitet och högskolor.

SSI håller beredskap dygnet runt mot olyckor med strålning. En tidig varning om olyckor fås genom svenska och utländska mätstationer och genom internationella varnings- och informationssystem.

SSI medverkar i det internationella strålskyddssamarbetet och bidrar därigenom till förbättringar av strålskyddet i främst Baltikum och Ryssland.

Myndigheten har idag ca 110 anställda och är belägen i Stockholm.

THE SWEDISH RADIATION PROTECTION AUTHORITY, SSI, is the government regulatory authority for radiation protection. Its task is to secure good radiation protection for people and the environment both today and in the future.

The Swedish parliament has appointed SSI to be in charge of the implementation of its environmental quality objective Säker strålmiljö ("A Safe Radiation Environment").

SSI sets radiation dose limits for the public and for workers exposed to radiation and regulates many other matters dealing with radiation. Compliance with regulations is ensured through inspections.

SSI also provides information, education, advice, carries out its own research and administers external research projects.

SSI maintains an around-the-clock preparedness for radiation accidents. Early warning is provided by Swedish and foreign monitoring stations and by international alarm and information systems.

The Authority collaborates with many national and international radiation protection endeavours. It actively supports the on-going improvements of radiation protection in Estonia, Latvia, Lithuania, and Russia.

SSI has about 110 employees and is located in Stockholm.

Statens strålskyddsinstitut
Swedish Radiation Protection Authority

Adress: Statens strålskyddsinstitut; S-171 16 Stockholm
Besöksadress: Solna strandväg 96
Telefon: 08-729 71 00, Fax: 08-729 71 08

Address: Swedish Radiation Protection Authority
SE-171 16 Stockholm; Sweden
Visiting address: Solna strandväg 96
Telephone: + 46 8-729 71 00, Fax: + 46 8-729 71 08

www.ssi.se